USGS
science for a changing world

Prepared in cooperation with the Legislative-Citizen Commission on Minnesota Resources and in collaboration with Iowa State University and the Minnesota Department of Health

Hydrogeology and Groundwater Geochemistry of Till Confining Units and Confined Aquifers in Glacial Deposits near Litchfield, Cromwell, Akeley, and Olivia, Minnesota, 2014–18

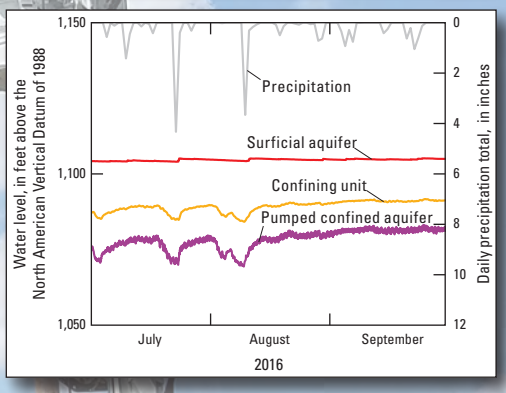

Scientific Investigations Report 2020–5127

U.S. Department of the Interior
U.S. Geological Survey

Cover photograph. (Clockwise from top left) Photographs showing (1) the Olivia water tower and the rotosonic drill rig, taken at the Olivia site, July 31, 2017, taken by Jared Trost, U.S. Geological Survey (USGS) hydrologist; (2) USGS hydrologic technician, Andrew Berg, and Iowa State University graduate student, Alyssa Witt, in the process of purging a piezometer after installation, taken at the Cromwell site, July 11, 2015, taken by James Stark, USGS Minnesota Water Science Center director; and (3) a Good Thunder formation till core sample taken at the Olivia site, August 9, 2017, taken by Jared Trost, USGS. (4) Plot showing precipitation and hydraulic head in piezometers during 3-month periods. (5) Photograph showing Minnesota Geological Survey Quaternary geologist, Maurice Nguyen, taking notes on till taken at the hydrogeology field camp site, May 24, 2017, taken by Jared Trost, USGS.

Hydrogeology and Groundwater Geochemistry of Till Confining Units and Confined Aquifers in Glacial Deposits near Litchfield, Cromwell, Akeley, and Olivia, Minnesota, 2014–18

By Jared J. Trost, Anna-Turi Maher, William W. Simpkins, Alyssa N. Witt, James R. Stark, Justin Blum, and Andrew M. Berg

Prepared in cooperation with the Legislative-Citizen Commission on Minnesota Resources and in collaboration with Iowa State University and the Minnesota Department of Health

Scientific Investigations Report 2020–5127

U.S. Department of the Interior
U.S. Geological Survey

U.S. Department of the Interior
DAVID BERNHARDT, Secretary

U.S. Geological Survey
James F. Reilly II, Director

U.S. Geological Survey, Reston, Virginia: 2020

For more information on the USGS—the Federal source for science about the Earth, its natural and living resources, natural hazards, and the environment—visit https://www.usgs.gov or call 1–888–ASK–USGS.

For an overview of USGS information products, including maps, imagery, and publications, visit https://store.usgs.gov/.

Suggested citation:
Trost, J.J., Maher, A., Simpkins, W.W., Witt, A.N., Stark, J.R., Blum, J., and Berg, A.M., 2020, Hydrogeology and groundwater geochemistry of till confining units and confined aquifers in glacial deposits near Litchfield, Cromwell, Akeley, and Olivia, Minnesota, 2014–18: U.S. Geological Survey Scientific Investigations Report 2020–5127, 80 p., https://doi.org/10.3133/sir20205127.

Associated data for this publication:
Maher, A.-T., Trost, J.J., Witt, A.N., Berg, A.M., Simpkins, W.W., and Stark, J.R., 2020, Geochemical data, water-level data, and slug test analysis results from till confining units and confined aquifers in glacial deposits near Akeley, Cromwell, Litchfield, and Olivia, Minnesota, 2015–2018: U.S. Geological Survey data release, https://doi.org/10.5066/P9IXC7D3.

Trost, J.J., Feinstein, D.T., and Jones, P.M., 2020, Heuristic MODFLOW models used to evaluate the effects of pumping groundwater from confined aquifers overlain by till confining units: U.S. Geological Survey data release, https://doi.org/10.5066/P9KOI6T3.

U.S. Geological Survey, 2019, USGS water data for the Nation: U.S. Geological Survey National Water Information System database, https://doi.org/10.5066/F7P55KJN.

ISSN 2328-0328 (online)

Acknowledgments

Funding for this study was provided by the Minnesota Environment and Natural Resources Trust Fund as recommended by the Legislative-Citizen Commission on Minnesota Resources and the U.S. Geological Survey's Cooperative Matching Funds program. Many people made contributions throughout this study. The authors wish to thank the numerous partners in this study that provided guidance in selecting field sites, including staff from the Minnesota Department of Natural Resources, Minnesota Geological Survey, University of Minnesota, and Minnesota Department of Health. Thanks to Bob Tipping, Maurice Nguyen, Amy Staley, and Caleb Wagner for core logging, geophysical surveys, and geologic interpretations and reports. Thanks to Scott Alexander for providing access to the University of Minnesota's hydrogeology field camp and for completing aquifer tests at this site for this study. Thanks to the Minnesota Department of Health staff who collected data for the aquifer tests at Litchfield and Cromwell. Thanks to the cities of Cromwell, Litchfield, and Olivia, and in particular, the municipal water systems operators of these cities, for their cooperation in this study. Thanks to Jan Falteisek and Erik Smith for providing technical reviews of this report.

A special thanks goes to Daniel Feinstein, U.S. Geological Survey, who completed the MODFLOW models discussed in this report.

Contents

Figures

Tables

Conversion Factors

U.S. customary units to International System of Units

Multiply	By	To obtain
	Length	
inch (in.)	2.54	centimeter (cm)
inch (in.)	25.4	millimeter (mm)
foot (ft)	0.3048	meter (m)
mile (mi)	1.609	kilometer (km)
	Area	
square mile (mi^2)	259.0	hectare (ha)
square mile (mi^2)	2.590	square kilometer (km^2)
	Volume	
gallon (gal)	3.785	liter (L)
gallon (gal)	0.003785	cubic meter (m^3)
gallon (gal)	3.785	cubic decimeter (dm^3)
million gallons (Mgal)	3,785	cubic meter (m^3)
	Flow rate	
foot per day (ft/d)	0.3048	meter per day (m/d)
gallon per minute (gal/min)	0.06309	liter per second (L/s)
gallon per year (gal/yr)	0.003785	cubic meter per year (m^3/yr)
inch per year (in/yr)	25.4	millimeter per year (mm/yr)

International System of Units to U.S. customary units

Multiply	By	To obtain
	Length	
millimeter (mm)	0.03937	inch (in.)
meter (m)	3.281	foot (ft)
	Volume	
cubic meter (m^3)	6.290	barrel (petroleum, 1 barrel = 42 gal)
liter (L)	33.81402	ounce, fluid (fl. oz)
liter (L)	2.113	pint (pt)
liter (L)	1.057	quart (qt)
liter (L)	0.2642	gallon (gal)
liter (L)	61.02	cubic inch (in^3)

Temperature in degrees Celsius (°C) may be converted to degrees Fahrenheit (°F) as follows:

$$°F = (1.8 \times °C) + 32.$$

Datum

Vertical coordinate information is referenced to the North American Vertical Datum of 1988 (NAVD 88).

Horizontal coordinate information is referenced to the North American Datum of 1983 (NAD 83).

Elevation, as used in this report, refers to distance above the vertical datum.

Supplemental Information

Specific conductance is given in microsiemens per centimeter at 25 degrees Celsius (µS/cm at 25 °C).

Concentrations of chemical constituents in water are given in either milligrams per liter (mg/L) or micrograms per liter (µg/L).

Results for measurements of stable isotopes of an element (with symbol E) in water, solids, and dissolved constituents commonly are expressed as the relative difference in the ratio of the number of the less abundant isotope (iE) to the number of the more abundant isotope of a sample with respect to a measurement standard.

Abbreviations

‰	per mil
14C yr BP	carbon-14 years before present
cal yr BP	calendar years before present
δ^2H	a measure of the ratio of stable isotopes hydrogen-2 and hydrogen-1
$\delta^{18}O$	a measure of the ratio of stable isotopes oxygen-18 and oxygen-16
DO	dissolved oxygen
HFC	hydrogeology field camp
K	hydraulic conductivity
KGS	Kansas Geological Survey
K_h	horizontal hydraulic conductivity
K_v	vertical hydraulic conductivity
MGS	Minnesota Geological Survey
NWIS	National Water Information System
NWQL	National Water Quality Laboratory
RWF	reverse water-level fluctuation
TU	tritium unit
USGS	U.S. Geological Survey

Hydrogeology and Groundwater Geochemistry of Till Confining Units and Confined Aquifers in Glacial Deposits near Litchfield, Cromwell, Akeley, and Olivia, Minnesota, 2014–18

By Jared J. Trost,[1] Anna-Turi Maher,[1] William W. Simpkins,[2] Alyssa N. Witt,[2] James R. Stark,[3] Justin Blum,[4] and Andrew M. Berg[1]

Abstract

Confined (or buried) aquifers of glacial origin overlain by till confining units provide drinking water to hundreds of thousands of Minnesota residents. The sustainability of these groundwater resources is not well understood because hydraulic properties of till that control vertical groundwater fluxes (leakage) to underlying aquifers are largely unknown. The U.S. Geological Survey, Iowa State University, Minnesota Geological Survey, and Minnesota Department of Health investigated hydraulic properties and groundwater flow through till confining units using field studies and heuristic MODFLOW simulations. Till confining units in the following late-Wisconsinan stratigraphic units (with locations in parentheses) were characterized: Des Moines lobe till of the New Ulm Formation (Litchfield, Minnesota), Superior lobe till of the Cromwell and Aitkin Formations (Cromwell, Minn.), and Wadena lobe till of the Hewitt Formation (hydrogeology field camp [HFC] near Akeley, Minn.). Pre-Illinoian till of the Good Thunder formation (Olivia, Minn.) was also characterized.

Hydraulic and geochemical field data were collected from sediment cores and a series of five piezometer nests. Each nest consisted of five to eight piezometers screened at short vertical intervals in hydrostratigraphic units including (if present) surficial aquifers, till confining units, confined/buried aquifers, and underlying bedrock. Till hydraulic conductivity was estimated from slug tests (horizontal [K_h]) and constant-rate aquifer tests in the confined aquifer (vertical [K_v]). Travel times through the till were evaluated with Darcy's law and stable isotope concentrations. A series of heuristic MODFLOW simulations were used to evaluate groundwater fluxes through till across the range of till hydraulic properties and pumping rates observed at the field sites.

The field data demonstrated variability in hydraulic properties between and within till stratigraphic units horizontally and vertically. The variability in hydraulic properties within and between sites resulted in substantial differences in groundwater flux through till. A conceptual understanding that emerges from the vertical till profiles is that they are not homogeneous hydrostratigraphic units with uniform properties; rather, each vertical sequence is a heterogeneous mixture of glacial sediment with differing abilities to transmit water.

Till thicknesses varied from 60 to 166 feet, and till textures ranged from a sandy loam (Hewitt Formation, HFC site) to a silt loam/clay loam (Good Thunder formation, Olivia site). Till K_h varied by one to three orders of magnitude within each piezometer nest. Four piezometer nests had downward hydraulic gradients ranging from 0.04 to 0.56, and one nest had a slight upward hydraulic gradient of 0.02. The Cromwell, HFC, and Litchfield 1 sites were examples of "leaky" tills with high K_v (0.001 to 1.1 feet per day [ft/d]) and geometric mean K_h (0.03 to 0.07 ft/d) and extensive vertical hydraulic connectivity between the confined aquifer and the overlying till. Estimated groundwater travel times through these sites ranged from 1 to 81 years, and two of these sites had tritium throughout their till profiles. The tills at the other two sites, Olivia and Litchfield 2, were effective confining units that had low K_v (0.001 to 0.0005 ft/d) and geometric mean K_h (0.0002 to 0.004 ft/d). The till piezometers at these sites had no drawdown response to short-term (up to 10 hours for Olivia and up to 5 days for Litchfield) high-capacity pumping from the confined aquifer. Estimated groundwater travel times through the tills at these sites ranged from 165 to nearly 1,800 years, and tritium was only detected in the upper one-third of these till profiles. Across all sites, the till vertical anisotropy (ratio of K_h to K_v) ranged by four orders of magnitude from 0.05 at the Cromwell nest to 70 at the Litchfield 1 nest. Stable isotopes of

[1]U.S. Geological Survey.

[2]Iowa State University.

[3]Minnesota State Legislative Water Commission.

[4]Minnesota Department of Health.

oxygen and hydrogen indicate that groundwater throughout all five till profiles is younger than the last glacial advance into Minnesota at about 11,000 years ago.

The heuristic modeling demonstrated that, for understanding sustainability of groundwater pumping from confined aquifers, knowledge of till hydraulic properties is just as important as knowledge of aquifer hydraulic properties. Substantial differences in groundwater fluxes into and through till were observed across hydrogeologic settings representative of the field sites. Over long periods of time (hundreds of years), pumping-induced hydraulic gradients are established in confined aquifer systems and, even in low hydraulic conductivity tills, these pumping-induced hydraulic gradients increase leakage into and through till compared to ambient conditions.

In conclusion, groundwater flowing vertically downward through till confining units (leakage) replenishes water pumped from confined aquifers. Till hydraulic properties, such as those presented in this report, provide important information that can be used to quantify leakage rates through till. Till hydraulic properties are variable over short distances and profoundly affect leakage rates, demonstrating the importance of site-specific till hydraulic data for evaluating the sustainability of groundwater withdrawals from confined aquifers.

Introduction

Confined aquifers of glacial origin overlain by till confining units provide drinking water to thousands of Minnesota residents. These till confining units are typically conceptualized as having low potential for transmitting water; thus, the confined aquifers below may be prone to unsustainable groundwater withdrawals. Quantification of the recharge (leakage) rate through till is essential to understanding the sustainability of groundwater pumping from confined aquifers. Although the well yields of these confined aquifers are sufficient for some Minnesota communities, sustainability issues can arise because of the small size of the aquifer or low groundwater recharge rates. Strain on the water supply can be the result of the water demand exceeding the recharge rate to the aquifer, or from reduction of the recharge rate to the aquifer because of changes in climate (Delin, 1986; Lindgren, 1996, 2002).

Buried aquifers can be confined or unconfined, and the field investigations of this study focused solely on confined aquifers. Groundwater in confined aquifers is isolated from the atmosphere at the point of discharge by poorly conductive geologic formations (for example, overlying till confining units), and the confined aquifer is subject to pressures higher than atmospheric pressure. This means that when a well is drilled through an overlying confining unit into a confined aquifer, water rises in the well to some level above the top of the aquifer. The water level in the well represents the confining pressure at the top of the aquifer (Driscoll, 1986). On the other hand, buried, unconfined aquifers do not have a confining pressure. When a well is installed in a buried unconfined aquifer, the water level in the well will be below the top of the aquifer.

Confined aquifers may be protected from anthropogenic contamination by a confining unit overlying them, but properties such as the hydraulic conductivity (K) and the thickness of the confining unit, the presence or absence of fracture flow, and the confining unit geochemical environment may either impede the flow of contaminants or allow the flow of contaminants through a confining unit to an underlying aquifer (Bradbury and others, 2006). Investigations concerning confining unit properties are less abundant compared to investigations on aquifer properties (Cherry and others, 2004). Field studies of hydrogeology and (or) geochemistry of till confining units have been completed in Alberta, Saskatchewan, Manitoba, Wisconsin, Iowa, and Minnesota (Grisak and Cherry, 1975; Fortin and others, 1991; Simpkins and Bradbury, 1992; Simpkins and Parkin, 1993; Witt, 2017). These studies reported a wide range of hydraulic properties and geochemical environments in till confining units. For instance, K in studied till confining units has been estimated to be as low as 6×10^{-6} feet per day (ft/d) (Simpkins and Parkin, 1993) and as high as 2×10^{-1} ft/d (Witt, 2017). Properties may also vary spatially throughout a till confining unit, and the presence of features such as sand lenses, erosional surfaces, joints, and fractures is locally important to the flux of groundwater in the till (Gerber and Howard, 2000).

To help understand the sustainability of groundwater resources in confined aquifers overlain by till confining units, the U.S. Geological Survey (USGS), Iowa State University, Minnesota Geological Survey, and Minnesota Department of Health investigated hydraulic properties and groundwater flow through till confining units using field studies and heuristic MODFLOW simulations. The results of this study provide insight to the sustainability of the groundwater resources being withdrawn from confined aquifer systems in Minnesota.

Purpose and Scope

The purpose of this report is to describe the hydrogeology and groundwater geochemistry of till confining units and confined aquifers in glacial deposits at four representative sites in Minnesota. The results of field studies and modeling approaches designed to quantify the variability of hydrologic properties and groundwater fluxes through till confining units to confined aquifers are described. The field studies were completed during 2014–18 near Litchfield, Cromwell, Akeley, and Olivia, Minnesota (fig. 1).

Description of Study Sites

Four field sites were selected for inclusion in this study. Field sites were representative of deposits from major glacial lobe extents in Minnesota. Sites were in three late-Wisconsinan deposits: the Des Moines lobe, the Superior

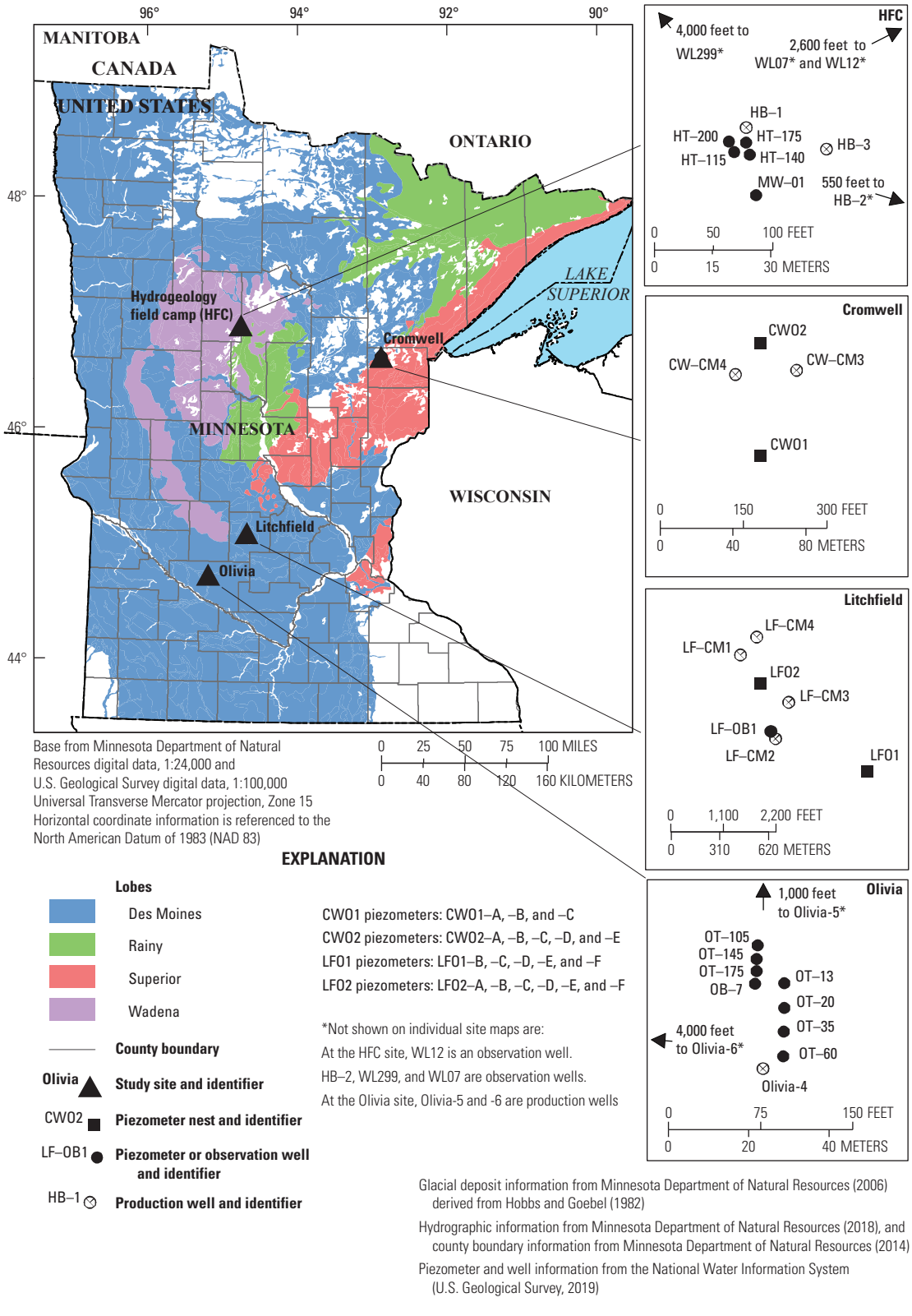

Figure 1. The location of the Litchfield sites (LFO1 and LFO2) and the Cromwell (CWO1/O2), hydrogeology field camp (HFC), and Olivia sites in Minnesota in relation to major glacial lobes of late-Wisconsinan deposits, and the piezometers and production wells at each site.

lobe, and the Wadena lobe, as well as one pre-Illinoian deposit underlying the Des Moines lobe (fig. 1; Hobbs and Goebel, 1982). Candidate field sites were required to have (1) a small number (less than five) of high-capacity production wells withdrawing water from a buried artesian (confined) aquifer contained in Quaternary deposits, as classified by the Minnesota Geological Survey (MGS); (2) a confined aquifer within 300 feet (ft) of land surface; (3) a completed wellhead protection plan (or comparable form of local site hydrogeological characterization); (4) a completed county geologic atlas (or comparable detailed geological data compilation); and (5) information on the integrity of the high-capacity well construction. Sites meeting these minimum criteria were identified and then municipalities or land owners were contacted to gauge their willingness in partnering with the USGS in the study.

The Litchfield and Olivia study sites are within the footprint of the Des Moines lobe in central Minnesota. The city of Litchfield, where the Litchfield site is located, has a population of 6,726 and is in central Minnesota (Meeker County) (U.S. Census Bureau, 2012). The population of Litchfield relies on four municipal wells that pump approximately 340 million gallons per year (Mgal/yr) (Haglund and Robertson, 2000). The Litchfield site had two piezometer nests installed for this study, referred to as the Litchfield 1 (LFO1) site and the Litchfield 2 (LFO2) site.

The town of Olivia, where the Olivia site is located, has a population of 2,484 and is 35 miles (mi) southwest of Litchfield (Renville County) (U.S. Census Bureau, 2012). The population of Olivia draws its water supply from two confined aquifers. The water use in the town of Olivia, from the confined aquifer in this study, is around 64 Mgal/yr (Robertson, 2011). The Olivia site had one piezometer nest installed for this study. The towns of Litchfield and Olivia draw municipal water from glacigenic confined aquifers of limited areal extent. The physical setting at both sites consists of low-relief ground moraine typical of the Des Moines lobe. Row-crop agriculture is the dominant land use in the region. The land area surrounding both sites usually receives about 27–29 inches (in.) of precipitation annually (Minnesota Department of Natural Resources, 2020).

The town of Cromwell has a population of 231 and is in the footprint of the Superior lobe in Carlton County (fig. 1) (U.S. Census Bureau, 2012). The population of Cromwell relies on two production wells pumping approximately 6 Mgal/yr from a glacigenic confined aquifer (Walsh, 2012). The Cromwell field site had two piezometer nests installed for this study, the Cromwell 1 (CWO1) and Cromwell 2 (CWO2) nests; however, the two nests are only about 160 ft apart and are primarily discussed as a single, merged site (CWO1/O2) throughout this report. The CWO1/O2 site is on a topographic high of hummocky topography consisting primarily of sand and gravel. Land cover consists of moderately forested woodlands and some agriculture. The annual precipitation around the town of Cromwell is about 29–31 in. (Minnesota Department of Natural Resources, 2020).

The hydrogeology field camp (HFC) site is within the footprint of the Wadena lobe on the far eastern edge of Hubbard County and is not located in a town (fig. 1). The town of Akeley, Minn., (not shown) is to the northwest of the field site. There are more than 60 observation wells at this location that are operated as part of the University of Minnesota's HFC. The HFC site had one piezometer nest installed for this study. The area is highly wooded, and numerous lakes are near the site. The annual precipitation in the area surrounding the HFC site is about 26–28 in. (Minnesota Department of Natural Resources, 2020).

Geologic Setting

The following is a summary of detailed geologic reports produced during this study (Wagner and Tipping, 2016; Staley and Nguyen, 2018; Staley and others, 2018) and the glacial history of the sites. Naming conventions and descriptions of the Quaternary-aged formations and members listed in this report are described in the Minnesota Geological Survey's definitive reference for Minnesota Quaternary geology titled "Quaternary lithostratigraphic units of Minnesota" (Johnson and others, 2016). Generalized lithologies are presented in the completion diagram figures (figs. 2, 3, 4, 5, and 6). The depths and thicknesses shown in the generalized lithologies in these figures are simplified compared to the detailed stratigraphy presented in the geologic reports (Wagner and Tipping, 2016; Staley and Nguyen, 2018; Staley and others, 2018).

Litchfield

At the Litchfield site, till of the Villard Member of the New Ulm Formation overlies the confined aquifer (Wagner and Tipping, 2016). The glaciofluvial deposit that composes the confined aquifer is most likely outwash of the Hewitt Formation (Wagner and Tipping, 2016). Till of the Villard Member was deposited by glacial ice (and its meltwater) that moved into Minnesota from the Winnipeg provenance to the north, eventually depositing the Pine City moraine (Johnson and others, 2016). The till age is not exactly known but is estimated as about 12,300 carbon-14 years before present (^{14}C yr BP) (about 14,450 calendar years before present [cal yr BP]) (Clayton and Moran, 1982; Johnson and others, 2016). More recent publications indicate that the deposition of the Pine City moraine is older, about 13,000 ^{14}C yr BP (about 16,000 cal yr BP) (Johnson and others, 2016). The lobe eventually advanced as far south as Des Moines, Iowa, by 14,000 ^{14}C yr BP.

The mean particle-size distribution of the till for the Litchfield site, determined by the MGS from two continuous till cores from the LFO1 and LFO2 sites, sampled at about 4-ft intervals, is 49-percent sand, 33-percent silt, and 18-percent clay (Wagner and Tipping, 2016). This distribution is similar to the equivalent till of the Alden Member of the Dows Formation near Ames, Iowa (Helmke and others, 2005b). Particle-size distribution of the LFO1 and LFO2 till

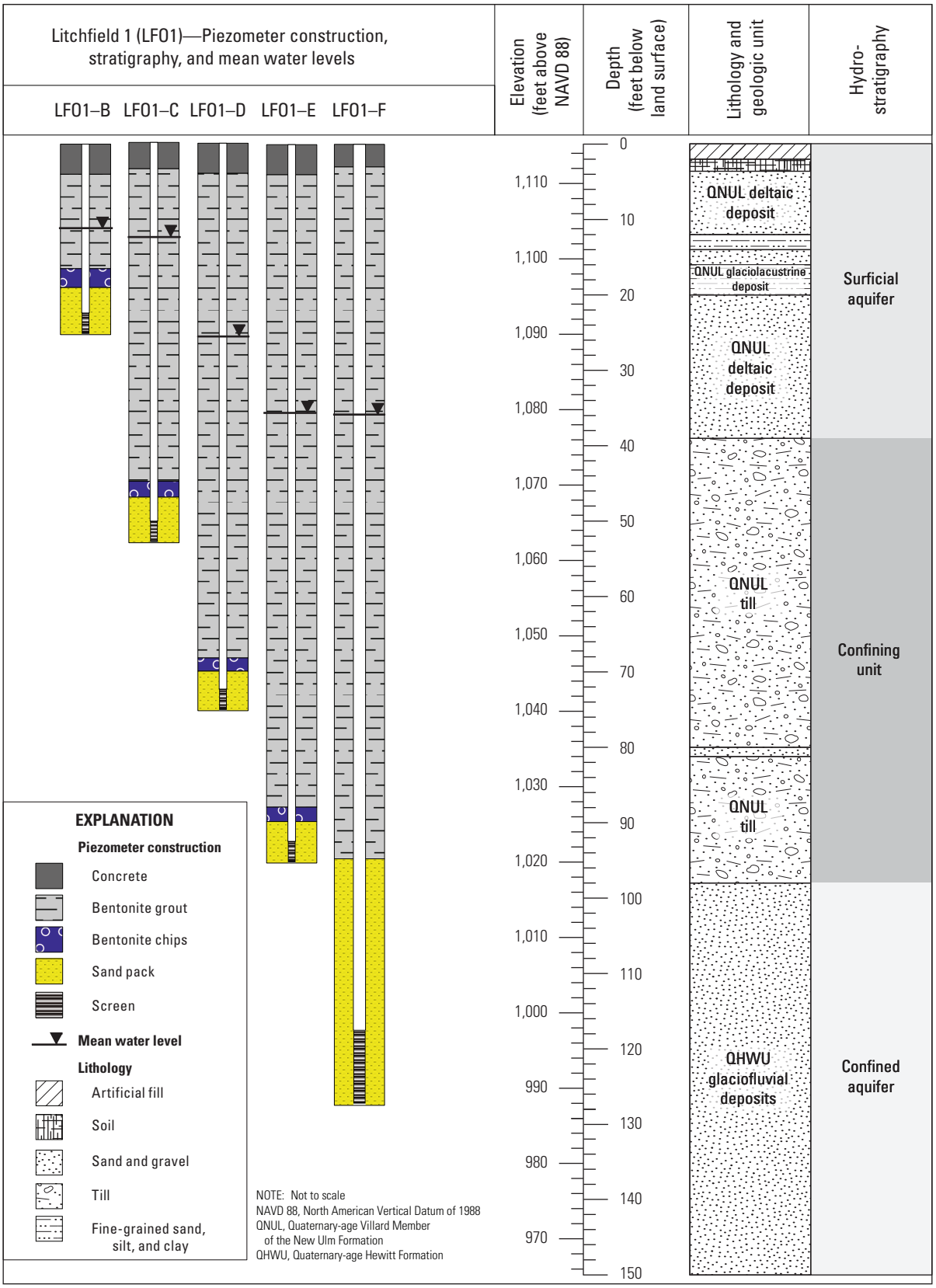

Figure 2. Litchfield 1 (LFO1) site piezometer construction, stratigraphy, and mean water levels. Stratigraphic information is based on the Minnesota Geological Survey analysis (Wagner and Tipping, 2016; Staley and others, 2018).

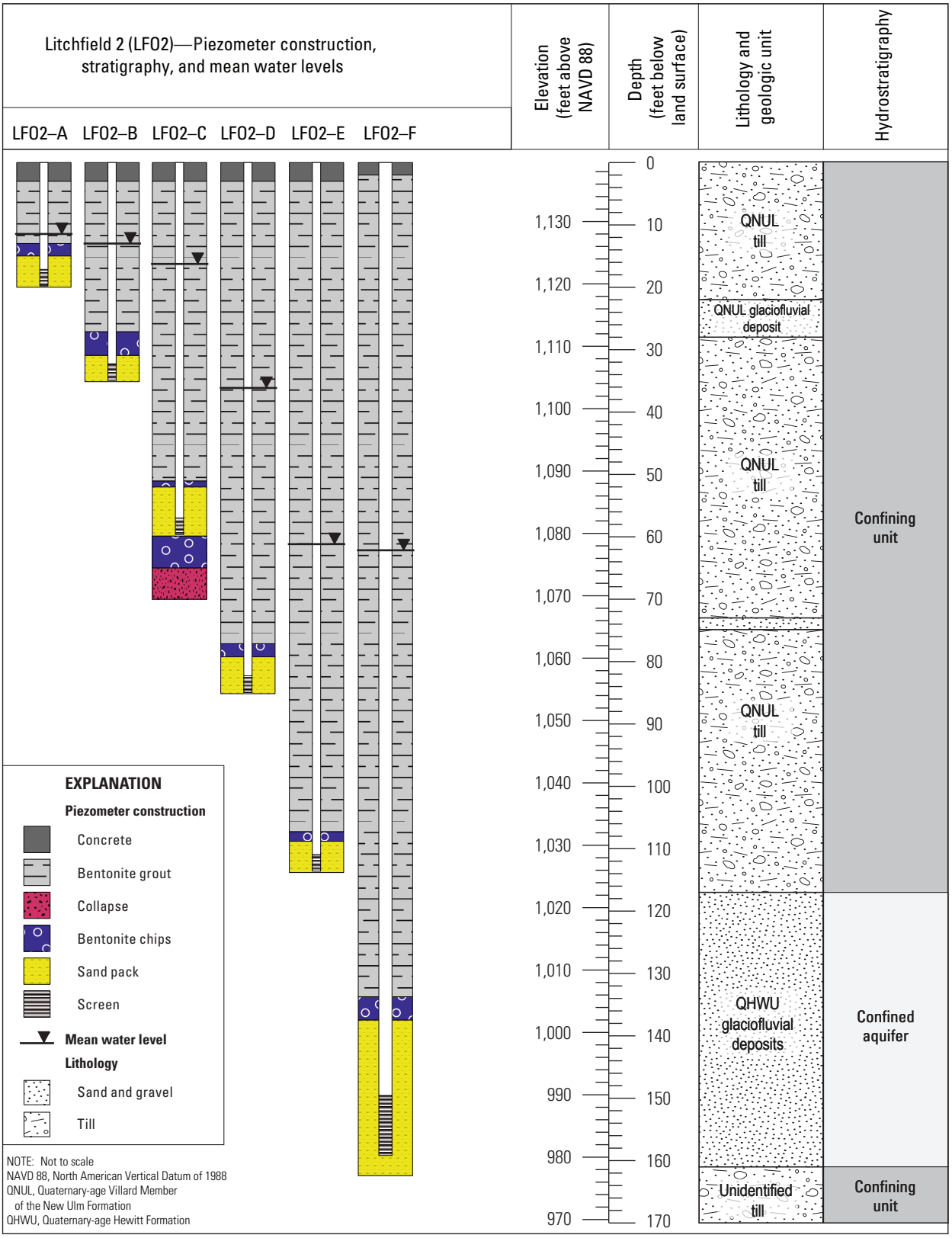

Figure 3. Litchfield 2 (LFO2) site piezometer construction, stratigraphy, and mean water levels. Stratigraphic information is based on the Minnesota Geological Survey analysis (Wagner and Tipping, 2016; Staley and others, 2018).

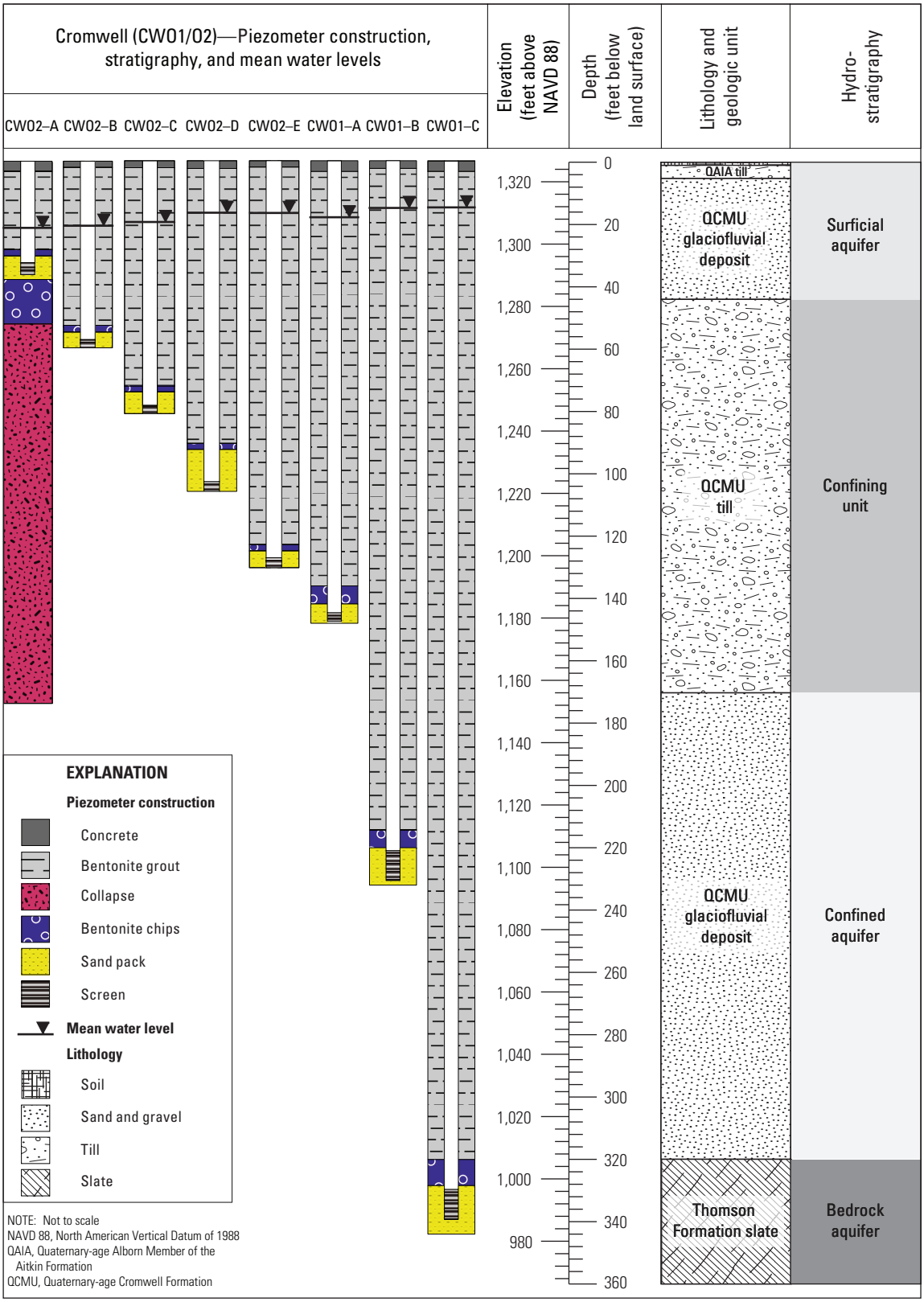

Figure 4. Cromwell (CWO1/O2) site piezometer construction, stratigraphy, and mean water levels. Stratigraphic information is based on Knaeble and Hobbs (2009) and the Minnesota Geological Survey analysis (Staley and others, 2018).

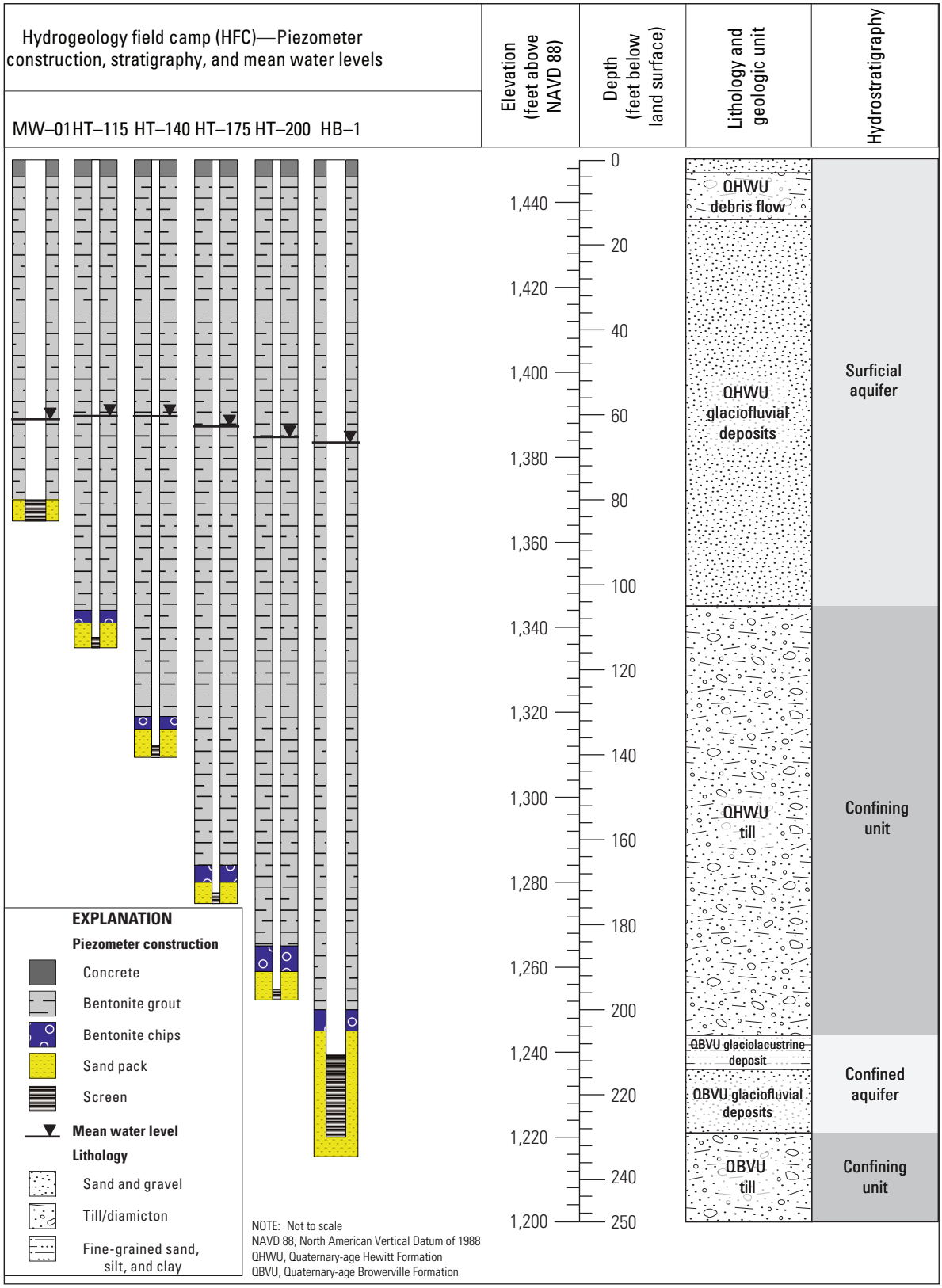

Figure 5. Hydrogeology field camp (HFC) site piezometer construction, stratigraphy, and mean water levels. Stratigraphic information is based on the Minnesota Geological Survey analysis (Staley and others, 2018).

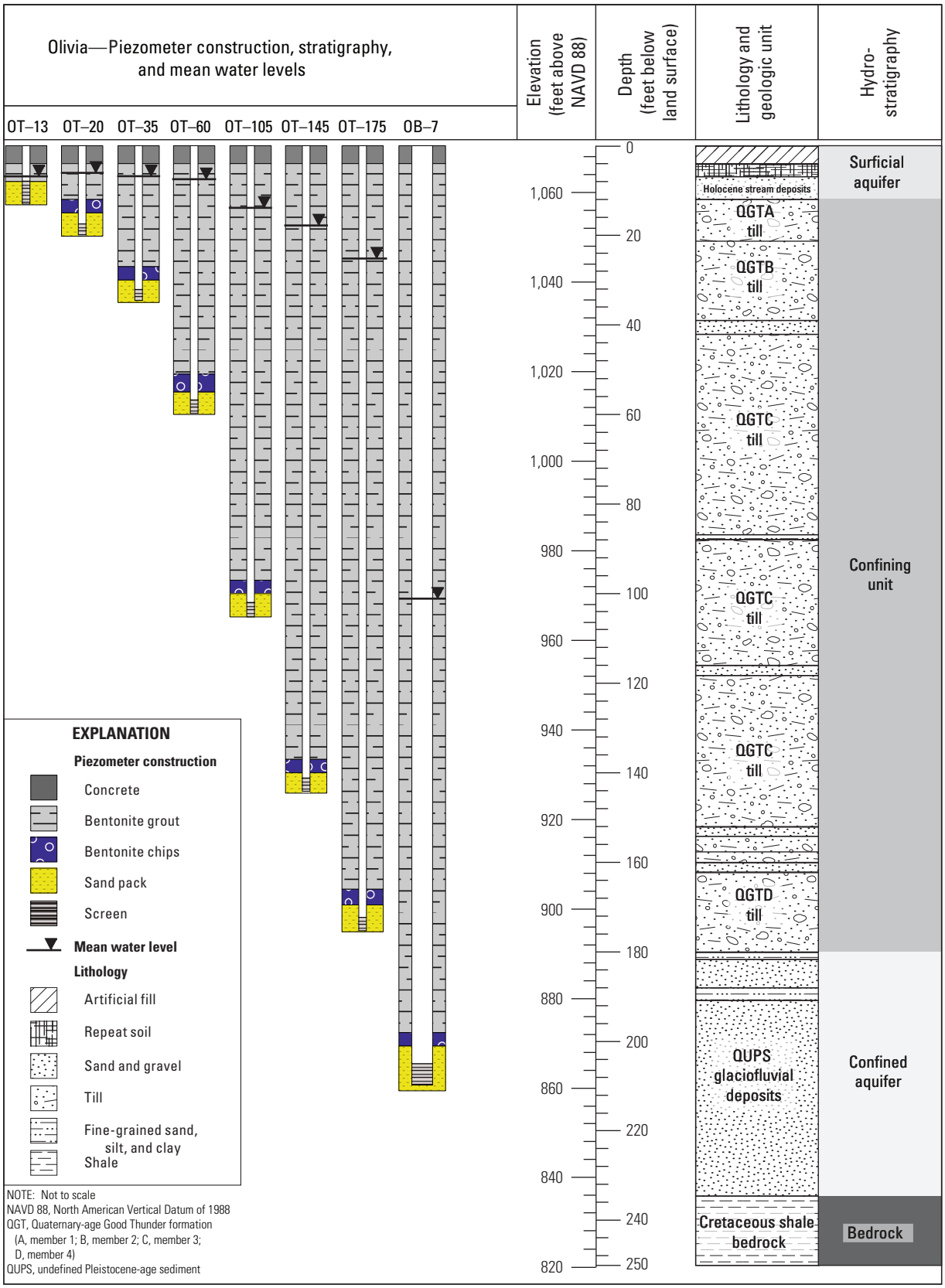

Figure 6. Olivia site piezometer construction, stratigraphy, and mean water levels. Stratigraphic information is based on the Minnesota Geological Survey analysis (Staley and others, 2018).

cores, from the MGS report by Staley and others (2018), was used to calculate separate mean particle-size distributions for the LFO1 and LFO2 sites. At LFO1, the mean particle size is 47-percent sand, 34-percent silt, and 19-percent clay, and at the LFO2 site, the mean particle size is 52-percent sand, 31-percent silt, and 17-percent clay (fig. 7*A*).

Sediment of the New Ulm Formation is yellowish brown and oxidized in the upper 15 ft, and grayish brown and unoxidized below this depth. Carbonate clasts and a calcareous matrix are present throughout, except in the top 3 ft of the LFO1 core. Fractures were described in the LFO1 and LFO2 cores to depths of about 60 and 90 ft, respectively. Most fractures lacked iron

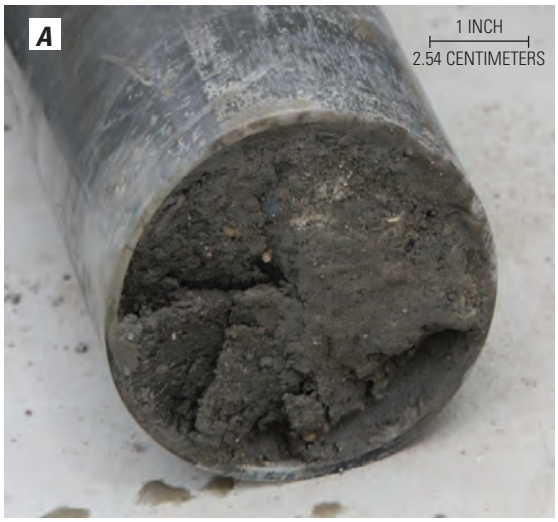

A. **Till of the New Ulm Formation from the Litchfield site. The mean particle size distribution of the till at the LFO1 site is 47 percent sand, 34 percent silt, and 19 percent clay; and at the LFO2 site is 52 percent sand, 31 percent silt, and 17 percent clay.**

B. **Till of the Cromwell Formation from the Cromwell site. The till has a mean particle size distribution of 57 percent sand, 31 percent silt, and 13 percent clay (greater than 100 percent because of rounding).**

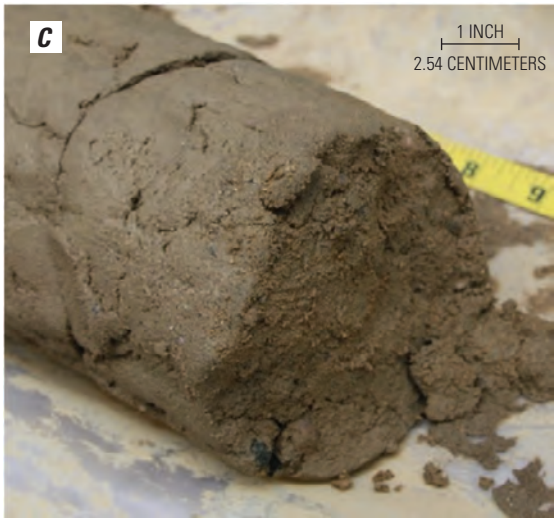

C. **Till of the Hewitt Formation from the HFC site. The till has a mean particle size distribution of 67 percent sand, 22 percent silt, and 11 percent clay.**

D. **Till of the Good Thunder formation from the Olivia site. The till has a mean particle size distribution of 37 percent sand, 40 percent silt, and 23 percent clay.**

Figure 7. Images of till from cores extracted from sites. *A*, till of the New Ulm Formation from the Litchfield site (LFO1 and LFO2); *B*, till of the Cromwell Formation from the Cromwell site; *C*, till of the Hewitt Formation from the hydrogeology field camp (HFC) site; *D*, till of the Good Thunder formation from the Olivia site. Mean particle-size information is from Wagner and Tipping (2016) and Staley and Nguyen (2018). [in, inch; cm, centimeter]

staining common to fracture surfaces in the equivalent till in Iowa (Helmke and others, 2005b). Some fractures may be artifacts of the coring process and subsequent unloading; however, McKay and Fredericia (1995) determined that till fractures can occur below depths where oxidation staining occurs.

Sediment sequences differ between the LFO1 (fig. 2) and LFO2 (fig. 3) sites. At the LFO1 site, fine-grained, sandy and silty deltaic and glaciolacustrine sediment with some gravel occurs above the till. Wagner and Tipping (2016) interpreted this as a deltaic deposit resulting from a series of meltwater plumes into Glacial Lake Litchfield (Meyer, 2015). The sand and gravel unit is not detected at the LFO2 site, which lies at about 25 ft higher in elevation than the LFO1 site (Wagner and Tipping, 2016). The confined sand and gravel aquifer unit begins at approximately 98 and 117 ft below land surface at the LFO1 site and the LFO2 site, respectively. Till thickness varies between the two piezometer nests. At the LFO1 site, the till is about 60 ft thick, and at the LFO2 site, the till is about 115 ft thick. The aquifer is about 44 ft thick at the LFO2 site, based on borehole geophysical logs and the generalized borehole lithostratigraphy (Wagner and Tipping, 2016). The confined aquifer sediments were not included in core samples at either LFO1 or LFO2, which is why alternative methods were used to determine confined aquifer thickness. The confined aquifer at the Litchfield sites may be underlain by pre-Wisconsinan till of the Sauk Centre Member of the Lake Henry Formation (Meyer, 2015).

Cromwell

The stratigraphic sequence at the Cromwell site (fig. 4) is more complex than that at the Litchfield site. The Superior lobe advanced and retreated from the Lake Superior Basin multiple times during the late-Wisconsinan glacial episode. As the climate warmed, the extent of those advances into Minnesota became successively smaller. The Cromwell Formation, which consists of till and glaciofluvial and glaciolacustrine sediment of the Superior provenance, is the primary glacial lithostratigraphic unit at the Cromwell site and in northeastern Minnesota. The exact age of the unit at Cromwell is not well constrained (Johnson and others, 2016). The St. Croix phase of the Superior lobe advanced ice over the Cromwell site in west-central and south-central Minnesota between 15,000 and 20,000 ^{14}C yr BP. The Superior lobe advanced over the Cromwell site later during the Automba phase between 13,500 and 14,000 ^{14}C yr BP (Jennings and Johnson, 2011). It was during ice retreat at the end of the Automba phase that till of the Cromwell Formation was likely deposited on top of the sand and gravel of the Cromwell Formation that compose the confined aquifer at the site. After the retreat of the Superior lobe, the St. Louis sublobe advanced over the Cromwell site from the northwest at about 12,500 ^{14}C yr BP (about 15,000 cal yr BP) and deposited the Alborn Member of the Aitkin Formation (Johnson and others, 2016; Staley and others, 2018).

Core samples were not retrieved from the CWO1 site, and the MGS reconstructed the geology through analysis of downhole gamma ray logs. Core samples were collected at the CWO2 site; however, the high frequency of clasts greater than 2 in. in diameter interfered with the coring process and resulted in the collection of fewer core samples than expected. Two glacigenic units were identified at the Cromwell site. Starting at land surface, 4 ft of silt loam till of the Alborn Member of the Aitkin Formation overlies 40 ft of sand and gravel outwash of the Cromwell Formation deposited during the Automba phase of the Superior lobe. The Alborn Member is likely responsible for the hummocky topography at the site. Below the sand and gravel deposits lies about 126 ft of sandy loam to loam till with cross-stratified, fine- to very coarse-sand and gravel layers, also likely deposited during the Automba phase. The confined aquifer below these deposits consists of a sand and gravel unit within the Cromwell Formation, underlain by Paleoproterozoic slate of the Thomson Formation (Boerboom, 2009).

Sediment of the Cromwell Formation and the Aitkin Formation was typically reddish brown, and a calcareous matrix was present in the core below 43.5 ft. The till of the Cromwell Formation had a mean particle-size distribution of 57-percent sand, 31-percent silt, and 13-percent clay (fig. 7*B*, greater than 100 percent because of rounding), which is about 8 percent more sand than till of the New Ulm Formation. Till of the Aitkin Formation was not analyzed for particle-size distribution.

Hydrogeology Field Camp

The HFC site (fig. 5) has glacial sediment deposits of the Wadena lobe. Glacial ice brought northeast sourced sediments from the Rainy provenance and deposited till, outwash, and lake sediments of the Hewitt Formation (Johnson and others, 2016). Two depositional events known as the Alexandria and Itasca phases have been identified. The Alexandria phase represents the first ice advance, and the Itasca phase is associated with a later, second ice advance (Knaeble and Hougardy, 2018). Deposits of both phases are assigned to the Hewitt Formation, which has an estimated age of about 30,000 ^{14}C yr BP (Johnson and others, 2016; Knaeble and Hougardy, 2018). This age indicates that the Wadena lobe was actively depositing sediments in the early part of late-Wisconsinan time (Johnson and others, 2016).

The till at the HFC site underlies a 105-ft-thick coarse-grained sand and gravel outwash deposit of the Hewitt Formation. The till of the Hewitt Formation is a sandy loam, with a mean particle size of about 67-percent sand, 22-percent silt, and 11-percent clay (fig. 7*C*; Staley and Nguyen, 2018). The till is brown in color and lacks shale clasts but has moderate carbonate clasts of around 10–25 percent (Staley and Nguyen, 2018). The thickness of the till unit is about 102 ft. The entirety of the till of the Hewitt Formation is considered one unit (Staley and Nguyen, 2018).

Below the till of the Hewitt Formation to a depth of 250 ft is pre-Wisconsinan lake sediments, outwash, and glacial till of the Browerville Formation (Staley and Nguyen, 2018). The confined aquifer below the Hewitt Formation is composed of fine-grained sand and gravel glaciolacustrine (glacial lake) sediments and outwash sediments of the Browerville Formation, and is about 23 ft in thickness (Staley and Nguyen, 2018). Immediately below the confined aquifer is till of the Browerville Formation, which starts at a depth of 230 ft below land surface and has a thickness of about 20 ft (Staley and Nguyen, 2018).

Olivia

At the Olivia site (fig. 6), till of the New Ulm Formation was expected to be present because thick sequences of Des Moines lobe tills have been mapped around the Olivia area (Knaeble, 2013; Bradt, 2017; Staley and Nguyen, 2018). During the Pleistocene, several glacial advances and retreats occurred in the study site area, with the most recent till deposition being the New Ulm Formation from the Des Moines lobe (Knaeble, 2013). The age range for Des Moines lobe glaciation in Minnesota is 16,000 to 12,000 cal yr BP (Knaeble, 2006); however, the till sequence at Olivia is interpreted to be of the Good Thunder formation, an informally named pre-Wisconsinan till (Staley and Nguyen, 2018). Radiocarbon-dated wood deposits from the Good Thunder formation provide an age estimate as greater than 48,500 ^{14}C yr BP (Knaeble, 2013).

Till of the Good Thunder formation present at Olivia is typically gray in color, with a loam to silty and clayey loam texture and a mean particle size of around 37 percent for sand, 40 percent for silt, and 23 percent for clay (fig. 7*D*). The till is high in carbonates (usually greater than 50 percent) and low in gray shale percentage (between 0 and 10 percent) and Cretaceous grains are present (between 1 and 10 percent) (Staley and Nguyen, 2018). Four possible members of the Good Thunder formation are present at Olivia, based on Cretaceous percentage and density changes through the till formation (Staley and Nguyen, 2018). The overall thickness of till of the Good Thunder formation at Olivia is about 166 ft. Sand bodies are also often present in the formation, stratigraphically dividing the different members (Staley and Nguyen, 2018).

Above the Good Thunder formation is a thin layer of Holocene sediment that is about 10 ft thick and is topped by about 4 ft of fill (Staley and Nguyen, 2018). Below the Good Thunder formation is a silt and fine- to coarse-grained sand aquifer, likely a glaciofluvial outwash deposit of uncertain origin (Staley and Nguyen, 2018). The confined aquifer is about 48 ft thick. Underneath the aquifer at a depth of 229.5 ft below land surface lies Cretaceous shale bedrock (Staley and Nguyen, 2018).

Methods of Study

The following section describes the study design, field sampling and analytical procedures, and the MODFLOW modeling approach. Drilling operations for core sample collection and installation of wells and piezometers are presented. Hydrologic data collection and analysis methods are discussed. Procedures for collecting and analyzing water quality samples are described. Finally, descriptions of the heuristic MODFLOW models are presented.

Field Study Design and Piezometer Installation

Piezometer "nests" were installed at each site to assess the vertical flux of water and transport of chemicals from land surface to the underlying confined aquifer system. A piezometer nest is a series of piezometers installed adjacent to one another and screened at separate short intervals below land surface. The nest design enables vertically discrete observations throughout the geologic profile from near land surface through the till into the confined aquifer. The nest design has been commonly used to investigate hydrologic properties of tills (for example, Simpkins and Parkin, 1993; Shaw and Hendry, 1998). Small diameter (1.25-in.) piezometers were installed in the confining units to reduce the volume of water required for observable water-level fluctuations in geologic materials with low *K*. Piezometers (or wells) with a 2-in. diameter were installed in the confined aquifers.

At the Litchfield and Cromwell sites, two nests were installed at each site, one of which was near a well field and one which was farther from a well field. After the initial installation, the two Cromwell nests (the CWO1 and CWO2 sites) were considered together as a single nest (CWO1/O2) and are mostly presented as such throughout this report. The near and far nest design was intended to facilitate aquifer test analyses. At the Olivia and HFC sites, only one piezometer nest was installed near a production well.

A total of 19 piezometers were installed in 2015 at the Litchfield and Cromwell sites for this study (table 1). The LFO1 site consisted of five piezometers and was about 1,500 ft from the nearest production well (figs. 1 and 2). The LFO2 site consisted of six piezometers, was within a well field, and was about 500 ft from the nearest production well (figs. 1 and 3). Five production wells are near the LFO1 and LFO2 sites (fig. 1). The CWO1 site consisted of three piezometers and was about 150 ft from the nearest production well (figs. 1 and 4). The CWO2 site consisted of five piezometers and was about 50 ft from the nearest production well (figs. 1 and 4). Two production wells were near the CWO1 and CWO2 sites. The CWO1 and CWO2 sites were 160 ft apart from each other and had piezometers that were sequential in depth.

Table 1. Well and piezometer identification, vertical placement, and mean water-level information.

[USGS, U.S. Geological Survey; ID, identifier; ft, foot; NAVD 88, North American Vertical Datum of 1988; BLS, below land surface; MN040, agency code representing the Minnesota Geological Survey in the U.S. Geological Survey's National Water Information System database; --, not calculated; HFC, hydrogeology field camp near Akeley, Minnesota]

Well or piezometer short name	Field site	Agency code[a]	USGS site ID[a]	Minnesota unique well number	Installed during this study	Hydrostratigraphy of screened interval	Land surface elevation (ft above NAVD 88)[a]	Screened interval (ft BLS)	Mean hydraulic head (ft above NAVD 88)	Mean water level (ft BLS)
LFO1–B	Litchfield	USGS	450814094315001	773062	Yes	Surficial aquifer	1,115.22	22.4–25.06	1,104.02	11.20
LFO1–C	Litchfield	USGS	450814094315002	773060	Yes	Till	1,115.45	50.23–52.89	1,103.11	12.34
LFO1–D	Litchfield	USGS	450814094315003	773059	Yes	Till	1,115.34	72.4–75.06	1,089.99	25.35
LFO1–E	Litchfield	USGS	450814094315004	773058	Yes	Till	1,115.15	92.41–95.07	1,079.56	35.59
LFO1–F	Litchfield	USGS	450814094315006	773057	Yes	Confined aquifer	1,115.19	117.5–127.12	1,079.49	35.70
LFO2–A	Litchfield	USGS	450832094321201	773056	Yes	Till	1,139.45	17.12–19.78	1,128.15	11.30
LFO2–B	Litchfield	USGS	450832094321202	773055	Yes	Till	1,139.29	32.26–34.92	1,126.34	12.95
LFO2–C	Litchfield	USGS	450832094321203	773054	Yes	Till	1,139.72	56.97–59.63	1,123.58	16.14
LFO2–D	Litchfield	USGS	450832094321204	773053	Yes	Till	1,139.18	82.27–84.93	1,103.33	35.85
LFO2–E	Litchfield	USGS	450832094321205	773052	Yes	Till	1,139.64	110.95–113.61	1,078.18	61.46
LFO2–F	Litchfield	USGS	450832094321206	773051	Yes	Confined aquifer	1,139.47	149.56–159.18	1,077.34	62.13
LF–OB1	Litchfield	MN040	450821094320601	607417	No	Confined aquifer	1,123.14	122–127	--	--
LF–CM1	Litchfield	MN040	450837094321601	764258	No	Confined aquifer	1,145.14	136.5–161.5	--	--
LF–CM2	Litchfield	MN040	450820094320801	607420	No	Confined aquifer	1,123.23	107–132	--	--
LF–CM3	Litchfield	MN040	450828094320601	632077	No	Confined aquifer	1,121.20	108–136	--	--
LF–CM4	Litchfield	MN040	450851094321201	632078	No	Confined aquifer	1,142.83	123–147	--	--
CWO1–A	Cromwell	USGS	464110092531401	773071	Yes	Till	1,326.28	144.56–147.36	1,307.34	18.94
CWO1–B	Cromwell	USGS	464110092531402	773070	Yes	Confined aquifer	1,326.29	220.91–230.53	1,311.21	15.08
CWO1–C	Cromwell	USGS	464110092531403	773069	Yes	Bedrock aquifer	1,326.25	329.63–339.25	1,311.19	15.06
CWO2–A	Cromwell	USGS	464112092531401	773068	Yes	Surficial aquifer	1,332.28	32.3–34.96	1,304.61	27.67
CWO2–B	Cromwell	USGS	464112092531402	773067	Yes	till	1,332.59	56.75–59.41	1,305.68	26.91
CWO2–C	Cromwell	USGS	464112092531403	773066	Yes	Till	1,332.33	78.7–81.36	1,306.91	25.42
CWO2–D	Cromwell	USGS	464112092531404	773065	Yes	Till	1,332.13	103.58–106.24	1,309.69	22.44
CWO2–E	Cromwell	USGS	464112092531405	773064	Yes	Till	1,332.44	125.78–128.44	1,309.53	22.91
CW–CM3	Cromwell	MN040	464109092530701	519761	No	Confined aquifer	1,327	180–190	--	--
CW–CM4	Cromwell	MN040	464111092531401	593593	No	Confined aquifer	1,327.88	210–230	--	--
HT–115	HFC	USGS	465652094394801	773075	Yes	Till	1,452.00	112.35–114.83	1,391.44	60.56
HT–140	HFC	USGS	465652094394802	773076	Yes	Till	1,452.39	137.77–140.25	1,391.43	60.96
HT–175	HFC	USGS	465652094394803	773077	Yes	Till	1,452.04	172.47–174.95	1,389.03	63.01

Table 1. Well and piezometer identification, vertical placement, and mean water-level information.—Continued

[USGS, U.S. Geological Survey; ID, identifier; ft, foot; NAVD 88, North American Vertical Datum of 1988; BLS, below land surface; MN040, agency code representing the Minnesota Geological Survey in the U.S. Geological Survey's National Water Information System database; --, not calculated; HFC, hydrogeology field camp near Akeley, Minnesota]

Well or piezometer short name	Field site	Agency code[a]	USGS site ID[a]	Minnesota unique well number	Installed during this study	Hydrostratigraphy of screened interval	Land surface elevation (ft above NAVD 88)[a]	Screened interval (ft BLS)	Mean hydraulic head (ft above NAVD 88)	Mean water level (ft BLS)
HT–200	HFC	USGS	465652094394804	773078	Yes	Till	1,452.04	195.22–197.7	1,387.59	64.45
HB–1	HFC	MN040	465653094394701	809697	No	Confined aquifer	1,451.98	210–230	--	--
HB–2	HFC	MN040	465651094394001	819726	No	Confined aquifer	1,454.83	214–224	--	--
HB–3	HFC	MN040	465652094394701	825587	Yes	Confined aquifer	1,453.03	213.33–223.53	1,387.18	65.85
MW–01	HFC	MN040	465652094394501	569489	No	Surficial aquifer	1,453.54	80–85	1,391.63	61.91
WL07	HFC	MN040	465711094392601	243680	No	Surficial aquifer	1,502.20	126.3–128.3	--	--
WL12	HFC	MN040	465712094404201	243843	No	Confined aquifer	1,467.42	340–344	--	--
WL299	HFC	MN040	465725094403207	243849	No	Confined aquifer	1,400.46	--	--	--
OT–13	Olivia	USGS	444630095002202	773086	Yes	Surficial aquifer	1,070.51	7.89–13.03	1,063.90	6.61
OT–20	Olivia	USGS	444630095002203	773085	Yes	Till	1,070.75	17.44–19.91	1,063.99	6.76
OT–35	Olivia	USGS	444630095002204	773084	Yes	Till	1,070.60	32.08–34.55	1,063.92	6.68[b]
OT–60	Olivia	USGS	444630095002205	773083	Yes	Till	1,070.67	56.74–59.77	1,063.27	7.40
OT–105	Olivia	USGS	444630095002206	773082	Yes	Till	1,071.61	101.95–104.94	1,056.45	15.16
OT–145	Olivia	USGS	444630095002207	773081	Yes	Till	1,071.44	141.15–144.13	1,052.90	18.54
OT–175	Olivia	USGS	444630095002208	773080	Yes	Till	1,071.46	172.26–175.26	1,045.09	26.37
OB–7	Olivia	USGS	444630095002209	773079	Yes	Confined aquifer	1,071.39	204.92–209.71	969.02	102.37
Olivia-4	Olivia	USGS	444630095002201	228797	No	Confined aquifer	1,071.00	204–228	--	--
Olivia-5	Olivia	USGS	444639095002201	228796	No	Confined aquifer	1,075.01	196–218	--	--
Olivia-6	Olivia	MN040	444637095013701	241525	No	Confined aquifer	1,087.00	333–343	--	--

[a]Data can be accessed from the USGS National Water Information System database (U.S. Geological Survey, 2019) using the USGS site ID.

[b]This water level is not a mean; it is the final water-level reading. The water level in this well took the study period to recover from being drawn down for well development, and therefore, the final water level best represented an approximate “static” water level.

A total of 13 piezometers and wells were installed in 2017 at the Olivia and HFC sites for this study (table 1). At the Olivia site, eight piezometers were installed about 60 ft from the nearest production well (figs. 1 and 6; table 1). Two other production wells were near the site, one about 1,000 ft from the piezometer nest and the other about 4,000 ft from the piezometer nest. At the HFC site, four piezometers were installed in the till about 20 ft from the nearest production well and one well was installed in the confined aquifer about 50 ft from the nearest production well (figs. 1 and 5). The HFC site also included several wells previously installed by the University of Minnesota, including two in the surficial aquifer and five in the confined aquifer (table 1).

Drilling operations for sediment core collection and piezometer installation varied across the four sites. The following is a general description, and detailed drilling and piezometer construction information is provided in appendix table 1.1. A hollow-stem auger rig was used for sediment core collection and installation at the LFO1, LFO2, and CWO2 sites. Hollow-stem methods are commonly used for till investigations because sediment core samples can be collected during drilling, and drilling fluids, which could contaminant the till formation, are not required (Simpkins and Bradbury, 1992; Shaw and Hendry, 1998). Sediment core samples were collected into acetate liners with a cutter head and split core barrel assembly. Rocks in the till impeded the installation of piezometers at the CWO1 site, so a direct mud rotary rig was used to install the three piezometers (CWO1–A, CWO1–B, and CWO1–C). Sample cuttings were collected from the drilling mud at the CWO1 site (Witt, 2017).

Rotary-sonic drilling methods were used for core collection and piezometer installations at the Olivia and HFC sites. Rotary-sonic drilling methods enabled continuous core collection and eliminated problems caused by cobbles and boulders in the till but did require water and drilling fluids. At the Olivia site, untreated water from the municipal supply system was used during drilling operations, and at the HFC site, water from the surficial aquifer was used during drilling operations. At each of the Olivia and HFC sites, one continuous sediment core profile extending from land surface to the confined aquifer was collected. Core samples were extruded from the core barrel directly into plastic sleeves (Staley and others, 2018). All installed piezometers were developed with an inertial pump to establish a good connection between the well screen and the surrounding geologic material.

At all sites, the piezometer screened intervals were determined with consideration of the site geology, the vertical distribution of sample points, and the driller's confidence in successful piezometer completion. Lithologic changes and oxidation state were documented from the sediment core samples collected during drilling operations. Piezometer screens were generally placed directly above lithologic boundaries, as recommended by Hart and others (2008). Lithological changes selected for piezometer screen placement were spaced somewhat uniformly within the till units. In some cases, the screened interval was determined by where the drillers were confident that a piezometer completion would be successful.

Hydrology

Several techniques were used to assess the hydrologic properties and leakage through till confining units at the four study sites: continuous and discrete water-level monitoring, slug tests, aquifer tests, and calculations according to Darcy's law to estimate recharge rates and travel times. Different techniques were used to evaluate the scale dependency of hydrologic measurements. Previous studies have demonstrated that K values increase with measurement scale; for example, laboratory measurements of K in till are significantly lower than field measurements of the same materials (Grisak and Cherry, 1975; Grisak and others, 1976; Bradbury and Muldoon, 1990).

Continuous and discrete monitoring of water-level responses to pumping and precipitation events can be used to qualitatively assess hydraulic connectivity between aquifers and till confining units (as was done for this study), but they can also be used to quantitatively estimate the vertical hydraulic conductivity (K_v) of till confining units (Cherry and others, 2004). Previous studies have used hydraulic head variations in confined aquifers and confining units induced by pumping over long periods (years to decades) as evidence for extremely low confining unit K_v values (for example, Husain and others, 1998). Other studies have monitored hydraulic head in surficial aquifers and confining unit material to determine confining unit K_v values (for example, Keller and others, 1989).

Laboratory tests and slug tests are commonly used to assess the hydraulic properties of till confining units, although these tests represent smaller volumes of till than aquifer tests. Vertical fractures or stratigraphic windows (zones of higher K through low-K material) can be important transport features through till, but the results of laboratory measurements on core samples rarely reflect these features (Cherry and others, 2004). Slug tests, in combination with sediment core samples, can indicate the presence and nature of important transport features, such as fractures or high-permeability zones, in till confining units if the slug tests happen to intersect those features (Cherry and others, 2004). Beyond potential identification of important transport features, slug tests have limited usefulness for determining the K_v of the till matrix because, in vertical holes, the slug response primarily depends on the horizontal component of the hydraulic conductivity (K_h). However, slug tests can indicate the presence of permeable zones, providing valuable insight concerning the internal nature of the confining unit (Cherry and others, 2004).

Aquifer tests designed with the specific purpose of determining till confining unit properties are another, larger scale approach to estimating the K_v of tills. Aquifer tests measure a much larger volume of till than slug tests and are more likely to capture the effects of features most important for transport through till (Cherry and others, 2004). The piezometers

installed as part of this study were used during an aquifer test at each site to measure hydraulic-head responses within the till confining unit and the pumped aquifer (Cherry and others, 2004). Several analytical methods, such as Neuman and Witherspoon (1972), can be used to determine confining unit properties from properly executed aquifer tests.

Water-Level and Precipitation Monitoring

Water levels in the piezometers and production wells were measured at discrete intervals by hand and logged every 15 minutes with pressure transducers in a subset of piezometers. These data were collected to determine how water levels and hydraulic gradients vary through time in surficial aquifers, till confining units, and confined aquifers. Manual water-level measurements were made in piezometers and wells using a Solinst or Keck electric tape or a Lufkin steel tape between July 2015 and April 2017 for the Litchfield and Cromwell sites and intermittently for the Olivia and HFC sites between October 2017 and October 2018. Submersible pressure transducers (OTT Orpheus Mini) recorded water-level and temperature data in 12 piezometers at the Litchfield and Cromwell sites between December 2015 and April 2017 (appendix table 1.1). OTT Orpheus Mini submersible pressure transducers also recorded water-level and temperature data in 14 piezometers and wells at the Olivia and HFC sites between October 2017 and October 2018 (appendix table 1.1).

Precipitation was also monitored continuously (every 15 minutes) with HOBO RG3 tipping bucket rain gages at the LFO2 site and the Cromwell site between December 2015 and April 2017, at the Olivia site between August 2017 and October 2018, and at the HFC site between June 2017 and October 2018.

All discrete and continuous water-level and precipitation data collected throughout this study were reviewed and approved according to USGS technical policies, which are available at https://water.usgs.gov/admin/memo/GW. The data can be retrieved from https://doi.org/10.5066/F7P55KJN by searching for the USGS site identifiers (USGS site ID column) listed in table 1. An R script for downloading these data is provided in the data release accompanying this report (Maher and others, 2020).

Mean water levels were calculated for each piezometer and then used to compute the mean hydraulic gradients for each piezometer nest. Water-level measurements were included in the calculation of the mean only when measurements were made at all piezometers in a nest within a short period. Discrete water-level measurements were used at the Litchfield and Cromwell sites because not all piezometers had continuous water-level data. A total of 16 synoptic water-level measurement runs between September 26, 2015, and April 24, 2017, were used to compute the mean water levels for the piezometers in the LFO1 and LFO2 nests. A total of 13 synoptic water-level measurement runs between August 12, 2015, and April 25, 2017, were used to compute the mean water levels for the piezometers in the CWO1/O2 nest. A "synoptic water-level measurement run" is when water levels in all piezometers at a given nest were measured within a 36-hour period. Continuous water-level data from transducers (recorded every 15 minutes or every hour) were used for calculating the mean water level for each piezometer in the Olivia and HFC nests (except OT–35, which was excluded from hydraulic gradient calculations). The period during which continuous water-level data were recorded in all piezometers in the Olivia nest is December 12, 2017, to October 10, 2018. The periods during which continuous water-level data were recorded in all piezometers in the HFC nest are September 11, 2017, to July 18, 2018, and August 26 to October 11, 2018.

Slug Tests

Rising-head and falling-head slug tests were completed in each piezometer to estimate *K*. Generally, three rising-head and three falling-head slug tests were completed for each piezometer, though some piezometers had fewer tests completed because of field conditions or slow recoveries. For each rising- or falling-head slug test, a solid polyvinyl chloride slug was rapidly added (falling-head test) or removed (rising-head test) from the piezometer and water-level measurements were recorded either manually or with a submersible pressure transducer. A Druck PDCR 1800 transducer and Campbell Scientific CR10X datalogger were used to record water levels at most piezometers, except a few piezometers at the Litchfield and Cromwell sites, which had only manual water-level measurements made with an electric tape. The manual measurements provided sufficient data quality in these piezometers because these piezometers are screened in units with *K* values less than 32 ft/d (Butler and others, 1996).

Slug test results were analyzed with the AQTESOLV program (version 4.5; Duffield, 2007) using the most appropriate methods, which included the Kansas Geological Survey (KGS) method for unconfined or confined settings (Hyder and others, 1994), the Butler method (Butler, 1998), and the Springer-Gelhar method (Springer and Gelhar, 1991). Analytical methods for each slug test were selected based on the hydrostratigraphic placement of the piezometers (unconfined versus confined), piezometer construction (all piezometers are partially penetrating), and the water-level response to the slug (nonoscillatory versus oscillatory). A discussion of method selection for slug test analyses is provided in appendix 2, and an example of an AQTESOLV analysis done for OT–20 at the Olivia site is shown in figure 8. The accompanying data release (Maher and others, 2020) contains all of the slug test water-level data and AQTESOLV analyses done for this study.

Data inputs of the AQTESOLV analyses are detailed in appendix tables 2.1 and 2.2. Field observations recorded during the slug tests, including static water levels, the volume of the slug used, the initial water-level displacement when the slug was added or removed from the piezometer, and the theoretical displacement volume of the slug, are listed in

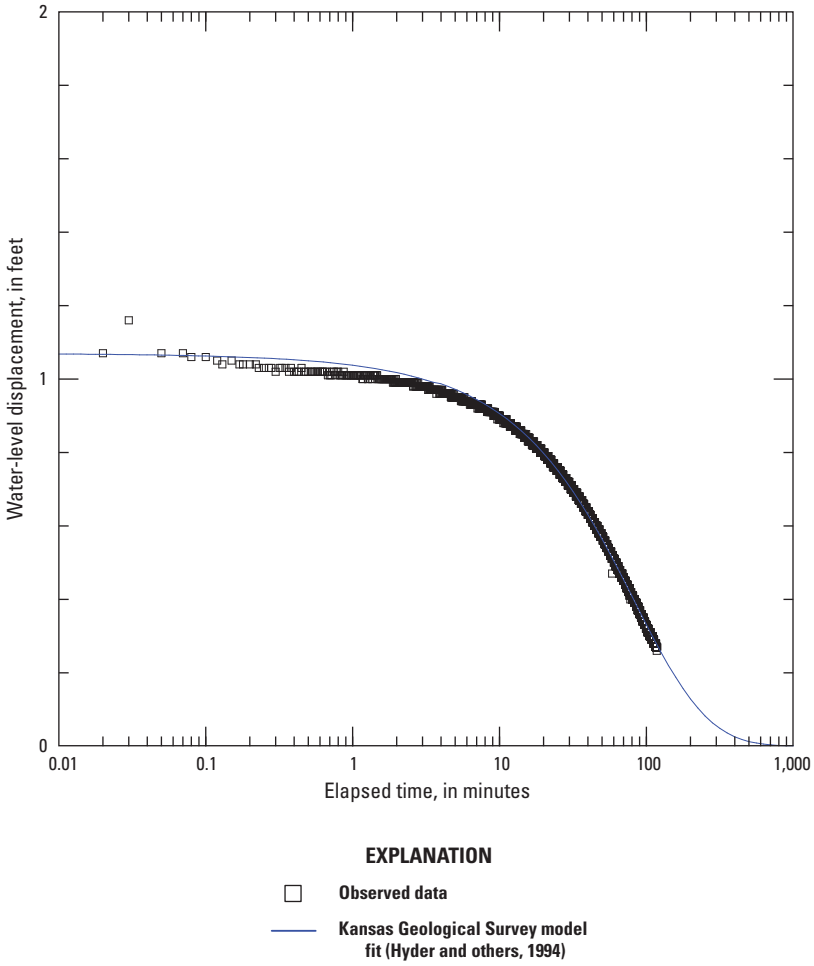

Figure 8. Example graphical slug test analysis output from AQTESOLV for piezometer OT–20. The plot shows observed water-level displacement versus elapsed time and the Kansas Geological Survey model fit to those data.

table 2.1. The theoretical displacement volume of a slug is the possible volume of water that can be displaced in a piezometer/well, calculated based on diameter and length of the slug, and the diameter of the piezometer/well (Cunningham and Schalk, 2011). The AQTESOLV parameters, information on water levels and aquifer properties, as well as piezometer construction, that were entered into the AQTESOLV program are detailed in table 2.2.

Aquifer Tests

The vertical arrangement of well screens near high-capacity production wells provided an opportunity to evaluate the K_v of tills from aquifer test data. Constant-rate pumping aquifer tests were completed at all sites to estimate the hydraulic properties of the aquifers and overlying till confining units at the Litchfield, Cromwell, Olivia, and HFC sites (table 2). An aquifer test was completed at the Cromwell site on May 24, 2017, and at the Litchfield site on June 29, 2017. An aquifer test was completed at the Olivia site from July 10 to July 13, 2018. Two aquifer tests were completed at the HFC site, but only the second test was valid. This second test was completed between July 18 and July 22, 2018. Water levels during the aquifer tests were measured with pressure transducers (OTT Orpheus Mini or Solinst) recording data at 1-minute intervals. Staff from the Minnesota Department of Health led the aquifer test planning and data analysis.

Several approaches were used to analyze the aquifer test data, many of which are available in AQTESOLV (table 2). Only the methods used to determine a representative bulk K_v for each aquifer test are listed in table 2; many more methods of analysis and more complete documentation are described in the detailed reports (Blum and Woodside, 2017; Lund and Blum, 2017; Blum, 2019a, b; Blum, 2020). Most of the methods used to determine the representative bulk K_v were "leaky confined aquifer" type tests including Neuman-Witherspoon (Neuman and Witherspoon, 1969), Hantush-Jacob (Hantush and Jacob, 1955), and Moench (1985).

Table 2. Summary of constant-rate aquifer tests and analytical approaches used to determine representative till vertical hydraulic conductivities (Blum and Woodside, 2017; Lund and Blum, 2017; Blum, 2019a, b).

[min, minute; gal, gallon; gal/min, gallon per minute; K_v, vertical hydraulic conductivity; --, unknown]

Site	Aquifer test name(s)	Minnesota unique number of pumped well(s)	Date/time pumping start	Date/time recovery start	Pumping duration (min)	Total discharge (gal)	Rate (gal/min)	Analytical method to determine representative till K_v	AQTESOLV or manual analysis
Cromwell	CW–CM4	593593	5/24/2017 12:10	5/25/2017 12:25	1,454.90	242,350	167	Neuman-Witherspoon (Neuman and Witherspoon, 1969)	AQTESOLV
Litchfield	Litchfield nest 1, composite	--	7/5/2017 19:00	7/10/2017 10:55	6,715	15,444,500	2,300	Neuman-Witherspoon (Neuman and Witherspoon, 1969)	AQTESOLV
Hydrogeology field camp (HFC)	HB–1	809697	7/20/2018 10:44	7/22/2018 12:02	2,958.15	Not reported	75	Hantush-Jacob (Hantush and Jacob, 1955)	AQTESOLV
Olivia	Olivia composite (Olivia-4 and Olivia-5)	228797 and 228796	7/11/2018 7:54	7/12/2018 17:46	1,210	Not reported	232–227	Moench (1985) case 1	AQTESOLV
Olivia	Olivia-4 and Olivia-5 time-delay analysis	228797 and 228796	7/11/2018 7:54	7/12/2018 17:46	1,210	Not reported	232–227	Wang (2001)	Manual

The Olivia site was a special case because there were no detectable vertical hydraulic (drawdown) responses observed in any till piezometers; only reverse water-level fluctuations (RWFs) were observed. This means that application of traditional "leaky confined aquifer" approaches that rely on drawdown responses for determining aquifer and confining unit properties is questionable. Blum (2020) applied a second type of test, a time-delay analysis based on Wang (2001), to the data from the Olivia site. The basic idea of the time-delay analysis is that the delay in time of the pressure wave reaching a point in the confining unit from the base of the confining unit is related to the hydraulic diffusivity of the confining unit. The hydraulic diffusivity can then be used to calculate the K_v of the confining unit if the specific storage of the confining unit is known or estimated (Wang, 2001; Blum, 2020); therefore, two representative bulk K_v values were determined for the Olivia site using different conceptual models, each with their own limitations. A more complete discussion of the time-delay analysis is available in Blum (2020).

Calculations of Groundwater Flow through Till According to Darcy's Law

Calculations based on Darcy's law were used to estimate travel times and leakage through till confining units into the confined aquifer (Simpkins and Bradbury, 1992; Hendry and Wassenaar, 1999; Witt, 2017; Maher, 2020). The following equations were used to compute discharge and travel time through till confining units. According to Darcy's law, discharge, Q, is calculated as follows:

$$Q = -KiA, \tag{1}$$

and the specific discharge (q) is calculated by dividing the discharge by the cross-sectional area:

$$\frac{Q}{A} = q = -Ki, \tag{2}$$

and a mean linear velocity (V_z) is calculated by dividing the specific discharge by the effective porosity of the till:

$$V_z = \frac{q}{n_e}, \tag{3}$$

and finally, a travel time through till (T) is calculated by dividing the till thickness by the mean linear velocity:

$$T = \frac{L}{V_z}, \tag{4}$$

where

Q is discharge (synonyms in this report include leakage through till and recharge to confined aquifer) (length cubed per unit time);
K is hydraulic conductivity (length per unit time);
i is the hydraulic gradient (length/length);
A is the cross-sectional area of flow (length × length);
q is specific discharge (length per unit time);
V_z is the mean linear velocity (length per unit time);
n_e is effective porosity (unitless);
T is travel time (time); and
L is the thickness of the till confining unit (length).

For all sites, an effective porosity of 0.25 was used for travel time calculations, which is within the range of values used in calculations for fluxes of groundwater or solutes through till (McKay and others, 1993). Because of large uncertainties in the sizes of the confined aquifers at each site, the calculations were done using a cross-sectional area (A) of 1 square mile (mi^2). The hydraulic gradient used in the calculation was the mean hydraulic gradient at each piezometer nest, determined by taking the mean of the hydraulic gradients among all till piezometers at a given site. The till thickness (L) was determined from cores at each well nest. Two calculations of travel time, specific discharge, and discharge were done for each piezometer nest: the first calculation was done using the geometric mean of all K_h values from slug tests, and the second calculation was done using the representative K_v value determined from each site's aquifer test. For the calculations done using the geometric mean K_h, isotropy between K_h and K_v was assumed.

Groundwater Geochemistry

Groundwater samples and pore-water samples were collected to evaluate the vertical distribution of anthropogenic chemicals, groundwater ages, and oxidation-reduction (redox) conditions from land surface through till confining units to the underlying confined aquifer. All groundwater sampling procedures and methods were completed according to the USGS "National Field Manual for the Collection of Water-Quality Data" (U.S. Geological Survey, variously dated).

Groundwater samples for laboratory analyses were collected after three well volumes were purged and water-quality field properties (dissolved oxygen [DO], pH, specific conductance, and temperature) were stable. Water quality properties were measured during the purging process with a YSI 6820 multiparameter sonde. Samples for stable isotopes of oxygen and hydrogen ($\delta^{18}O$ and $\delta^{2}H$, respectively) and tritium analyses were collected raw, without filtration. Samples collected for cation analysis were filtered through a 0.45-micron filter into a polyethylene bottle, acidified to a pH less than 2 with nitric acid, and chilled on ice until analysis. Samples for anion analysis and alkalinity were filtered through a 0.45-micron filter into a polyethylene bottle and chilled on ice

until analysis. Samples for nutrients (ammonia, nitrite, nitrate, and phosphorus) were filtered through a 0.45-micron filter into a brown polyethylene bottle and chilled on ice until analysis. Alkalinity (in milligrams per liter as calcium carbonate) was determined on filtered samples within 24 hours of sample collection using a Hach Digital Titrator and the inflection-point method. Listed in table 3 are the analyses completed on groundwater samples.

Pore-water samples were extracted from till core samples to evaluate differences in water chemistry between hydraulically conductive flow paths (groundwater) and water bound within the till matrix (pore water). Pore water was extracted from 6-in.-long subsamples of core sections extracted from boreholes during drilling operations. These subsamples were collected at or near the screened interval of a piezometer and prepared for storage and analysis in a similar manner to Gerber and Howard (1996). Core subsamples were scraped clean on the outside to remove potential contamination from drilling equipment or fluid. The subsamples were then wrapped in at least two layers of plastic wrap, taped, wrapped in at least two layers of aluminum foil, taped again, labeled, and then bagged. The core subsamples were then sent to the San Diego Geochemistry Laboratory at the USGS California Water Science Center where a hydraulic press was used to extract pore fluid. Pressures between 8,000 and 9,500 pounds per square inch were used to extract the pore fluid. Listed in table 3 are the analyses completed on pore-water (interstitial water) samples.

The following are brief descriptions of analytical methods used to determine concentrations of analytes in groundwater and pore-water samples. Ammonia concentrations measured in samples at the USGS National Water Quality Laboratory (NWQL) were determined with a salicylate-hypochlorite colorimetry method (Fishman, 1993). Dissolved phosphorus concentrations measured in samples at the USGS NWQL were determined by colorimetry according to U.S. Environmental Protection Agency method 365.1 (Odell, 1993). Anion concentrations measured in samples at either the University of Minnesota Geochemistry Laboratory or the Ion Chrom Analytical Laboratory were determined by anion chromatography using a Dionex ICS 5000 with an AS19 4-micron (2-x 250-millimeter) column (Maher and others, 2020). At the USGS NWQL, anion concentrations were determined by ion chromatography, and cation concentrations were determined by inductively coupled plasma atomic emission spectroscopy (Fishman and Friedman, 1989; Fishman, 1993; American Public Health Association and others, 1998). Nitrate plus nitrite concentrations measured in samples at the USGS NWQL were determined with an enzyme reduction-diazotization colorimetry method (Patton and Kryskalla, 2011), and nitrite concentrations were determined by colorimetry (Fishman, 1993). Stable isotope analyses were done at the Iowa State Stable Isotope Laboratory on a Picarro L2130–i Isotopic Liquid Water Analyzer with autosampler and ChemCorrect software. Reference standards for isotopic corrections varied between runs and are identified in the accompanying data release (Maher and others, 2020). Tritium concentrations in samples at the University of Waterloo Environmental Isotope Laboratory were determined by electrolytic enrichment and an LKB Wallace 1220 Quantulus counter (Maher and others, 2020).

All geochemical data from non-USGS laboratories are provided in a data release accompanying this report, along with an R script to retrieve geochemistry data from the USGS National Water Information System (NWIS; Maher and others, 2020). Alternatively, USGS NWIS water-quality data are available at https://doi.org/10.5066/F7P55KJN and can be retrieved using the USGS site identifiers listed in table 1.

Quality assurance samples were collected during the field study, including field replicates, field blanks, and split samples sent to separate laboratories. A summary of quality assurance at USGS laboratories and comparisons between USGS and non-USGS laboratories is provided in appendix 3. A summary of the quality assurance information from non-USGS laboratories is included in the metadata of the data release accompanying this report (Maher and others, 2020).

Groundwater Modeling

Assessing the sustainability of groundwater withdrawals from buried confined aquifers in glacial sediments is challenging because their hydrogeologic settings at locally relevant scales are highly uncertain. The field investigations at the Litchfield site, in particular, established that the hydrologic properties of till overlying confined aquifers can be highly variable over short distances. Furthermore, the extent of confined aquifers and their connections to other buried and possibly confined aquifer systems are not well understood because of the complex glacial geologic history of Minnesota. The MGS has mapped buried aquifers (sand bodies that may or may not be confined) using the best available data (well logs from well installations) through the County Geologic Atlas Program; however, there are still large uncertainties about the connectivity and extent of buried aquifer systems. The field studies presented in this report could not address questions about water movement with and without pumping because the sites were near production wells that consistently pumped groundwater. To better understand how till properties, aquifer properties, and pumping affect fluxes of water through till, a series of heuristic steady-state groundwater-flow models was developed (table 4). The heuristic models do not represent the actual physical locations that were sampled in this study and thus the models are not “calibrated.” Rather, the models utilize a generalized structure in which a subset of system properties was varied in order to evaluate how hydrogeologic setting and groundwater pumping affect fluxes of water through till into confined aquifers. The software package, Groundwater Vistas (Environmental Simulations Incorporated), was used to develop MODFLOW-2005 (Harbaugh, 2005) models for this analysis. The specific goal of the modeling effort was to evaluate the variability in water fluxes into and through till

Table 3. Summary of water-quality sampling events, analytes, and analytical laboratories used for water sample analysis.

[USGS, U.S. Geological Survey; WG, groundwater sample; WI, interstitial (pore) water; --, no samples collected]

Laboratory	Analytes	Well nest				
		Litchfield 1 (LFO1)	Litchfield 2 (LFO2)	Cromwell (CWO1/O2)	Hydrogeology field camp (HFC)	Olivia[a]
		Sample medium and month of sampling event				
USGS field staff	Alkalinity, water-quality field properties: specific conductance, dissolved oxygen, temperature, pH	WG: July 2015 WG: May 2016	WG: July 2015 WG: May 2016	WG: July 2015 WG: May 2016	WG: Sept.–Oct. 2017	WG: Sept.–Oct. 2017
Rick Knurr (University of Minnesota and Ion Chrom Analytical Laboratory)	Major anions: bromide (Br), chloride (Cl), acetate (CH_3CO_2), fluoride (F), sulfate (SO_4), thiosulfate (S_2O_3); nutrients: nitrite (NO_2), nitrate (NO_3), phosphate (PO_4)	WI: June 2015 WG: July 2015 WG: May 2016	WI: June 2015 WG: July 2015 WG: May 2016	WG: July 2015 WI: July 2015 WG: May 2016	WI: May 2017	WI: Aug. 2017 WG: Sept.–Oct. 2017
USGS National Water Quality Laboratory	Major anions: Br, Cl, F, SO_4; major cations: potassium (K), calcium (Ca), magnesium (Mg), manganese (Mn), sulfur (S), iron (Fe), sodium (Na); nutrients: ammonia (NH_3), total phosphorus (P), NO_2, NO_3	--	WG: May 2016	WG: May 2016	WG: Sept.–Oct. 2017	WG: Sept.–Oct. 2017
Iowa State University Stable Isotope Laboratory	Stable isotopes: oxygen-18 ($\delta^{18}O$) and hydrogen-2 ($\delta^{2}H$)	WI: June 2015 WG: July 2015 WG: May 2016	WI: June 2015 WG: July 2015 WG: May 2016	WG: July 2015 WI: July 2015 WG: May 2016	WI: May 2017 WG: Sept.–Oct. 2017	WI: Aug. 2017 WG: Sept.–Oct. 2017
University of Waterloo, Ontario, Canada, Environmental Isotope Laboratory	Enriched tritium (^{3}H)	WG: May 2016	WG: May 2016	WG: May 2016	WG: Sept.–Oct. 2017	WG: Sept.–Oct. 2017
San Diego Geochemistry Laboratory (USGS California Water Science Center)	Pore-water extraction from cores, specific conductance, pH	WI: June 2015	WI: June 2015	WI: July 2015	WI: May 2017	WI: Aug. 2017

[a]Piezometer OT–35 was never sampled at this nest.

Table 4. Model parameter values used in the heuristic groundwater model scenarios and the naming scheme used for each model run.

[K_v, vertical hydraulic conductivity; K_h, horizontal hydraulic conductivity]

Model parameter value	Unit	Low parameter value	Base model parameter value (Naming convention)	High parameter value	Source(s) that informed model property values
Permutation model run					
K_v of upper till and lower unit	Feet per day	0.001 (Lv)	0.05 (Mv)	2 (Hv)	[a, b]
Lateral connectivity of buried aquifer to adjacent till and aquifers (K_h of middle unit)	Feet per day	0.05 (Lc)	5 (Mc)	30 (Hc)	[a, b, c]
Buried sand body (aquifer) size	Mile × mile	1.0×0.5 (Ls)	3.0×1.5 (Ms)	5.0×2.5 (Hs)	[c]
Variation model run					
Buried sand body (aquifer) K_h	Feet per day	30 (BSkh_L)	100 (MsMvMc)	400 (BSkh_H)	[a, b]
Thickness of upper till	Feet	40 (UTtk_L)	80 (MsMvMc)	160 (UTtk_H)	[d, e]
Total pumping rate	Gallons per minute	300 (TOTq_L)	900 (MsMvMc)	2,250 (TOTq_H)	[f]
Screen length and penetration of production wells	Screen length and location in aquifer	40-foot screen in lower aquifer layer (Ppen_L)	80-foot screen across both aquifer layers (full penetration) (MsMvMc)	40-foot screen in upper aquifer layer (Ppen_H)	[g]
K_h of surficial unit; K_v of surficial unit	Feet per day; feet per day	5.0; 0.5 (SURF_L)	70; 7.0 (MsMvMc)	400; 40 (SURF_H)	[a, b, e]
Recharge rate	Inches per year	2 (SURF_L)	4 (MsMvMc)	8 (SURF_H)	[h]
Thickness of surficial unit	Feet	80 (SURF_L)	40 (MsMvMc)	40 (SURF_H)	[a, b, e]
Transmissivity of buried sand body (aquifer) and K_h used to determine transmissivity	Feet squared per day; feet per day	4,400; K_h=55.5 (CRtrlk)	8,000; K_h=100 (MsMvMc)	8,990; K_h=112.4 (LFtrlk)	[a, b, e]
Low and high parameter values are calculated from the leakance of upper till as observed in Litchfield and Cromwell aquifer tests (expressed as vertical hydraulic conductivity)	Feet per day	0.6769 (CRtrlk)	0.05 (MsMvMc)	0.0016 (LFtrlk)	[a, b]

[a]Lund and Blum, 2017.

[b]Blum and Woodside, 2017.

[c]Meyer, 2015.

[d]Wagner and Tipping, 2016.

[e]Witt, 2017.

[f]Minnesota Department of Natural Resources, 2017.

[g]Minnesota Department of Health, 2017.

[h]Smith and Westenbroek, 2015.

to confined aquifers that are being pumped across the range of hydrogeologic settings observed at the field sites. All of the models and output data are available through the model archive (Trost and others, 2020).

The basic structure of the heuristic model domain was about 20 mi by 20 mi with a cell size of 500 ft by 500 ft (shown in fig. 9). The model contained seven layers: a surficial unit that contained several rivers and lakes, three layers of "upper" till that represented the confining unit, two layers that contained the buried sand aquifer and a "middle" unit, and a layer of "lower" till. Under nonpumping conditions, the hydraulic head in the buried sand aquifer indicated a confined aquifer; however, the persistence of confined conditions throughout all model runs was not tracked, so the sand unit is referred to as a "buried sand unit" or "buried aquifer" to encompass the possibility of confined or unconfined conditions for all model runs. For most models runs, the surficial unit (layer 1) was 40 ft thick, the till unit was 80 ft thick (layers 2–4), the buried sand unit and surrounding middle unit (layers 5–6) were 80 ft thick, and the lower till unit was 200 ft thick (layer 7, fig. 9). Differences in layer thicknesses for specific model runs are listed in table 4. The buried aquifer was in the middle of the model domain to minimize the potential for boundary conditions to directly affect water fluxes in the aquifer. Three hypothetical production wells were screened in the buried sand aquifer. The north and south model boundaries were specified head boundaries, and the east and west model boundaries were no-flow boundaries. A regional north-to-south horizontal hydraulic gradient of 0.001 was specified. A vertical downward hydraulic gradient of 0.15 was assigned to model boundary cells. A constant recharge rate of 4 inches per year (in/yr) was applied at the surface of the model for all but two model runs, which is the statewide mean from Smith and Westenbroek (2015). Lakes and streams were generally simulated as groundwater discharge features with head-dependent flux boundaries using the MODFLOW RIV and DRN packages, respectively (Harbaugh and others, 2000). Lakes and streams were assigned bed conductances of 1 ft/d and 5 ft/d, respectively. All model input files, output files, and executables are available through a model archive (Trost and others, 2020).

Several model parameters, including the K_v and K_h of till and aquifer material, till thickness, buried aquifer size, pumping rate, and penetration of production wells, were varied in the model scenarios (table 4). The range of model parameter values chosen for evaluation were informed by the observations made at the field sites and other applicable studies and datasets. Also listed in table 4 is the naming convention for the model runs, which corresponds to figures and tables of model output later in the report.

Steady-state model runs beginning with Ls, Ms, or Hs compose a set of "permutation runs" in which ranges of parameters for specific parts of the model system were evaluated (table 4). The names of the permutation model runs are six-letter codes representing the relative values (H = high, M = middle, and L = low) of the three hydraulic properties varied among simulations. The high (H) and low (L) model parameter values are inclusive of Litchfield and Cromwell, typically slightly greater than or less than observations at these sites. The three hydraulic properties that varied were the maximum lateral dimensions of the buried sand unit in model layers 5 and 6 (naming convention = "s"), the upper till K_v in model layers 2–4 (naming convention = "v"), and the K_h in the middle unit in model layers 5 and 6 surrounding the buried sand unit (naming convention = "c"). In all permutation runs, the K_h of the upper till (layers 2–4) was fixed at 0.05 ft/d. The K_v of the middle unit (layers 5–6) was assigned the same value as the K_v of the till in layers 2–4. For example, from table 4, a model run titled LsMcHv means the buried sand unit in layers 5 and 6 was assigned the low size of 1.0 mi by 0.5 mi, the middle unit (layers 5 and 6) was assigned the "middle" K_h of 5 ft/d, and the till units (layers 2–4) were assigned the "high" K_v of 2 ft/d. The "base model" is labeled MsMvMc and contained model parameter values that represented an approximate midpoint among observations from the field study sites.

A set of "variation" steady-state model runs was also completed (table 4). In this set of model runs, six additional properties were evaluated through comparison to the base model, MsMvMc. Model run names ending in "_H" indicate the "high" parameter value, and names ending in "_L" indicate the low parameter value. These high and low values were also informed by field data collected as part of this study. The model runs titled CRtrlk and LFtrlk stand for "Cromwell transmissivity like" and "Litchfield transmissivity like." In these model runs, the transmissivity of the buried aquifer and the leakance of the upper till unit were assigned values determined from the Cromwell and Litchfield aquifer test results (Blum and Woodside, 2017; Lund and Blum, 2017).

Several response variables were extracted from the model output and compared among the model runs. To check for boundary effects on water fluxes, the change in flux from constant head cells on the north and south model boundaries was compared between ambient (pumping turned off) and stressed (pumping turned on) periods. The following response variables were compared: (1) the source of water to buried aquifer, (2) pumping-induced leakage of water from the surficial unit in layer 1 to the till in layer 2, and (3) the maximum drawdown in the surficial unit (layer 1) and the till unit (layer 3). The programs for extracting model output are provided in the model archive (Trost and others, 2020).

For the source of water to the buried aquifer, the relative contributions of water entering the buried aquifer from above, from the sides, and from below were compared among model runs. The leakage of water from the surficial unit in layer 1 to the till in layer 2 was quantified within a 5-mi by 5-mi "local area" (red outline in fig. 9) centered on the production wells and buried aquifer. The following equation was used to compute leakage as a percentage of total inputs into layer 1 within the 5-mi by 5-mi local area:

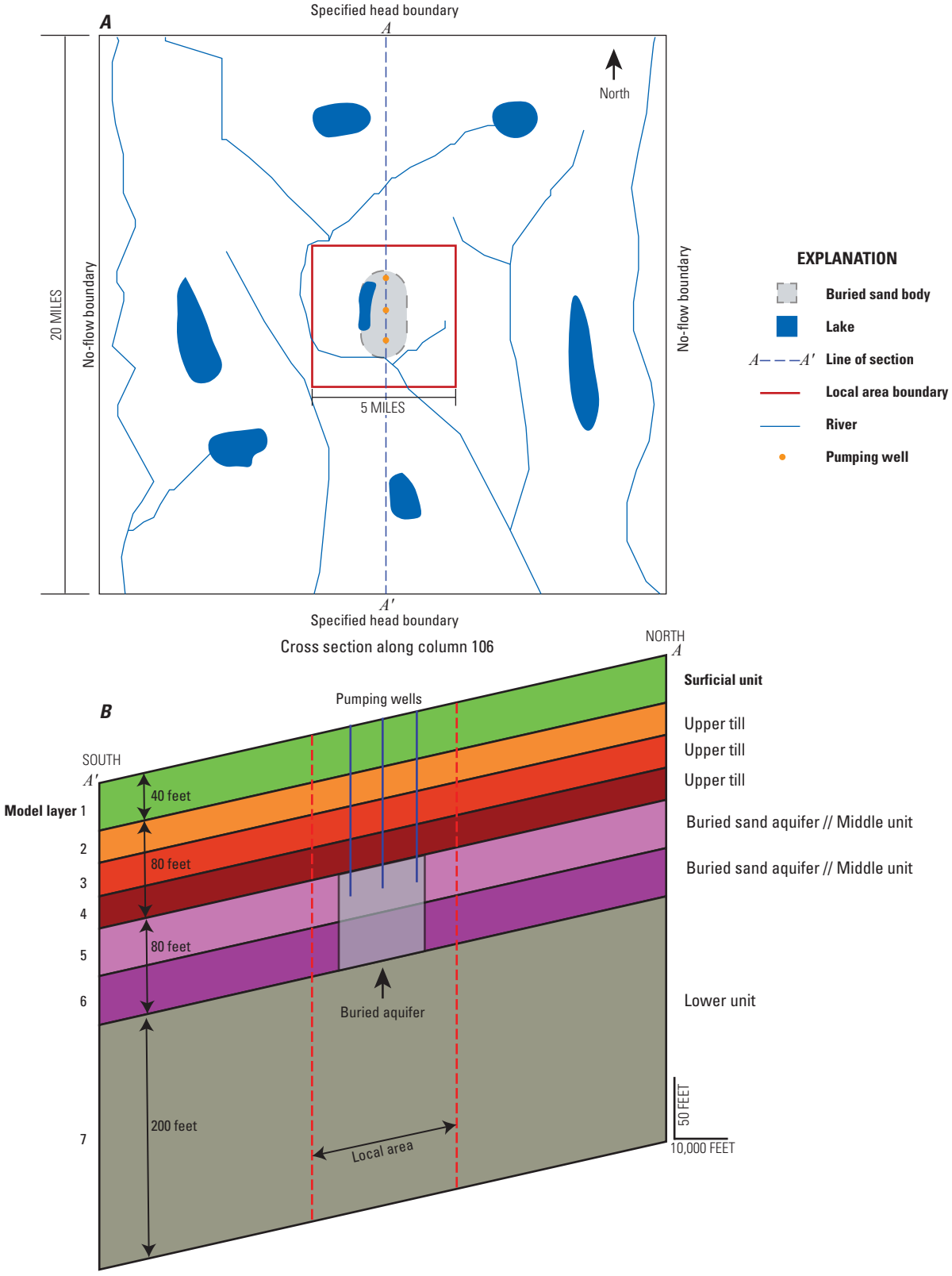

Figure 9. Heuristic MODFLOW model layout. *A*, top view; *B*, cross-sectional view.

$$L_{D,PCT} = \frac{V_D}{(V_R + V_L + V_I)} \times 100, \quad (5)$$

where

$L_{D,PCT}$ is the percentage of downward leakage from layer 1 to layer 2,

V_D is the volume of water flowing downward from layer 1 to layer 2,

V_R is the volume of groundwater recharge within the local area (water reaching the water table from precipitation and percolating through soil),

V_L is the volume of groundwater inputs entering the local area from the sides and below, and

V_I is the volume of induced flow from local streams into layer 1 within the local area (typically zero or very small).

The pumping-induced increase in leakage was then calculated as the difference between the percentage of downward leakage during ambient and stressed (pumped) periods. The recharge rate was 4 in/yr for all but two model runs (SURF_L, SURF_H, table 4), so increases in the percentage of downward leakage from ambient to stressed conditions indicated a pumping-induced reduction in lateral groundwater flow out of the local area and (or) a reduction in the contribution of groundwater discharge to lakes and streams within the local area (fig. 9).

Characterization of Glacial Till and Aquifer Systems

The following section presents the hydrogeological and geochemical findings along with sources of uncertainty associated with field methods. Evaluations of the MODFLOW heuristic models are also presented. The "Hydrogeology" subsection describes hydraulic properties of the till and confined aquifer units. The "Groundwater Geochemistry and Water Quality" subsection presents the results and interpretations of chemical analyses. The "Sources of Uncertainty" subsection describes important factors related to field procedures that may affect the conclusions of this study. The "Interpretive Groundwater Modeling" subsection describes variations in groundwater flux through till caused by pumping from buried aquifers in different hydrogeologic settings.

Hydrogeology

Several physical and hydrogeological properties of the till and confined aquifer units at each site are summarized in table 5. In the following sections, a qualitative evaluation of the vertical profiles of hydraulic-head responses to pumping and weather, a discussion of *K* distributions in till, and calculations of leakage (recharge) through till confining units are presented.

Hydraulic-Head Responses to Pumping and Weather

The piezometer nests at the Litchfield, Cromwell, and Olivia sites were installed near high-capacity production wells, and aquifer tests were completed at all the study sites, providing an opportunity to observe hydraulic-head fluctuations to pumping in vertical till profiles (fig. 10). Water levels in piezometer screens hydraulically isolated from the aquifer being pumped were not expected to have a drawdown response from pumping stress over the short-term (several hours up to 5 days) pumping cycles that occurred during this study (Cherry and others, 2004). If water levels in till piezometers demonstrate a drawdown response to short-term pumping, it indicates a likely hydraulic connection between the confined aquifer and the till piezometer. Hydraulic connections are possible because of a conductive matrix with high percentages of sand (for example, tills at the HFC and Cromwell sites) or from fractures in more clayey till (Cherry and others, 2004). If, for example, a piezometer intersected or was near a fracture that is hydraulically connected to the aquifer being pumped, then it is likely that a drawdown response would be observed in that piezometer (Cherry and others, 2004). Similarly, hydraulic connectivity from the surface downward can be examined by water-level responses in till piezometers to snowmelt or other substantial infiltration events (Cherry and others, 2004).

The LFO1 and LFO2 sites showed decreasing hydraulic-head values with depth and an overall downward hydraulic gradient (figs. 10*A*,*B* and 11*A*,*B*). At both sites, the downward hydraulic gradients increased with depth through the till, with the largest hydraulic-head losses occurring near the base of the till (fig. 11*A*,*B*). The downward hydraulic gradient was larger at the LFO2 site compared to the LFO1 site. Continuous water-level data at the LFO1 and LFO2 sites show varying responses to the pumping of the high-capacity production wells (fig. 10*A*,*B*). In the two aquifer piezometers, LFO1–F and LFO2–F, a clear daily to subdaily oscillation in hydraulic head from the high-capacity wells is evident. The LFO2 site is nearer to the high-capacity production wells, and as expected, LFO2–F shows a much larger oscillation in hydraulic head, as much as 4 ft, from pumping than LFO1–F, which shows only about 1-ft variations in hydraulic head (fig. 10*A*,*B*). Both confined aquifer piezometers show three large decreases in hydraulic head in July and August 2016 (fig. 10*A*,*B*). These large drops occurred during dry periods and ended during or just before precipitation events, indicating that these water-level fluctuations are likely caused by a high-capacity irrigation system that withdrew water from a confined aquifer system hydraulically connected to the confined aquifer used by high-capacity production wells. According to the Minnesota Department of Natural Resources (2020), there are several agricultural irrigation wells within about 1 mi from the Litchfield site, with the closest irrigation well about one-half mi away.

Table 5. Summary of physical and hydraulic properties of till and confined aquifers at the Litchfield 1 (LFO1), Litchfield 2 (LFO2), Cromwell (CWO1/O2), Olivia, and hydrogeology field camp (HFC) sites.

[--, no data or not applicable; K_h, horizontal hydraulic conductivity; K_v, vertical hydraulic conductivity; <, less than]

Property	Unit	Site				
		Litchfield 1 (LFO1)[a]	Litchfield 2 (LFO2)[a]	Cromwell (CWO1/O2)[b]	Hydrogeology field camp (HFC[c])	Olivia[d,e]
Glacial lobe	--	Des Moines	Des Moines	Superior	Wadena	Winnipeg provenance
Age[f]	--	Late-Wisconsin	Late-Wisconsin	Late-Wisconsin	Late-Wisconsin	Pre-Illinoian
Till properties						
Geologic formation[f]	--	New Ulm, Villard Member	New Ulm Villard Member	Cromwell	Hewitt	Good Thunder
Mean till grain size[f]	Percent (sand:silt:clay)	47:34:19	52:31:17	57:31:13	67:22:11	37:40:23
Till texture[f]	--	Loam to sandy loam	Loam to sandy loam	Sandy loam	Sandy loam to loamy sand	Clay loam to loam
Mean lithologic composition[f]	Percent (crystalline:carbonate:shale)	56:28:16	56:28:16	98:3:0	97:3:0	45:53:2
Till thickness	Feet	60	115	120	100	166
Hydraulic gradient through till	Dimensionless	0.56 downward	0.48 downward	0.02 upward	0.04 downward	0.13 downward
Slug test geometric mean K_h	Feet per day	0.07	0.0002	0.06	0.03	0.004
Slug test K_h range	Feet per day	0.02–0.4	0.00001–0.001	0.006–0.3	0.0003–0.4	0.0001–0.03
Aquifer test representative K_v	Feet per day	0.001	0.001	1.1	0.031	0.0012[d] 0.0005[e]
Aquifer test K_v range	Feet per day	<0.0001–0.02	<0.0001–0.02	0.8–4.1	0.011–0.037	0.00012–0.003
Vertical anisotropy (representative K_v/geometric mean K_h)	Dimensionless	70	0.20	0.05	1.0	3.3[d] 8.0[e]
Hydraulic gradient across till/confined aquifer boundary	Dimensionless	0.01 downward	0.02 downward	0.05 upward	0.02 downward	2.26 downward
Confined aquifer properties (determined from aquifer tests)						
Transmissivity	Feet squared per day	9,000	9,000	4,400	1,850	8,230
Thickness	Feet	29	29	145	14	54
K_h	Feet per day	310	310	30	132	152
Vertical anisotropy	Dimensionless	1	1	0.5	1	1
Storativity	Dimensionless	0.000075	0.000075	0.0002	0.000058	0.000054
Leakage factor	Feet	21,000	21,000	--	2,630	2,570
Well efficiency	Percent	--	--	--	0.1	0.5

[a]Aquifer test results from Blum and Woodside, 2017.

[b]Aquifer test results from Lund and Blum, 2017.

[c]Aquifer test results from Blum, 2019a.

[d]Aquifer test results from Blum, 2019b.

[e]Aquifer test results from Blum, 2020.

[f]Staley and others, 2018.

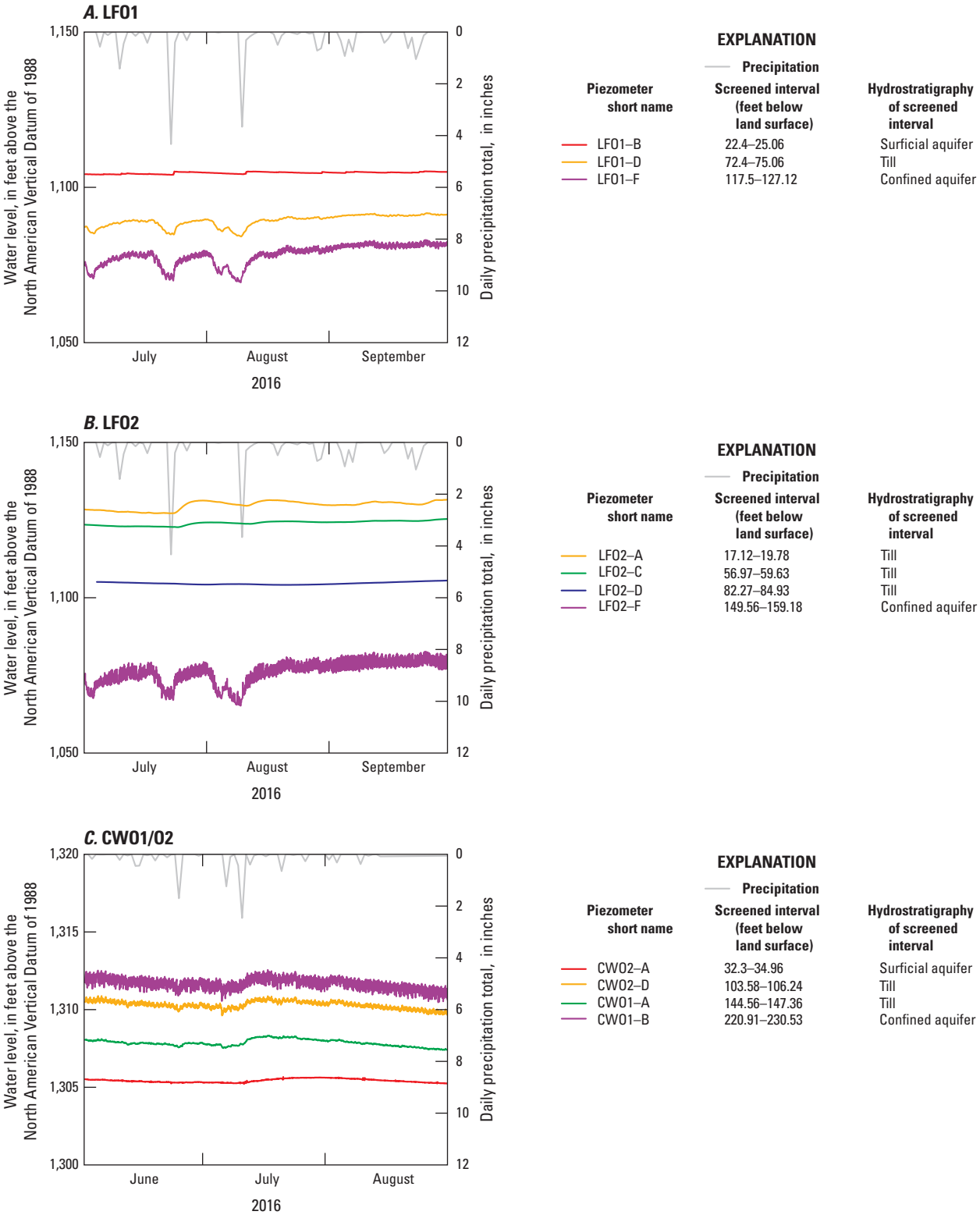

Figure 10. Precipitation and hydraulic head in piezometers during 3-month periods. *A*, the LFO1 nest at the Litchfield site; *B*, the LFO2 nest at the Litchfield site; *C*, the CWO1/O2 nest at the Cromwell site; *D*, the hydrogeology field camp (HFC) site; *E*, the Olivia site.

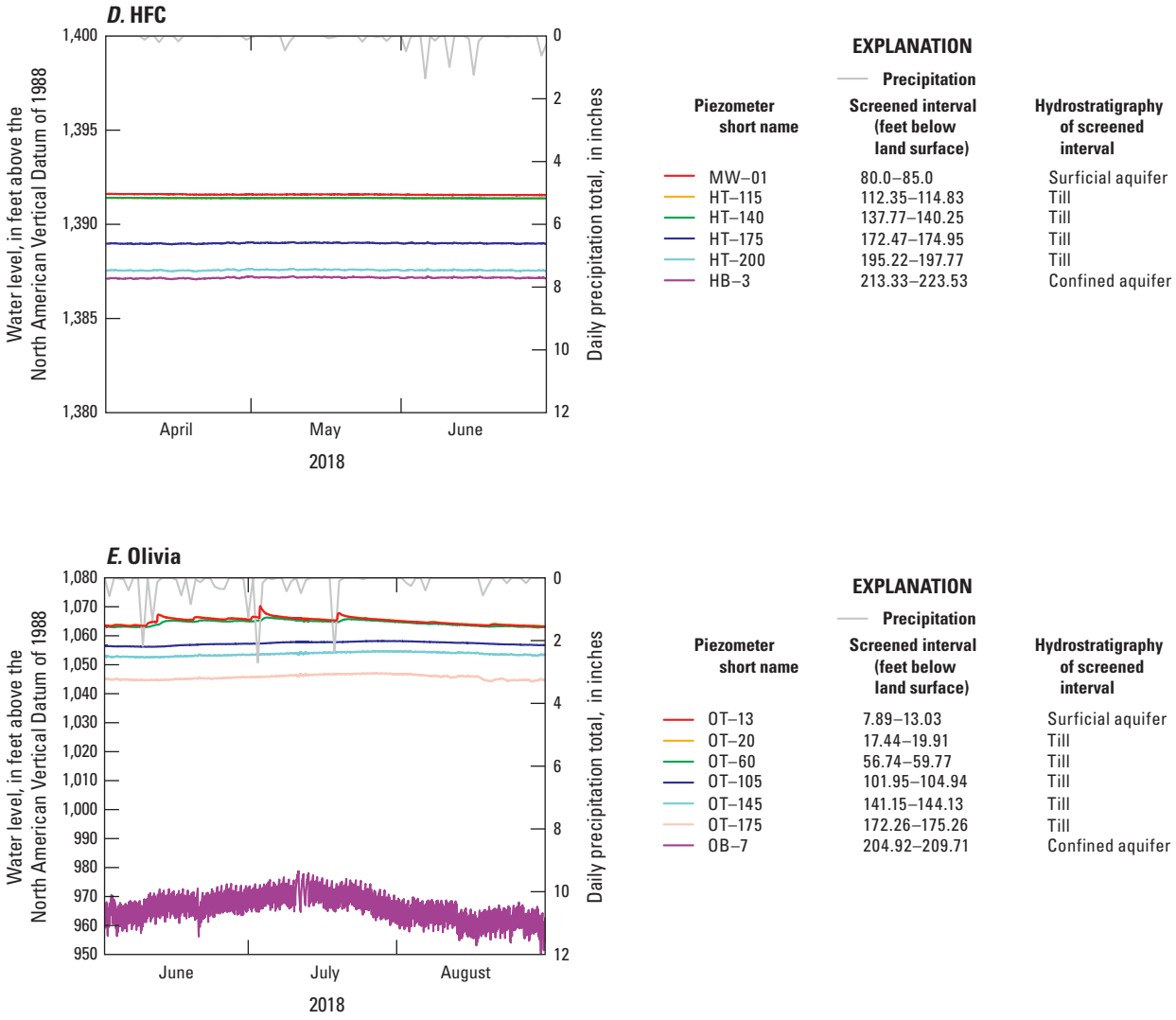

Figure 10. Precipitation and hydraulic head in piezometers during 3-month periods. *A*, the LFO1 nest at the Litchfield site; *B*, the LFO2 nest at the Litchfield site; *C*, the CWO1/O2 nest at the Cromwell site; *D*, the hydrogeology field camp (HFC) site; *E*, the Olivia site.—Continued

Hydraulic-head data from the LFO2 site demonstrate the presence of a till confining unit that limits hydraulic connectivity through the till profile (fig. 10*B*). Water-level fluctuations from pumping stress are not apparent at LFO2–D, 30 ft above the till/aquifer boundary. There is not a large sand lens that could dampen the hydraulic-head fluctuation response between the till/aquifer boundary and LFO2–D (fig. 3). This piezometer also did not demonstrate a drawdown response during the aquifer test after 24 hours of pumping at 787 gallons per minute (gal/min) (Blum and Woodside, 2017). This indicates there is a confining unit within 30 ft of the till/aquifer boundary that limits the hydraulic connectivity between the aquifer and the till.

Water levels in LFO2–A (screened about 17–20 ft below land surface) and LFO2–C (screened about 57–60 ft below land surface) responded similarly to large precipitation events (fig. 10*B*), indicating hydraulic connectedness through the till from 20 to 60 ft below land surface. Patterns in water levels at LFO2–D did not resemble those of LFO2–A, indicating that LFO2–D is also reasonably hydraulically isolated from surficial processes. Taken together, this indicates that the most effective confining unit at LFO2 exists above and below LFO2–D and that at least the upper 60 ft of till at the LFO2 site are hydraulically connected.

A different “leaky” response was observed at the far nest, the LFO1 site. LFO1–D is screened in till about 25 ft above the top of the confined aquifer/till boundary, and water-level patterns in this piezometer closely resemble those observed in the confined aquifer. Even the daily oscillations from the cycling on and off of the production wells are evident at LFO1–D, indicating a reasonable hydraulic connection from the aquifer through the bottom 25 ft of till (fig. 10*A*). During the aquifer test at the Litchfield site, drawdown was observed in all the till piezometers (LFO1–C, LFO1–D, and LFO1–F),

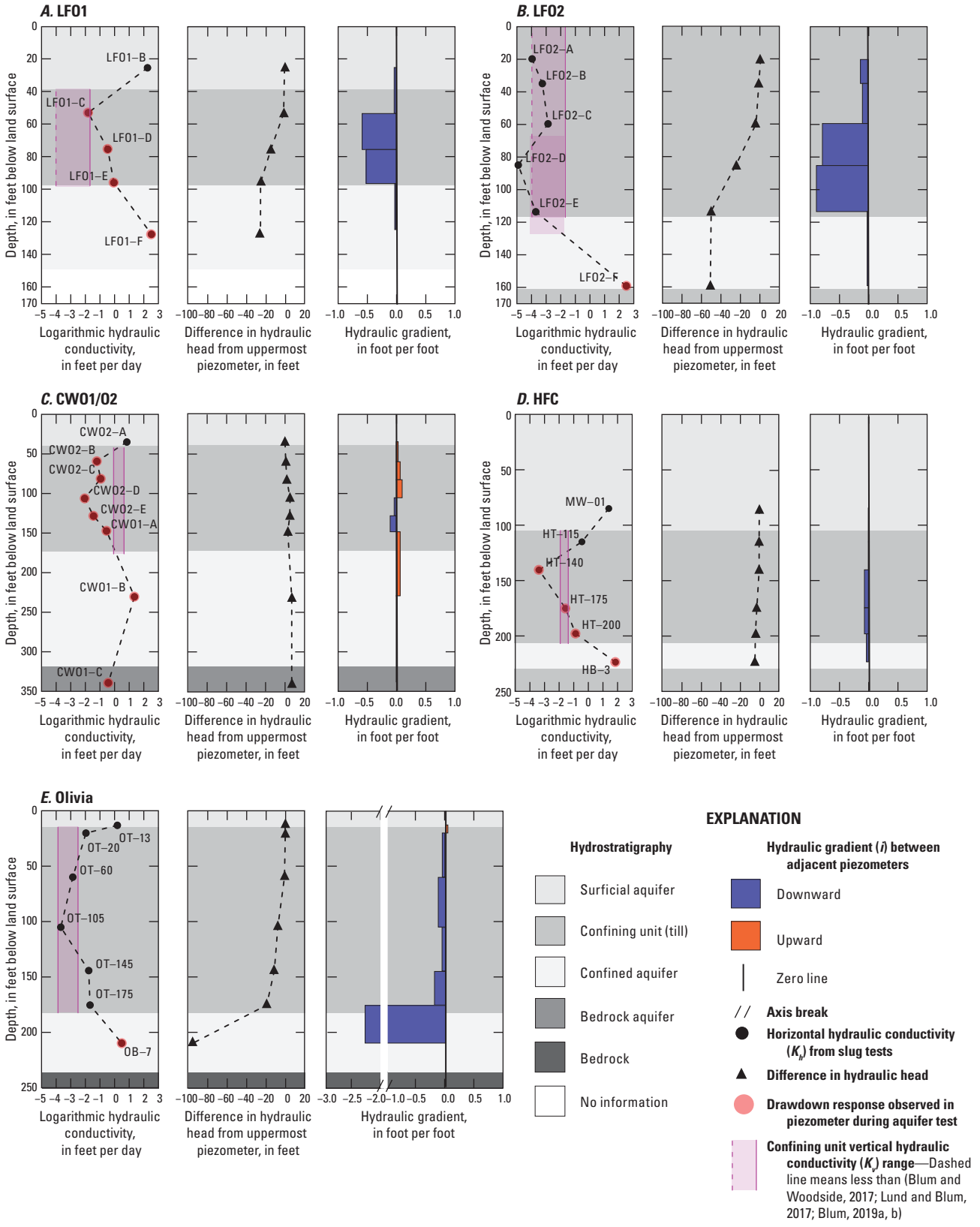

Figure 11. Hydraulic information for each piezometer nest including hydraulic conductivity, differences in hydraulic head, and hydraulic gradients among piezometers. *A*, at the LFO1 nest at the Litchfield site; *B*, at the LFO2 nest at the Litchfield site; *C*, at the CWO1/O2 nest at the Cromwell site; *D*, at the hydrogeology field camp (HFC) site; *E*, at the Olivia site.

indicating a hydraulic connection through most of the till layer. Water-level patterns at LFO1–D bear a stronger resemblance to the confined aquifer than to the surficial aquifer, which is monitored by LFO1–B. Sharp water-level rises in LFO1–B are linked to rainfall events. Further time-series analysis is needed to determine if the routine pumping signal is apparent in the LFO1–B well. The till at the LFO1 site is only about 58 ft thick, and nearly one-half of this sequence is hydraulically connected between the top of the confined aquifer and LFO1–D.

The hydraulic-head data from the Cromwell site (CWO1/O2) demonstrate a "leaky" till unit. At this site, a slight upward hydraulic gradient (fig. 11*C*) was observed. All the piezometers with continuous water-level data showed similar seasonal patterns in water levels (fig. 10*C*). Throughout the profile, from the surficial aquifer (CWO2–A) down to the bedrock (CWO1–C), an increase in water levels was observed in July 2016 (fig. 10*C*). Subdaily oscillations in hydraulic head caused by pumping from nearby high-capacity production wells are evident in the bedrock aquifer (CWO1–C, data not shown but are available at U.S. Geological Survey [2019]), the confined aquifer (CWO1–B), and two till piezometers (CWO1–A and CWO2–D) but not in the surficial aquifer (CWO2–A). Drawdowns were observed in all till piezometers installed at this site (CWO2–B through CWO1–A) during the aquifer test (fig. 11*C*; Lund and Blum, 2017). The till at the CWO1/O2 site is about 130 ft thick, and CWO2–B is screened about 14 ft below the top of the till. This means that hydraulic connectivity was observed through 90 percent of the till thickness at the Cromwell site.

The hydraulic-head data from the Olivia site demonstrate that parts of the till are an effective confining unit, limiting hydraulic connectivity between the confined aquifer and overlying till. The Olivia site has an overall downward hydraulic gradient (fig. 11*E*). The vertical hydraulic gradient between OT–13 in the surficial aquifer and OT–20 near the top of the till (confining) unit is small (0.03) and, depending on the time of year, can have a slightly upward vertical gradient. Mainly, the lack of a vertical hydraulic gradient between OT–13 and OT–20 indicates that there is primarily horizontal groundwater flow through the surficial aquifer in which OT–13 is screened. The vertical hydraulic gradient between OT–20 and OT–60 is also small (0.02) but is downward through the till throughout the year. Larger downward vertical hydraulic gradients exist from OT–60 through OT–175. An extremely large hydraulic gradient (2.26) exists between the piezometer screened in the bottom of the till, OT–175, and the piezometer screened in the confined aquifer, OB–7 (fig. 11*E*). Large vertical hydraulic gradients such as this have been observed in confining units before, and at the Olivia site, the large vertical hydraulic gradient may be due to the presence of thin layers of glaciolacustrine sediments near the bottom of the till unit (Hart and others, 2008). During a 10-hour aquifer test, the confined aquifer was pumped at 232 gal/min, and no drawdown response was observed in any till piezometers, including OT–175, which is only 12 ft above the till/aquifer boundary (Blum, 2019b); however, the lack of a hydraulic response was confounded because of RWFs (fig. 12*A*).

The upper part of the tills at the Olivia site, to a depth of at least 60 ft, are hydraulically connected. Groundwater recharge events, especially in spring/summer, cause hydraulic-head increases (of as much as about 3–5 ft) in piezometers OT–13, OT–20, and OT–60 (fig. 10*E*). Geologic descriptions and textural analyses of the till from about 30 to 60 ft are not appreciably different from 60 to 150 ft, indicating that fractures may explain the hydraulic connections in the upper part of the till. No visible fractures were reported in the geologic description of the cores (Staley and Nguyen, 2018), but fractures without visible staining are present in tills (Cherry and others, 2004; Helmke and others, 2005a, b).

Hydraulic-head observations at the Olivia site were unique in that water levels in several till piezometers demonstrated RWFs in response to pumping (see RWF discussion in the next section). Routine pumping by high-capacity production wells from the confined aquifer typically caused hydraulic-head changes of about 10 ft at well OB–7, which is screened in the confined aquifer. At first glance, OT–175 and OT–145 seem to be responding hydraulically to the pumping (fig. 10*E*); however, the fluctuations at these piezometers are RWFs, meaning water levels increased in response to pumping. Shown in figure 12*A* are hydraulic heads during the aquifer test completed in July 2018. Well OB–7 demonstrates a typical drawdown response when the pump turns on; however, the piezometers OT–175, OT–145, OT–105, and OT–60 all demonstrate varying degrees of RWF in that water levels in these wells increase as the hydraulic head in the aquifer decreases. Analysis of the RWF from the aquifer test data reveals no hydraulic response from any of these piezometers to the pumping; rather, the hydraulic-head changes are attributed to a poroelastic response of the system to pumping (Blum, 2019b).

The hydraulic-head data from the HFC site demonstrate a somewhat "leaky" till unit. The overall vertical hydraulic gradient at the HFC site is also downward but small (fig. 11*D*). The largest hydraulic gradients occur in the bottom half of the till profile. In contrast to the other sites, the confined aquifer at the HFC site is not continuously pumped, so the hydraulic heads measured at this site represent a static condition. The hydraulic-head difference between HT–115, which is screened about 10 ft below the top of the till confining unit, and HT–140, which is screened about 25 ft lower in the till unit is small (0.01 ft). Indeed, the hydrographs for these two piezometers overlap in figure 10*D* and the mean hydraulic gradient between these two piezometers is near zero (fig. 11*D*). There is a narrow band of higher sand content between these piezometers (Staley and Nguyen, 2018), which could be a zone of increased horizontal groundwater flow and might explain why there is such a small hydraulic gradient between these piezometers. There is a small vertical hydraulic gradient of 0.005 between MW–01 (in the surficial aquifer) and HT–115 (uppermost till piezometer).

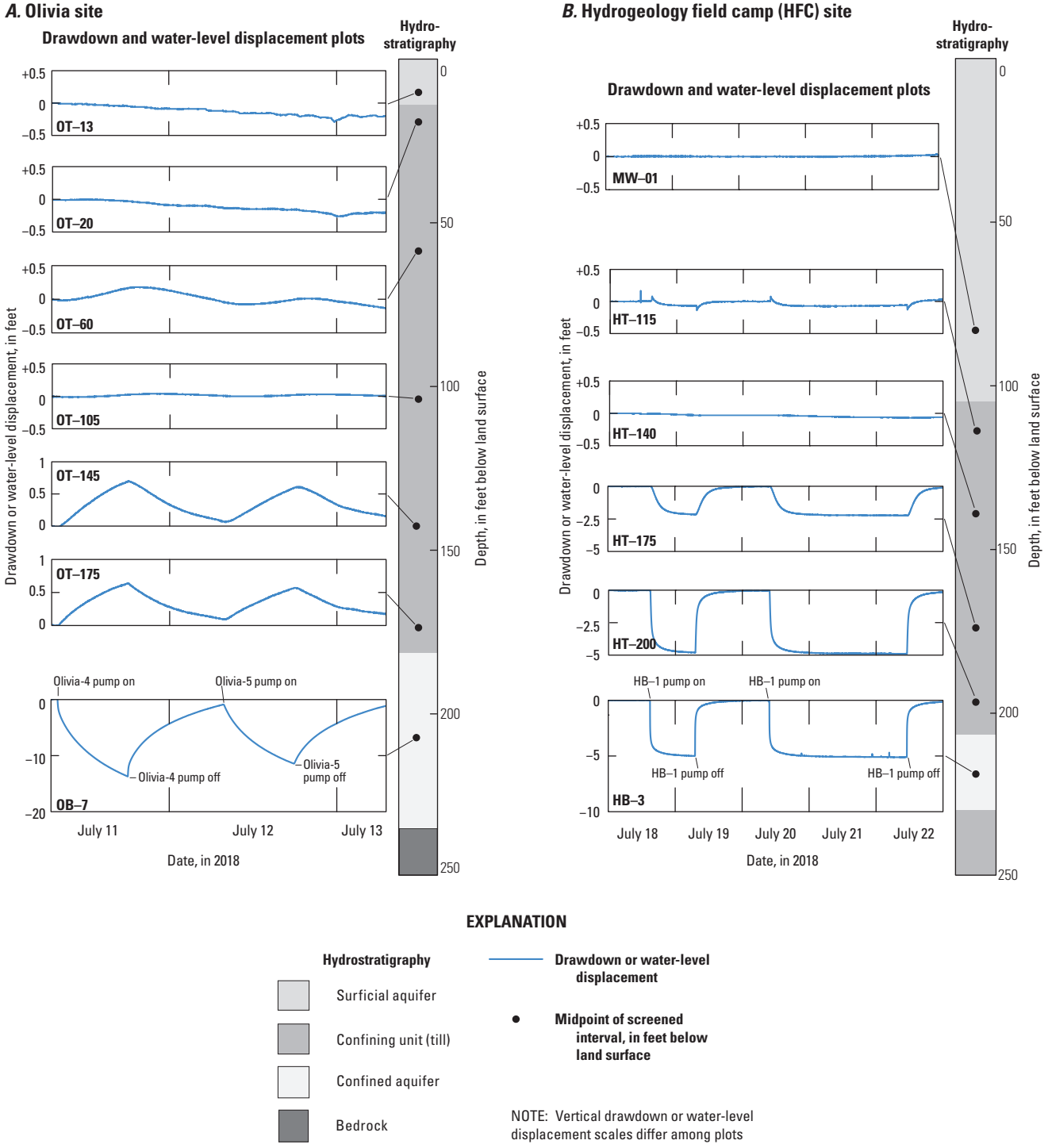

Figure 12. Drawdown and water-level displacement in piezometer nests during constant-rate aquifer tests. *A*, at the Olivia site; *B*, at the hydrogeology field camp (HFC) site near Akeley, Minnesota.

Hydraulic connections were observed throughout the till profile at the HFC site, although these were difficult to observe until the system was pumped. The unsaturated zone above the surficial aquifer is thick (over 60 ft) compared to the other sites in this study, and immediate responses to rainfall events were not noticeable; there is little to no variability in hydraulic head from April to June 2018 (fig. 10*D*). The only time water was pumped at this site was during aquifer tests. When the surficial aquifer was pumped for an aquifer test in 2017, a drawdown response was observed down to HT–175, which is 71 ft below the top of the till unit. During the 2018 aquifer test, when the confined aquifer below the till was pumped, a drawdown response was observed up through the till at piezometers HT–200, HT–175, and HT–140 (figs. 11*D* and 12*B*). This indicates that there are hydraulic connections throughout the till profile, and if this confined aquifer were pumped regularly such that a stronger downward hydraulic gradient was established, there could be fast downward groundwater flow through the sandy till.

Reverse Water-Level Fluctuations

RWF responses were observed in till piezometers during aquifer tests at three of the four study sites. At the Cromwell and HFC sites, brief RWF responses were observed when pumps were turned on or off. At the Olivia site, a prolonged RWF response that lasted the duration of the aquifer test was observed in several till piezometers (fig. 12*A*; Lund and Blum, 2017; Blum, 2019a, b). These RWF observations are usually attributed to a poroelastic response, or a "deformation-induced effect" (Hsieh, 1996), where pumping in the aquifer causes a reduction in pressure, which then leads to the expansion of water and a compression of the aquifer skeleton (Kim and Parizek, 2005; Berg and others, 2011). Deformation of the aquifer skeleton can then lead to strains that can cause confining units to have RWF responses. Often, these are either a brief response at the beginning of the pumping, where there is a temporary increase in the water level in the confining unit, called the Noordbergum effect, or a quick, temporary drop in water level at the end of pumping, called the Rhade effect (Kim and Parizek, 2005; Berg and others, 2011). Noordbergum and Rhade effects are clearly visible in HT–115 during the aquifer test at the HFC site (fig. 12*B*). At the Cromwell site, piezometers CWO2–B and CWO2–C demonstrated the Noordbergum and Rhade effects as the pump cycled on and off during the aquifer test period (Lund and Blum, 2017; Blum, 2020).

Evaluation of the Cromwell RWF data indicated hysteretic RWF responses to pumping and recovery when steady-state hydraulic gradient conditions in till were not achieved, but the hysteresis disappears when steady-state conditions are achieved (Blum, 2020). Under nonsteady-state conditions at the Cromwell site, the recovery RWF response is much larger than the pumping RWF response. At the Olivia site, the opposite is true. At the Cromwell site, there is an upward hydraulic gradient, and at the Olivia site, there is a downward hydraulic gradient; therefore, the apparent hysteresis of the RWF response is caused by the direction and strength of the ambient vertical hydraulic gradient (when inelastic deformation of the confining unit is negligible) (Blum, 2020). The prolonged RWF response in the till (confining unit) at the Olivia site is unusual because it lasted for the entire aquifer test (fig. 12*A*). The pumping time (10 hours) for the Olivia site aquifer test was not long enough to achieve a steady-state hydraulic gradient, and thus nonhysteretic RWF responses, within the till confining unit. It is estimated that a minimum pumping period of 20–30 days would be required to achieve steady-state conditions in the confining unit till at the Olivia site (Blum, 2019b).

Hydraulic Conductivity

A total of 141 slug tests were completed on the piezometers for this study. The calculated K_h values are summarized in table 6. Slug test model fit residual statistics and confidence intervals of K_h estimates are provided in appendix table 2.3. All the water-level data, AQTESOLV files, and graphical outputs are available in the data release accompanying this report (Maher and others, 2020).

Generally, K_h estimates from slug tests were repeatable with narrow confidence intervals. Repeated slug test estimates of K_h for a single till piezometer generally varied by one order of magnitude or less (table 6). For till piezometers, the magnitude of the 95-percent confidence interval of K_h estimates was small relative to the estimated K_h value, having a mean of 12 percent (appendix table 2.3). The model fit to the slug test data for one till piezometer, LFO2–A, was an outlier; the magnitude of the confidence interval value was large, 180 percent, relative to the K_h value. Estimates of K_h for aquifers (confined and unconfined) were more variable than estimates of K_h for till (table 6; appendix table 2.3).

The estimates of K_v from aquifer tests at each study site are shown in table 5 and figure 11. Two types of values are presented, a "representative bulk K_v" and a range of K_v values. These numbers are taken from several reports from the Minnesota Department of Health (listed in table 5). The representative bulk K_v is considered the single best K_v estimate for each site and is used for travel time estimates and comparisons with K_h values. The range of reasonable K_v estimates is shown in figure 11. The range in K_v estimates (table 5) results from variations in simplifying assumptions and application of different analytical solutions to estimating K_v from the aquifer test data. The detailed methodology is available in the reports referenced in table 5.

At the Litchfield site, mean K_h values from slug tests range from 306 ft/d for the sand and gravel aquifer to about 1×10^{-5} ft/d for till (fig. 11 and table 6). The geometric mean K_h values of till at the LFO1 and LFO2 sites are 7×10^{-2} ft/d and 2×10^{-4} ft/d, respectively (table 5). These values for K_h are within previously observed values for Des Moines lobe till, although the K_h values at the LFO1 site were slightly higher than expected (Simpkins and Parkin, 1993; Helmke and

Table 6. Summary of horizontal hydraulic conductivity (K_h) values from slug tests, lithology of sediments at the piezometer screen, and the methods used to determine K_h values from slug test data.

[K_h, horizontal hydraulic conductivity; E, scientific notation denoting exponentiation; for example 1.78E+02 = 1.78×10²; Springer-Gelhar, Springer and Gelhar, 1991; KGS, Kansas Geological Survey model, Hyder and others, 1994; Butler, Butler, 1998]

Piezometer	Mean K_h	Minimum K_h	Maximum K_h	Falling-head tests	Rising-head tests	Lithology at well screen	Slug test analysis method
	Feet per day			Count			
Litchfield field sites							
LFO1–B	1.78E+02	1.05E+02	2.44E+02	3	3	Silty to coarse sand	Springer-Gelhar
LFO1–C	1.57E−02	1.50E−02	1.63E−02	1	1	Till	KGS
LFO1–D	3.40E−01	2.53E−01	4.27E−01	1	1	Till	KGS
LFO1–E	8.88E−01	5.04E−01	1.55E+00	3	3	Till/sand and gravel	KGS
LFO1–F	3.34E+02	2.78E+02	3.89E+02	2	2	Sand and gravel	Butler
LFO2–A	1.10E−04	2.17E−05	1.99E−04	1	1	Till	KGS
LFO2–B	5.52E−04	2.09E−04	8.95E−04	1	1	Till	KGS
LFO2–C	1.34E−03	1.34E−03	1.34E−03	1	1	Till	KGS
LFO2–D	1.22E−05	1.22E−05	1.22E−05	1	0	Till	KGS
LFO2–E	1.95E−04	1.11E−04	2.80E−04	1	1	Till	KGS
LFO2–F	3.06E+02	2.28E+02	3.74E+02	3	3	Sand and gravel	Butler
Cromwell field sites							
CWO1–A	2.84E−01	2.63E−01	3.06E−01	1	1	Till	KGS
CWO1–B	2.31E+01	1.91E+01	2.81E+01	3	3	Sand and gravel	Butler (1), KGS (5)
CWO1–C	3.49E−01	2.48E−01	5.62E−01	3	3	Slate	KGS
CWO2–A	6.88E+00	4.71E+00	9.57E+00	3	3	Sand and gravel	KGS
CWO2–B	6.21E−02	5.89E−02	6.54E−02	1	1	Till	KGS
CWO2–C	1.12E−01	1.02E−01	1.23E−01	1	1	Till	KGS
CWO2–D	8.97E−03	6.15E−03	1.18E−02	1	1	Till	KGS
CWO2–E	3.60E−02	3.55E−02	3.65E−02	1	1	Till	KGS
Hydrogeology field camp field sites							
MW–01	2.49E+01	1.94E+01	3.15E+01	3	3	Sand and gravel	Springer-Gelhar
HT–115	3.64E−01	3.37E−01	3.77E−01	3	3	Till	KGS
HT–140	4.16E−04	2.61E−04	5.06E−04	3	3	Till	KGS
HT–175	2.78E−02	1.51E−02	6.45E−02	3	3	Till	KGS
HT–200	1.36E−01	1.24E−01	1.54E−01	3	3	Till	KGS
HB–3	7.27E+01	6.50E+01	8.03E+01	3	3	Sand and gravel	Butler
Olivia field sites							
OT–13	1.55E+00	1.12E+00	1.97E+00	3	3	Sand and gravel	KGS
OT–20	1.09E−02	6.50E−03	1.46E−02	3	3	Till	KGS
OT–35	6.07E−06	6.07E−06	6.07E−06	0	1	Till	KGS
OT–60	1.38E−03	6.47E−04	2.27E−03	3	2	Till	KGS
OT–105	2.11E−04	1.00E−04	3.41E−04	3	3	Till	KGS
OT–145	1.71E−02	6.45E−04	3.32E−02	3	3	Till	KGS
OT–175	2.09E−02	1.28E−02	3.02E−02	3	3	Till	KGS
OB–7	3.07E+00	1.44E+00	4.17E+00	3	3	Sand and gravel	KGS

others, 2005a, b). Only two piezometers were used to estimate the geometric mean K_h value of till at the LFO1 site. LFO1–E, which was intended to be screened solely in till, seems to be connected to the aquifer and was excluded from the geometric mean calculations. The large difference in mean K_h values between the two study sites in Litchfield was unexpected. The mean sand content in the till at the LFO1 site (47 percent) was lower than the mean sand content of the till at the LFO2 site, yet the K_h was two orders of magnitude higher at LFO1 compared to LFO2. The large difference between these sites could be due to differences in till deposition, a greater effect of till fractures on the hydraulic observations at the LFO1 site compared to the LFO2 site, or localized effects on the borehole wall from drilling operations (see "Sources of Uncertainty" section). The LFO2 site K_h values may be more indicative of the properties of the till matrix rather than fractures. Alternatively, installation procedures may have affected some piezometers more than others and may explain some of the large differences between these two nests (see "Sources of Uncertainty" section).

At the Olivia site, mean K_h values ranged from about 3 ft/d for sand and gravel to a low of about 2×10^{-4} ft/d for till (table 6, fig. 11*E*). The geometric mean K_h of the slug tests in the till confining unit is 4×10^{-3} ft/d (table 5), which is higher than at the LFO2 site, despite the lower sand and higher clay content at the Olivia site compared to the LFO2 site. As previously discussed, the upper part of the till at the Olivia site (to a depth of 60 ft) is hydraulically connected, with some data indicating that fractures may be present. The till deposit at the Olivia site is older (pre-Illinoian) than the deposit at the Litchfield site and could therefore be more weathered and may explain, in part, the higher K values observed at the Olivia site. One extremely low K_h outlier, about 6×10^{-6} ft/d, observed at piezometer OT–35 (table 5), was not considered for the calculation of the geometric mean K_h or plotted on figure 11. This piezometer had only one "slug" test completed that lasted for 14 months. The well was purged after installation in August 2017, and the water levels had not fully recovered before the study's data collection ended. It is hypothesized that the screen of this piezometer was affected by bentonite during the installation process; however, water samples were not collected to evaluate this hypothesis. An alternative hypothesis is that this till piezometer does not intersect any fractures and is a demonstration of a clayey till matrix response.

At the Cromwell site, mean K_h values ranged from about 23 ft/d for sand and gravel to about 9×10^{-3} ft/d for till (table 6, fig. 11*C*). The geometric mean K_h value for all slug tests in the till confining unit is 0.06 ft/d (table 5). The till K_h values at this site were remarkably similar to the till K_h values at the LFO1 site, despite a 10-percent difference in sand content and 6-percent difference in clay content (table 5).

At the HFC site, mean K_h values ranged from about 73 ft/d in sand and gravel to about 4×10^{-4} ft/d in till for the slug test results (table 6, fig. 11*D*). The geometric mean K_h value in the till confining unit is 3×10^{-2} ft/d (table 5), which again is similar to the LFO1 site despite a 20 percent higher sand content at the HFC site compared to the LFO1 site (table 5).

The material near the piezometer/well screen is the main material controlling the K_h value during a slug test (Cherry and others, 2004). Slug tests measure the horizontal hydrologic properties of a small (compared to aquifer tests) volume of till surrounding the sand pack, on the order of cubic meters (Bradbury and Muldoon, 1990). Studies have reported that a standard slug test has a sample volume of about 24 cubic meters for depths of 1–3.7 meters (Seo, 1996; Beckie and Harvey, 2002; Young and others, 2020). Thus, slug tests can be greatly affected by anything that affects the piezometer's connection to the geologic material being measured. Some such factors are discussed in the "Sources of Uncertainty" section.

Indeed, site-averaged textural compositions and till geometric mean K_h values were not well correlated in this study. This indicates that, at the localized scale measured with slug tests, textural compositions were not the primary driving factor for estimates of till hydraulic properties; for example, the correlation coefficient of the logarithm of the geometric mean K_h and site-average percentage of sand (number of samples = 5 sites) is 0.27. If the mean K_h value of each individual piezometer is paired with the nearest textural composition data from cores (Wagner and Tipping, 2016; Staley and Nguyen, 2018), the correlation coefficient between the logarithmic K_h and percentage of sand does not substantially improve; the correlation coefficient is 0.29 across 21 till piezometers. For this comparison, textural samples were collected within 2 ft vertically of the well screen, on average.

To further illustrate that textural composition is not a good indicator of K_h estimates in till, K_h values were plotted on a soil texture trilinear diagram in figure 13*A*. The K_h of till piezometers varied substantially across the range of soil textural compositions measured in this study (fig. 13*A*); for example, sediments classified as loam had K_h estimates that varied by four orders of magnitude. Two samples that were classified as clay loam or silt loam had higher K_h values than several samples classified as loam despite having higher clay and silt contents (fig. 13*A*).

In contrast, during aquifer tests, hydraulic responses in a much larger volume of till, on the order of hundreds of cubic meters, are measured. The bulk K_v values determined from aquifer tests for each site correlate much more strongly with the site-averaged percentage of sand in the till. Across the five sites, the correlation coefficient between percentage of sand and the logarithm of the bulk K_v is 0.61. The bulk K_v values from aquifer tests are even more strongly correlated with the percentage of clay at each site with a correlation coefficient of −0.73. These correlations improve if the logarithm of time-delay bulk K_v at the Olivia site (0.0005 ft/d) is used rather than the leaky confined aquifer bulk K_v at the Olivia site (0.0012 ft/d). These two correlations indicate that bulk till textural composition is an important factor controlling leakage through till to underlying aquifers at the scale measured with aquifer tests.

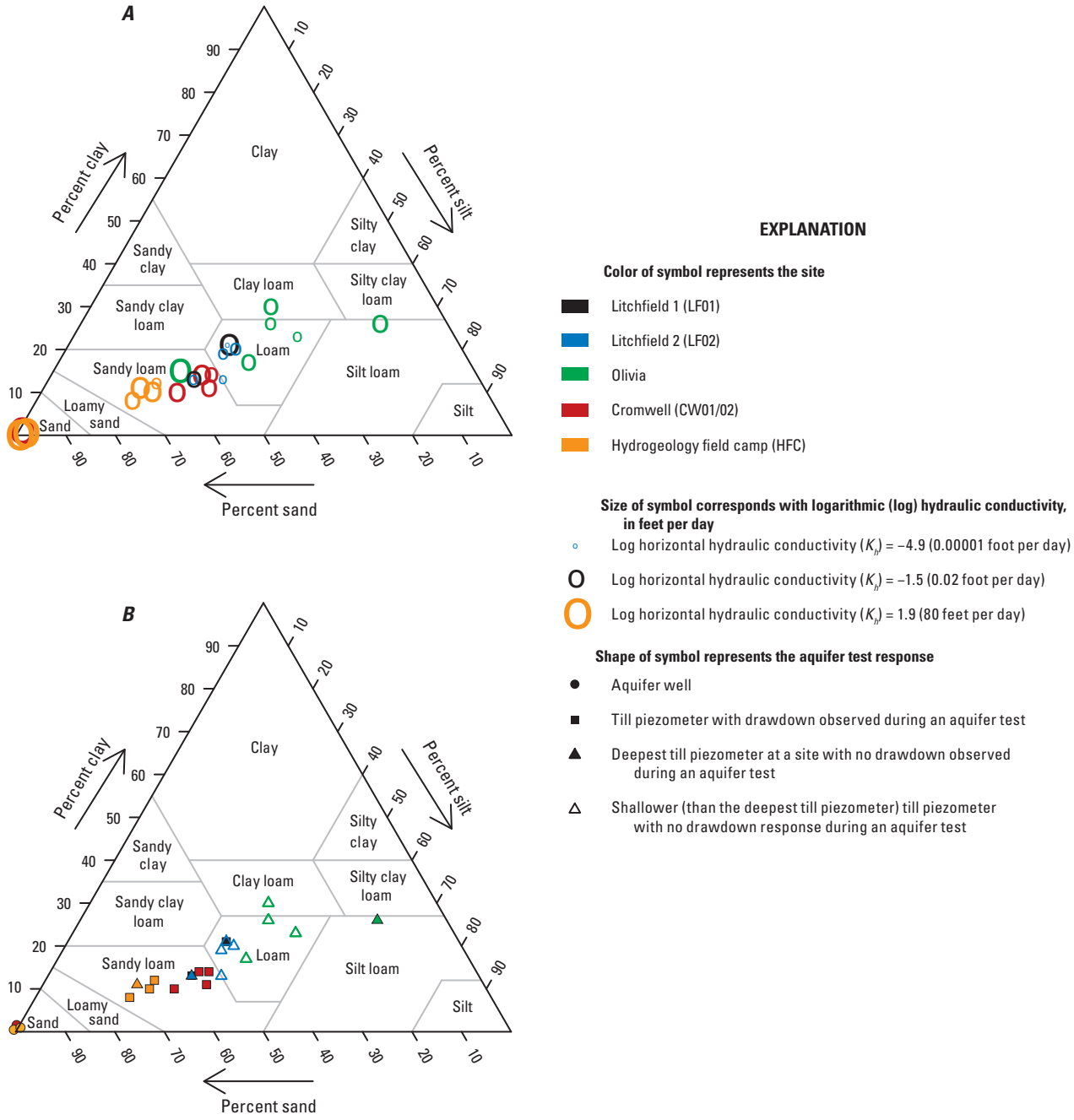

Figure 13. Trilinear plots showing the relation between sand, silt, and clay contents near the screened interval of piezometers and (*A*) horizontal hydraulic conductivity (K_h) estimates; (*B*) the presence or absence of an aquifer test drawdown response.

The vertical anisotropy, herein defined as the ratio of K_h to K_v, varies widely across the sites and the geometric mean K_h estimates are not well correlated with the bulk K_v estimates (correlation coefficient of 0.48). In modeling applications, anisotropy is commonly a specified parameter, and this study provides measured values of anisotropy in till. Confining units can have higher anisotropy compared to aquifers, with K_h possibly being higher because of stratification or K_v possibly being higher because of fractures (Cherry and others, 2004). Overall, the vertical anisotropy ranges by four orders of magnitude from 0.05 at the Cromwell site to 70 at the LFO1 site (table 5). In a single till unit at the Litchfield site, the vertical anisotropy varies by three orders of magnitude, from 0.20 to 70. Values of vertical anisotropy greater than 1 indicate tills that are more horizontally conductive than vertically conductive whereas vertical anisotropy values of less than 1 indicate the opposite. The textural composition is not well correlated with anisotropy. Only one site, the HFC site, had nearly equal K_v and K_h values, as indicated by its anisotropy value near 1.

Although K values provide information about a formation's ability to transmit water, evidence of hydraulic connections during periods of stress provide information about actual flow paths that may behave differently than those predicted from estimated K values. Qualitatively, the importance of till textural composition to hydraulic connections between till and underlying aquifers is shown in figure 13*B*; connections that only become apparent when a large pumping stress is present in the system. The aquifer tests completed for this study were a much more prolonged, continuous pumping stress compared to the routine pumping by municipalities. The triangle symbols in this plot represent piezometers that did not demonstrate a drawdown response during the aquifer test whereas square symbols represent piezometers that did demonstrate a drawdown response. Almost every piezometer screened in till with at least 55-percent sand and less than 15-percent clay had a drawdown response. Conversely, almost every piezometer with less than 55-percent sand and more than 15-percent clay did not demonstrate a drawdown response. There are a couple of outliers to this general classification, but overall, there is a consistent separation among these tills as to which materials demonstrate hydraulic connectivity during pumping stress.

Leakage (Recharge) through Tills

Calculations of travel time through the till, specific discharge, and leakage from till according to Darcy's Law vary by three to four orders of magnitude across the sites (table 7). At three of four sites, a downward hydraulic gradient through the till was observed, so the calculations represent the downward flux of water through till into the confined aquifer. At the Cromwell site, there was an upward hydraulic gradient, so the calculations represent the upward flux of water from the confined aquifer through the till to the surficial aquifer.

Specific discharge is given in inches and represents leakage from till as volume divided by a cross-sectional area (eq. 2). In most cases, the calculated specific discharge is constrained by the properties of the till (table 7). In other words, specific discharge from the till is less than or equal to precipitation-driven annual groundwater recharge to the water table aquifer, as estimated by Smith and Westenbroek (2015). Two specific discharge rates, 176 in/yr at LFO1 and 86 in/yr at the Cromwell site, are substantially greater than the precipitation-driven groundwater recharge to the water table aquifer (table 7). In these cases, the specific discharge across the till/confined aquifer boundary cannot be realized in a simple one-dimensional flow system where the only input to groundwater is diffuse recharge from precipitation directly above the vertical profile of interest. Lateral groundwater flow could supply additional water such that these fluxes could be realized. In fact, this is likely occurring at the Cromwell site. At the Cromwell site, the hydraulic gradient is slightly upward, and one hypothesis is that the groundwater is flowing laterally from a distant recharge location to the confined aquifer at the Cromwell site (Witt, 2017).

At all sites except for the HFC site, mean linear velocities and travel times vary widely between calculations using the geometric mean K_h from slug tests and the K_v from aquifer tests. The two types of calculations (K_h and K_v) require slightly different assumptions and represent different volumes of till and water. Calculations of travel time that use the geometric mean K_h assume isotropy between K_h and K_v. Calculations of travel time that use the bulk K_v assume that the hydraulic gradient and till thicknesses determined at each piezometer nest are representative of a large till volume.

When the geometric mean K_h from slug tests is used to calculate travels times through till, the resulting travel times vary from 1 year to more than 900 years (table 7). Interestingly, these extremes were observed at LFO1 and LFO2, respectively, which are one-half mi apart. The geometric mean K_h calculations represent localized flow conditions, and the wide range of travel times at the Litchfield site demonstrates two different vertical flow paths through which water travels to the confined aquifer.

When the bulk K_v from aquifer tests is used to calculate travel times through till at all sites, estimated travel times vary over a much larger range, from 4 to nearly 1,800 years. The minimum estimated travel time occurs at the Cromwell site and the maximum occurs at the Olivia site. For the Litchfield sites, calculations with the bulk K_v produce far different travel times compared to calculations with the geometric mean K_h. Using the bulk K_v, the estimated travel time through till at LFO1 is 75 years and at LFO2 is 165 years. The same K_v value was used for both nests, and the difference in travel time estimates results from different till thicknesses (60 ft at LFO1, 115 ft at LFO2) and hydraulic gradients (0.56 at LFO1 and 0.48 at LFO2). The Olivia and Cromwell sites also have a large difference in travel time estimates from the bulk K_v compared to the geometric mean K_h.

The Olivia site has two representative bulk K_v values, one from a traditional leaky confined aquifer approach and one from a time-delay analysis (tables 2, 5). Both of these methods have limitations, but given the complicated RWF responses observed at the site, both K_v estimates are considered reasonable. Varying the bulk K_v by only one order of magnitude has implications for estimating the travel time through the till at the Olivia site. The leaky confined aquifer method K_v is 0.001 ft/d, which when used in Darcy calculations, produces a travel time through the till of 738 years. The time-delay analysis K_v is 0.0005 ft/d, which produces a travel time through till of 1,772 years (table 7).

A comparison between the areal extent of till/aquifer surface required to meet the pumping rates of the high-capacity wells (table 7) and the mapping of confined aquifers reveals uncertainty about aquifer geometry and (or) the source of water to wells. The areal estimates assume (1) the only source of water to the confined aquifer is leakage from overlying till and (2) the bulk K_v from aquifer tests is a representative K for the leakage that occurs in response to pumping for water supply.

Table 7. Hydraulic characteristics of till, annual pumping rates, and estimates of vertical travel time and water flux through 1 square mile of till based on Darcy's law for each study site.

[*i*, mean hydraulic gradient; ft, foot; in/yr, inch per year; ft/d, foot per day; *q*, specific discharge (leakage); *Q*, recharge (leakage) from till; gal/yr, gallon per year; mi², square mile; K_h, horizontal hydraulic conductivity; E, scientific notation denoting exponentiation; for example 3.1E+09 = 3.1×10^9; --, no data or not applicable; K_v, vertical hydraulic conductivity]

Site name	*i* (dimensionless)	Till thickness (ft)	Potential groundwater recharge (in/yr)[a]	Hydraulic conductivity source	Hydraulic conductivity (ft/d)	Mean linear velocity (ft/d)	Travel time through till (years)	*q* (in/yr)	*Q* (gal/yr)	Pumping (gal/yr)	Area of till required to meet pumping demand (mi²)
Litchfield 1 (LFO1)	0.55 downward	60	4 to 8	Slug test geometric mean K_h	0.07	0.2	1	176	3.1E+09	3.4E+08	--
				Aquifer test K_v (Blum and Woodside, 2017)	0.001	0.002	74	2.4	4.2E+07		8
Litchfield 2 (LFO2)	0.48 downward	115	4 to 8	Slug test geometric mean K_h	0.0002	0.0003	913	0.4	6.6E+06	3.4E+08	--
				Aquifer test K_v (Blum and Woodside, 2017)	0.001	0.002	165	2.1	3.6E+07		9
Cromwell (CWO1/O2)	0.02 upward	120	4 to 8	Slug test geometric mean K_h	0.06	0.004	80	4.5	7.8E+07	6.0E+06	--
				Aquifer test K_v (Lund and Blum, 2017)	1.10	0.08	4	86	1.5E+09		--
Hydrogeology field camp (HFC)	0.04 downward	100	4 to 8	Slug test geometric mean K_h	0.03	0.005	57	5.3	9.2E+07	0.0E+00	--
				Aquifer test K_v (Blum, 2019a)	0.03	0.005	50	6.0	1.0E+08		0
Olivia	0.13 downward	166	2 to 6	Slug test geometric mean K_h	0.004	0.002	217	2.3	4.0E+07	6.5E+07	--
				Aquifer test K_v (Blum, 2019b)	0.001	0.0006	738	0.7	1.2E+07		6
				Aquifer test K_v, time-delay analysis Blum, 2020)	0.0005	0.000257	1,772	0.3	4.9E+06		13

[a]Smith and Westenbroek, 2015.

According to the Darcy's law calculations, and assuming that overlying till contributes all the water to the aquifer, Litchfield's groundwater pumping requires between 8 and 9 mi^2 of till to meet the pumping demands and Olivia's pumping requires 6 to 13 mi^2 (table 7). These areal extents are larger than the areal extents of the aquifers as mapped in geologic maps based on well and borehole logs. The Renville County Geologic Atlas shows that the areal extent of the confined aquifer at Oliva is only 0.08 mi^2 (Bradt, 2017), and the Meeker County Geologic Atlas shows an approximate areal extent of the aquifer at Litchfield of 3 mi^2 (Meyer, 2015). The Olivia aquifer test indicated an aquifer boundary within 350 ft of the production well, and well records indicate that the aquifer is most likely a buried alluvial channel with a complex shape (Blum, 2019b). The glacial deposits at Litchfield are a complex mixture of till layers and sand bodies with many possible lateral connections between buried sand bodies (Meyer, 2015).

The source of water to the confined aquifers is much more complex than the simple conceptual system discussed here of one-dimensional flow from land surface through till to a confined aquifer. Uncertainty of the distribution of till hydraulic properties, the extent of confined aquifers, and the connections between aquifers make evaluations of the sustainability of groundwater pumping from confined aquifers challenging. This uncertainty about the structure of the subsurface provided the impetus for developing the heuristic models, rather than site-specific models for this study. In a later section of this report, heuristic MODFLOW models are used to evaluate the flux of water into and through till in a variety of hydrogeologic settings and pumping rates representative of the field sites.

Groundwater Geochemistry and Water Quality

Several laboratories provided analytical services for this study. The data from each laboratory were acceptable for the purposes of our study, unless otherwise noted in the text of this report. A summary of the quality assurance evaluation for these laboratories is provided in appendix tables 3.1 and 3.2 and in the metadata of the data release accompanying this report (Maher and others, 2020). Included in table 3.1 is information on replicates and blanks compiled during laboratory analyses, and included in table 3.2 are comparisons between split samples of analytes analyzed at two laboratories. All the geochemical data are available through the USGS NWIS database (U.S. Geological Survey, 2019) and the data release accompanying this report; guidance for accessing the data in NWIS is also provided in the data release (Maher and others, 2020).

Background Information

Background information and context for interpreting the geochemical constituents evaluated in this study are presented in this section. Information is included for stable isotopes of water (^{18}O and ^{2}H), enriched tritium, chloride, chloride to bromide ratios, nitrate, phosphorus, oxidation-reduction (redox) conditions, and major ions.

During the Wisconsinan glaciation, glacial ice locked up a large part of the ^{16}O and H from precipitation in the northern hemisphere, thus leaving most of the ^{18}O and ^{2}H in the oceans, where it became enriched in those isotopes. Till deposited by that ice under a cold climate may retain some of that isotopic signature, manifested by $\delta^{18}O$ values approaching −30 per mil (‰) and $\delta^{2}H$ values approaching −200 ‰ (Remenda and others, 1994). Unfractured, thick, and unweathered confining units in North America have been determined to hold glacial-age groundwater when the residence time of the groundwater is long enough (Remenda and others, 1994).

Enriched tritium was released into the atmosphere during the hydrogen bomb testing in the 1950s and 1960s. Today, it is used as an indicator of relative groundwater "age." Groundwater age is an indication of when water in the groundwater system was last exposed to the atmosphere. If there are detectable levels of tritium (greater than 0.8 tritium unit [TU]), then at least some of the water in the sample is considered to have been in the atmosphere "postbomb" and likely reached the groundwater system sometime after the 1950s. Samples with detectable concentrations could be a mixture of old, prebomb water and postbomb water, but at least some postbomb water is present. If there is no detectable tritium, then the sample water is considered to be "prebomb" and the water likely reached the groundwater system before the 1950s. For this report, samples with detectable tritium are considered to have "modern," post-1950s water, and samples without detectable tritium are considered to be "old," pre-1950s water. The special case of high tritium concentrations (greater than 15 TU) is also considered because groundwater tritium peaks related to the bomb peak that occurred in the mid-1960s have a tritium concentration of 15 TU or greater (Berg, 2019).

Chloride concentrations can be naturally occurring in groundwater or affected by anthropogenic activities. Salt (sodium chloride) can occur naturally in groundwater from the presence of halite deposits, weathering of bedrock, briny water, seawater, surficial materials, soils, and volcanic activity (Mullaney and others, 2009). In the United States, salt use has been increasing, mainly because of deicing activities, since the 1950s (Mullaney and others, 2009). Minnesota is known to have an influx of chloride from road salt contamination or wastewater correlated with urban land use (Kroening and Ferrey, 2013). Anthropogenic salt contamination in groundwater can come from sources other than deicing, including landfills that have food waste and products containing salt, water softeners, septic systems, household use, and agricultural use (Mullaney and others, 2009). Agricultural salt groundwater contamination can come from animal feed, fertilizers, and pesticides. Some fertilizers have potassium chloride, which raises chloride levels but not sodium levels in water resources (Mullaney and others, 2009).

In a survey of sand and gravel aquifers in Minnesota, chloride concentrations in groundwater were generally less

than 25 milligrams per liter (mg/L) in rural settings and greater than 25 mg/L in urban settings, with some urban groundwater having chloride concentrations greater than 250 mg/L (Kroening and Ferrey, 2013). Even though groundwater in rural settings generally had low chloride concentrations, anthropogenically sourced chloride was commonly present, making establishment of accurate background (nonanthropogenic) chloride concentration challenging (Kroening and Ferrey, 2013). Background chloride levels in Quaternary sediments in Canada and Illinois are generally between 15 and 20 mg/L (Howard and Beck, 1993) and between 1 and 15 mg/L (Kelly and others, 2012), respectively. Some aquifers contained in Cretaceous-age formations in southwestern and south-central Minnesota are known to have naturally high concentrations of chloride, as much as 1,500 mg/L (Kroening and Ferrey, 2013). Upward flux of groundwater from aquifers in older formations, such as the Red River-Winnipeg aquifer contained in the Ordovician-age Red River and Winnipeg Formations in northwestern Minnesota, has been known to increase salinity in groundwater in the overlying sediments (Ruhl and Adolphson, 1986), though this type of flow system is not represented at the piezometer nests of this study.

Chloride and bromide concentrations and ratios have been used by many scientists to evaluate the presence of groundwater contamination, such as from septic tanks and road salt (for example, Katz and others, 2011). The anions chloride and bromide are conservative tracers in water because neither anion has substantial ion exchange reactions at low temperatures, both are soluble, both are not likely to be adsorbed to mineral surfaces, and they only form minerals during extreme evaporation (Alcalá and Custodio, 2008).

A broad range of thresholds of chloride concentrations and chloride/bromide ratios have been used to classify samples as containing anthropogenically sourced chloride or not. In a national study that examined thousands of wells, groundwater samples with a chloride concentration between 20 and 100 mg/L and a chloride/bromide ratio between 400 and 1,100 were statistically more likely to contain other contaminants indicative of septic discharge; thus, chloride and chloride/bromide were determined to be a useful screening tool for identifying wells affected by septic systems (Katz and others, 2011). The Katz and others (2011) study was solely focused on screening for septic contamination rather than the effect of other sources such as road salt and fertilizers. In a statewide evaluation of chloride in groundwater in Minnesota, Kroening and Ferrey (2013) concluded that groundwater with a chloride concentration of less than 7 mg/L and a chloride/bromide ratio less than 200 was unaffected by anthropogenically sourced chloride, groundwater with a chloride concentration between 7 and 30 mg/L and a chloride/bromide ratio between 200 and 1,000 was "intermediate," and groundwater with a chloride concentration greater than 30 mg/L and a chloride/bromide ratio greater than 1,000 was definitely affected by anthropogenically sourced chloride. The term "intermediate" was used ambiguously and could indicate a mixed sample that contained some anthropogenically sourced chloride, or it could indicate samples that were difficult to classify as affected by anthropogenically sourced chloride. A report by Berg (2018, p. 23) for a northwestern Minnesota county (Clay County) states "chloride is elevated if concentrations are greater than or equal to 5 [parts per million] ppm. It is anthropogenic if chloride/bromide ratios are greater than 250." In Renville County, Minn. (the county containing the Olivia site), samples with a chloride concentration greater than 5 mg/L, a bromide concentration greater than 0.07 mg/L and a chloride/bromide ratio greater than 200 were used to classify samples as having anthropogenically sourced chloride (Bradt, 2017). At low bromide concentrations, defined as three times the minimum reporting limit, the chloride/bromide ratio becomes a much less reliable indicator of anthropogenically sourced chloride (Brian G. Katz, Environmental consultant and former USGS research hydrologist, written commun., July 2, 2020).

The chloride concentration and the chloride/bromide ratio are simply screening metrics to identify locations potentially affected by anthropogenic inputs. It is clear from the diversity of classification schemes discussed previously that there is plenty of room for interpreting chloride and chloride/bromide ratio data. The data are best used in conjunction with other chemical data to determine the presence of anthropogenic contamination at a given site. For this study, the classification scheme of chloride greater than 5 mg/L and a chloride/bromide ratio of 250 proposed by Berg (2018) was used to classify samples. Samples with concentrations less than these criteria were considered to not have anthropogenically sourced chloride. Samples with concentrations slightly greater than these criteria were classified as "intermediate," in that they may or may not have anthropogenically sourced chloride. Samples with values greater than these criteria, but with concentrations of bromide less than 0.03 mg/L (three times the reporting limit of bromide) were also classified as not having anthropogenically sourced chloride. Concentrations of more analytes indicative of anthropogenic contamination would be beneficial to improve the classification of the samples as affected by anthropogenic chemicals.

Nitrogen fertilizers are the primary cause of increasing nitrate concentrations in groundwater throughout the United States (Spalding and Exner, 1993; Sebilo and others, 2013). Other anthropogenic sources of increased nitrate include waste from animals and contaminated rainfall because of the combustion of fossil fuels (Kroening and Ferrey, 2013). Nitrate concentrations in groundwater are 1.1 mg/L or less in areas of Minnesota without nitrate from anthropogenic activities (Kroening and Ferrey, 2013). In Minnesota, the aquifers most affected by nitrate contamination are shallow sand and gravel aquifers underlying agricultural areas (Kroening and Ferrey, 2013).

Phosphorus concentrations in Minnesota groundwater have been determined to be more strongly related to geology, rather than land use (Kroening and Ferrey, 2013). Rocks and sediments that contain phosphorus-bearing minerals can weather and contribute phosphorus to groundwater (Kroening and Ferrey, 2013). Shale is one such rock, and sand and gravel aquifers in Minnesota deposited by glacial lobes sourced

from the west/northwest tend to have higher phosphorus concentrations because of the presence of carbonates and shale, compared to aquifer material deposited by northeast glacial lobes (Kroening and Ferrey, 2013). Anthropogenically sourced phosphorus in groundwater is usually from fertilizer use or waste (Minnesota Pollution Control Agency, 1999). Concentrations of phosphorus can also increase with increasing residence time, which may be associated with elevated iron and manganese (Minnesota Pollution Control Agency, 1999). Groundwater with low redox potentials can result in the dissociation of iron-phosphorus minerals, releasing adsorbed phosphorus (Burkart and others, 2004). The median phosphorus concentration for buried aquifers in Quaternary-age deposits in Minnesota is 0.124 mg/L (Minnesota Pollution Control Agency, 1999).

The oxidation-reduction (redox) state of groundwater is an important factor in determining the presence of harmful constituents in groundwater (McMahon and others, 2011). Some common byproducts of reducing environments are manganese, ferrous iron, hydrogen sulfide, and methane (McMahon and others, 2009). Zones can form in the subsurface where one electron-accepting process can dominate. Zones commonly form in subsurface recharge areas of aquifers. Near the point of recharge, at the beginning of a groundwater-flow path, DO reduction is the dominant process, followed by a zone of nitrate reduction below, followed by a zone of ferric iron reduction, and then the deepest zone is usually one of sulfate reduction (McMahon and others, 2011). These zones follow flow paths, and commonly, increasing age in groundwater systems coincides with increased reducing conditions (McMahon and others, 2011). Under reducing conditions, nitrate is typically not of concern because it is readily reduced, but other constituents become problematic for human health. The most common contaminants are geogenic; that is, they are "naturally" occurring in the system and are not introduced from anthropogenic activities. For example, under reducing conditions, phosphorus concentration can increase because of dissociation of iron-phosphorus minerals (Burkart and others, 2004), arsenic can be released, and certain metals can become soluble (McMahon and others, 2011).

Characterizing the major ion geochemistry of groundwater provides information about how groundwater geochemical composition evolves with residence time, through contact with different geologic units, and effects from anthropogenic activities. Major ion chemistry is useful for defining hydrochemical facies (Blanchette and others, 2010). Previous research has indicated cation exchange of sodium on sediments with calcium and magnesium along the direction of groundwater flow, leading to more calcium- and magnesium-dominated groundwater in water near the beginning of a flow path and more sodium-dominated groundwater associated with older water that is farther along a flow path (Hendry and Schwartz, 1990).

Groundwater Age and Evidence for Infiltration of Anthropogenic Chemicals

Stable isotopes of oxygen and hydrogen indicated no evidence of glacial-age groundwater greater than 11,000 years old in the till confining units at any site. This aligns with the range of travel times predicted from the Darcy calculations using either geometric mean K_h or K_v, which ranged from 1 to nearly 1,800 years across the sites. Values of $\delta^{18}O$ ranged from −7.4 to −12.0 ‰, and values of $\delta^{2}H$ ranged from −84.1 to −55.7 ‰ (fig. 14), both of which are well outside the range of glacial-aged water. All but one sample fell along the global meteoric water line (fig. 14). The two northern sites, HFC and Cromwell, generally had lower $\delta^{18}O$ and $\delta^{2}H$ values than the two southern sites, Olivia and Litchfield. This pattern is expected because fractionation increases with distance from the Gulf of Mexico, causing $\delta^{18}O$ and $\delta^{2}H$ values to decrease with increasing latitude. The only sample that plots distant from the global meteoric water line (Craig, 1961) is from a surficial aquifer well, MW–01, at the HFC site. This sample is most likely an evaporative signal, indicating that surface water from nearby lakes is recharging the surficial aquifer (Palmer and others, 2007). Stable isotope values from pore water are consistent with the groundwater samples from piezometers (fig. 14). These data indicate that the groundwater values mostly reflect what is in the till rather than an artifact left from the drilling process.

Enriched tritium indicates differences in travel times through till among the sites that generally corroborate travel time estimates from Darcy's law. Tritium data indicate faster fluxes of groundwater through till at the HFC and LFO1 sites compared to the Olivia and LFO2 sites (fig. 15). Tritium values greater than 1 TU were detected in all till piezometers at the HFC and LFO1 sites, indicating the presence of modern water throughout these till profiles. Both sites have a tritium peak within the till confining units. The tritium peak is near the bottom of the till at the LFO1 site, whereas at the HFC site, the tritium peak is near the top of the till unit. The peak value at the LFO1 site was 16.1 TU, and the peak at the HFC site was 21.1 TU, both of which fall in the range of a mid-1960s bomb peak tritium value.

At the LFO1 site, assuming piston flow and the tritium peak at LFO1–E represents water that reached the surficial aquifer in 1966, groundwater took 50 years (1966–2016) to travel from the water table surface to the deepest till piezometer (LFO1–E). This is within the range of travel times (1 to 74 years) estimated with hydraulic data according to Darcy's law (table 7). At the LFO1 site, travel time estimates made using tritium data are expected to be toward the high side of the Darcy calculations because the tritium travel time estimate includes vertical travel through a 30-ft thickness of surficial aquifer in addition to the till profile, whereas the Darcy calculations in table 7 only include travel through the till profile. Assuming the distance traveled is from the mean water table surface (11.20 ft below land surface, measured in the

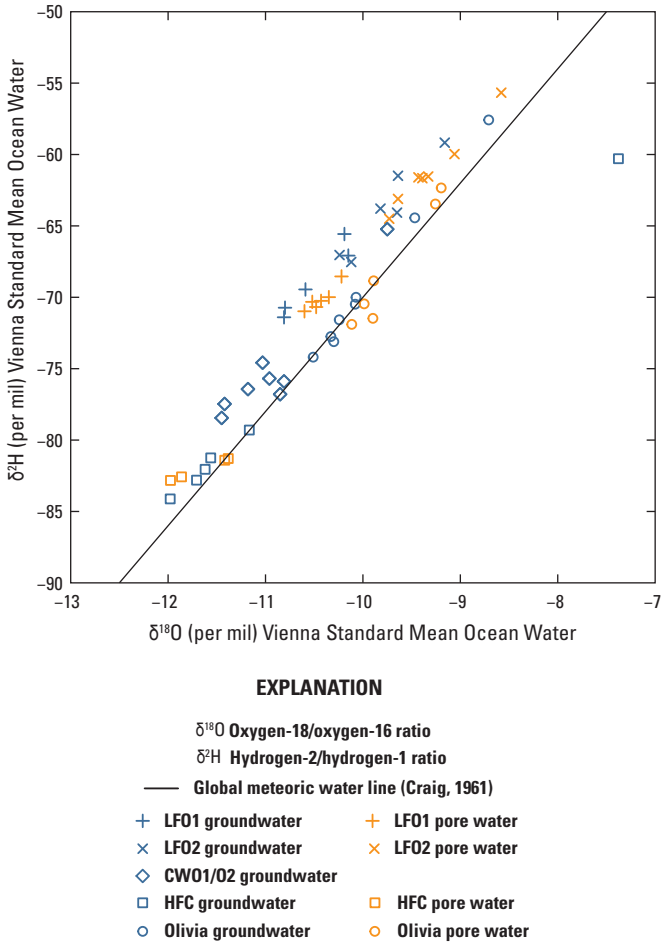

Figure 14. Comparison of oxygen-18/oxygen-16 ratios ($\delta^{18}O$) and hydrogen-2/hydrogen-1 ratios ($\delta^{2}H$) with the global meteoric water line for groundwater and pore-water samples from the Litchfield 1 (LFO1), Litchfield 2 (LFO2), Cromwell (CWO1/O2), Olivia, and hydrogeology field camp (HFC) sites.

shallowest well of the nest, LFO1–B, table 1) to the midpoint of the LFO1–E screen (93.74 ft below land surface, table 1), the mean linear velocity according to the tritium data is 0.0045 ft/d. This is within the range of mean linear velocities of 0.002 to 0.2 ft/d computed according to Darcy's law (table 7).

At the HFC site, assuming that the tritium peak at HT–115 represents water that reached the surficial aquifer in 1967, the travel time from the water table surface through a 53-ft thickness of saturated material, including 42 ft of surficial aquifer and 11 ft of till, was 50 years (1967–2017). This translates to a mean vertical linear velocity of 0.0029 ft/d. The Darcy's law calculation indicates a faster vertical travel time through till: 50–56 years to travel a vertical distance of 100 ft with a mean vertical linear velocity of 0.005 ft/d.

At the LFO2 and Olivia sites, tritium concentrations of about 5–6 TU are only seen in the upper one-third of the till units (fig. 15*B*,*E*). At the LFO2 site, tritium was only detected in the two uppermost till piezometers, to about 35 ft into the till, and at the Olivia site, tritium was only detected in the uppermost till piezometer, at a depth of about 8 ft into the till; therefore, most of the till thickness at these sites contained nonmodern water (older than 1953). The Darcy's law calculations of travel time through till at these sites are in the hundreds of years, so in a general sense, the tritium data corroborate the Darcy's law travel time calculations.

At the Cromwell site, tritium concentrations of around 5 TU are present in the surficial aquifer and the confined aquifer, but not the till in between (fig. 15*C*). The hydraulic gradient data and the tritium data indicate that recharge to the confined aquifer enters the system somewhere upgradient in the same buried aquifer system or perhaps through a stratigraphic window in the overlying till confining unit where the hydraulic gradient in the till is downward. The till sequence observed near the production well may therefore have little direct effect on the quality and quantity of water at the Cromwell site. Rather, anthropogenic activities and geologic materials at a distal recharge area (yet to be defined) may affect the water observed in the confined aquifer at the Cromwell site.

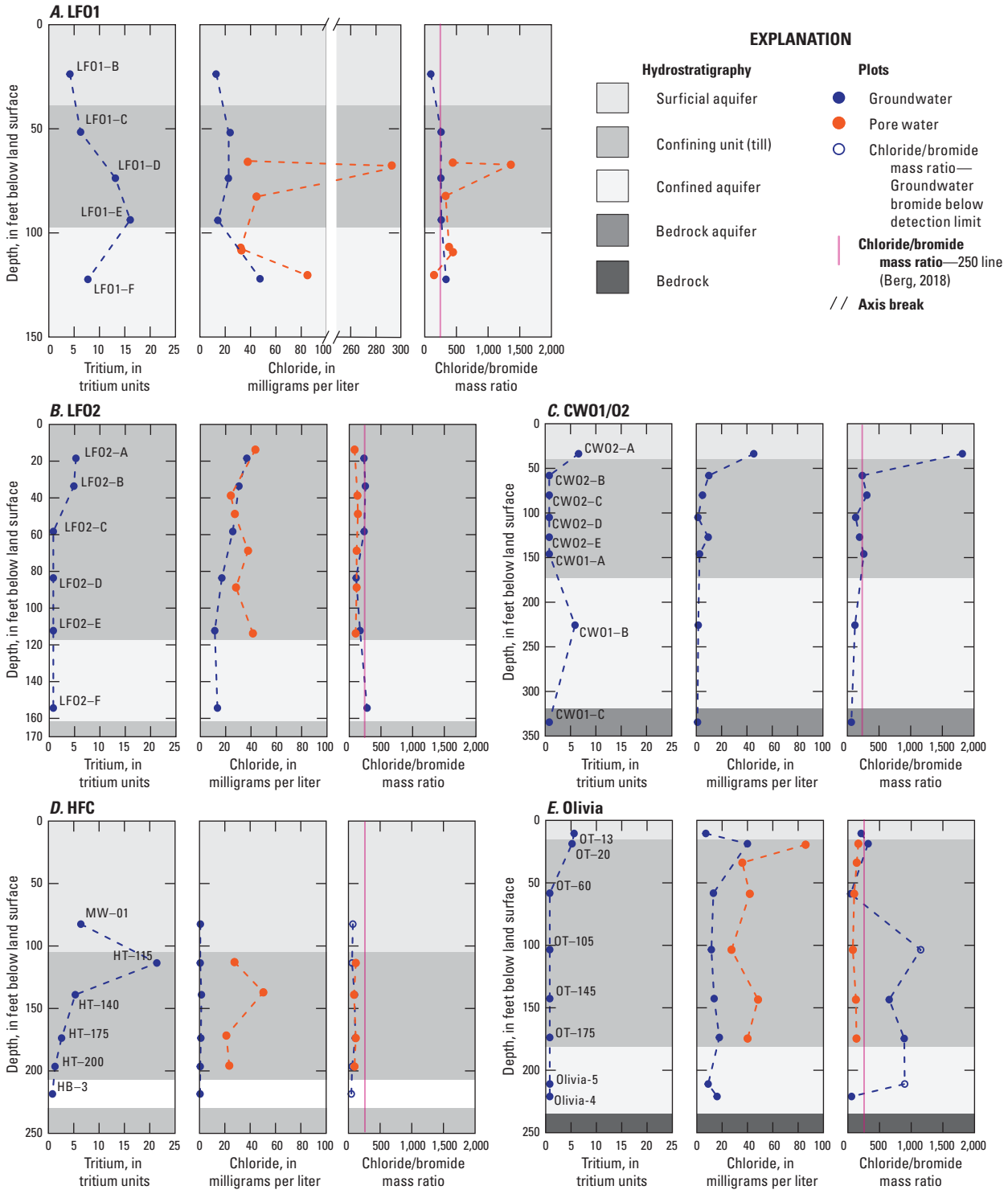

Figure 15. Vertical profiles of tritium, chloride concentrations, and chloride/bromide mass ratios in groundwater and pore-water samples. *A*, from the Litchfield 1 (LFO1) site; *B*, from the Litchfield 2 (LFO2) site; *C*, from the Cromwell (CWO1/O2) site; *D*, from the hydrogeology field camp (HFC) site; *E*, from the Olivia site.

Anthropogenically sourced chloride inputs are variable among the four study sites. Three of the sites, Litchfield, Cromwell, and Olivia, are in developed municipalities with high road densities and likely higher road salt applications compared to the HFC site, which is in the middle of a large forested area with few roads. Furthermore, the land surrounding the towns of Litchfield and Olivia is predominantly row-crop agriculture, which likely receives additional fertilizer inputs containing chloride.

Chloride concentrations, as well as chloride/bromide mass ratios in the groundwater at the Litchfield, Cromwell, and Olivia sites, indicate some anthropogenically sourced chloride is present in the till profiles, though the depth of penetration varies by site. A chloride/bromide ratio greater than 250 is considered to be an indicator of possible anthropogenically sourced chloride for this discussion (Berg, 2018). Except for the LFO1 site, all pore-water chloride/bromide mass ratios indicate no anthropogenically sourced chloride. At the LFO1 site, groundwater and pore-water chloride/bromide ratios are greater than or near 250 (fig. 15*A*).

Chloride concentration profiles at the LFO1 and LFO2 sites were different (fig. 15*A*,*B*). At the LFO1 site, pore-water and groundwater chloride concentrations in the till unit were all around 20–40 mg/L, except for one pore-water outlier that was near 300 mg/L. Most pore-water chloride concentrations are higher than groundwater chloride concentrations. Groundwater from the confined aquifer has stronger indicators of anthropogenically sourced chloride compared to the values observed in the till. The groundwater chloride/bromide mass ratios are between 250 and 261 in the till unit whereas in the confined aquifer, the groundwater chloride/bromide mass ratio is 336 and the chloride concentration is 47.07 mg/L. At LFO2, the highest concentration of chloride in groundwater, about 40 mg/L, was in the shallowest piezometer, and then chloride decreases in groundwater through the till unit. Pore water has concentrations that range from 20 to slightly greater than 40 mg/L in the till unit. In contrast to the LFO1 site, most pore-water concentrations and chloride/bromide mass ratios at LFO2 are lower than groundwater concentrations. Similar to the LFO1 site, the chloride concentration in the confined aquifer at the LFO2 site was greater than the concentration in the deepest till piezometer just above the confined aquifer. The chloride/bromide mass ratio in the confined aquifer at LFO2 was 278, higher than any ratio observed in the till at LFO2. At both nests, LFO1 and LFO2, the confined aquifer had stronger evidence for anthropogenically sourced chloride than the lower portion of the till, a possible indication of a chloride source reaching the confined aquifer in an area not represented by LFO1 or LFO2. In the confined aquifer, groundwater flow will primarily be horizontal toward the production wells. The water sampled from the confined aquifer piezometers may be representative of a different, perhaps larger, area than the till directly above and may explain why confined aquifer chloride concentrations are higher than till concentrations.

At the CWO1/O2 site, which has an overall upward hydraulic gradient through the vertical transect, groundwater chloride concentrations ranged from 1 to 45 mg/L and decreased with depth to near background values in the till and confined aquifer (fig. 15*D*). Chloride/bromide mass ratios are near or below 250 in the till and confined aquifer, but the surficial unit demonstrates a chloride/bromide mass ratio nearing 2,000, which is a strong indication of anthropogenically sourced chloride (fig. 15*D*). Because of the upward gradient at this well nest site, the chloride in the surficial aquifer at the location of the CWO1/O2 nest is not likely to reach the confined aquifer, though chloride could reach the confined aquifer where recharge to that aquifer occurs.

At the HFC site, the pore-water samples had higher chloride concentrations than groundwater samples. The chloride concentrations ranged from 0.46 to 50 mg/L (fig. 15*D*). All groundwater samples had chloride concentrations less than 5 mg/L, whereas chloride concentrations in pore-water samples were all greater than 20 mg/L. The pore-water chloride concentrations at the HFC site are comparable to pore-water chloride concentrations at other sites; however, the groundwater chloride concentrations at the HFC site are consistently lower than the chloride concentrations at the other sites. The groundwater concentrations of chloride at several piezometers at the CWO1/O2 site are also low among the sites, indicating that background chloride tends to be lower in sandier tills.

The Olivia site chloride concentrations in groundwater and pore water were fairly consistent throughout the till, with the exception of samples collected at about 20 ft below land surface. Groundwater and pore water concentrations were about double at this depth compared to all other till concentrations (fig. 15*E*). Chloride concentrations at this site ranged from 7 to 86 mg/L. Similar to the HFC and LFO1 sites, all pore-water samples at the Olivia site have higher chloride concentrations than the groundwater samples at similar depth intervals. Groundwater chloride concentrations were generally less than 20 mg/L whereas pore-water chloride concentrations were between 30 and 40 mg/L (fig. 15). Groundwater in the three deepest till piezometers at the Olivia site had the highest chloride/bromide mass ratios, ranging from 652 to 1,150, of all of the till piezometers at all the sites. The high ratios at depth were generally caused by extremely low or nondetectable bromide concentrations as opposed to high chloride concentrations. At low bromide concentrations, defined as three times the minimum reporting limit, the chloride/bromide ratio becomes a much less reliable indicator of anthropogenically sourced chloride (Brian G. Katz, Environmental consultant and former USGS research hydrologist, written commun., July 2, 2020). The minimum reporting limit at the USGS NWQL for bromide is 0.01 mg/L, so the chloride/bromide ratio becomes less reliable at bromide concentrations of 0.03 mg/L or lower. In Renville County, chloride/bromide ratios were determined to be a less reliable indicator of anthropogenically sourced chloride at a bromide concentration of less than about 0.07 mg/L (Bradt, 2017); therefore the high chloride/bromide ratios at the Olivia site do not necessarily indicate anthropogenically sourced chloride.

One hypothesis for the low bromide concentrations at the Olivia site is bromide sorption to clay. To evaluate this hypothesis, bromide concentrations of pore water and groundwater were compared with clay content of colocated samples from detailed grain size analyses across all sites (Staley and others, 2018). No strong correlations between bromide and clay content were evident. Bromide can sorb to clays in certain circumstances. At some pH levels, bromide can adsorb to clay minerals such as kaolinite and montmorillonite as well as iron and aluminum oxides (Goldberg and Kabengi, 2010). The mineral adsorption of bromide can occur at a pH of as much as 8; however, there is minimal adsorption at a pH of greater than 7 (Goldberg and Kabengi, 2010). Almost all piezometers had groundwater with a pH greater than 7. Only two piezometers had a groundwater pH slightly lower than 7. These two piezometers were shallow (greater than 20 ft below land surface) and possibly affected by a more recent influx of precipitation. Given all of these observations, bromide adsorption was probably not an important factor for the low bromide concentrations observed in till at the Olivia site.

Differences in chloride concentrations between groundwater and pore water were observed at the sites where both types of water were sampled. At three sites (LFO1, HFC, and Oliva), pore-water chloride was generally greater than groundwater chloride and at one site (LFO2), the opposite was observed. The differences in chloride concentrations between pore water and groundwater may be due to several processes. One hypothesis is that the sampled water came from different sampling scales. The till cores collected and squeezed for pore water were 6 in. long and 4 in. in diameter and contained a water volume of about 0.31 liter (L; 0.08 gallon [gal]) assuming a porosity of 25 percent, whereas groundwater samples represented a 5-ft screen and a borehole annulus diameter of 6.75 in., which contained about 8.8 L (2.3 gal) of water. Thus, the chloride concentration of pore water represented a much smaller sample volume compared to groundwater. A second hypothesis is that evaporation or other effects from sample handling procedures could have affected the chloride concentration of pore-water samples differently than groundwater samples because the two sample types were handled differently. Cores were wrapped in plastic and shipped to a laboratory where pore water was extracted weeks to months after sample collection. The pore water was then shipped to a second laboratory for analysis. Groundwater samples were collected in bottles, sealed immediately, and then shipped to a laboratory for analysis. The $\delta^{18}O$ and $\delta^{2}H$ values did not indicate an evaporation effect in the pore water from the till core samples. A third hypothesis is that drilling operations introduced groundwater with chloride concentrations different than ambient conditions to the formation. The pore-water samples would have been minimally affected by drilling fluids because the cores were collected ahead of the fluid injection point. The groundwater samples were collected after completion of drilling, and so could have been much more affected by the water used during the drilling process. This hypothesis cannot be fully evaluated because the water used for drilling operations at each site was not sampled.

Dissolved Nitrate, Dissolved Phosphorus, and Oxidation-Reduction (Redox) Conditions in Groundwater

Nitrate was detected infrequently and at low concentrations in groundwater samples across all study sites. The highest concentration of 1.78 mg/L as nitrogen was measured in the shallowest piezometer at the Cromwell site. This is the only sample with a concentration higher than the statewide ambient nitrate concentration of 1.1 mg/L (Kroening and Ferrey, 2013). The shallowest piezometer at the Olivia site had a concentration of 1.06 mg/L as nitrogen, and all other samples had nitrate concentrations less than 0.4 mg/L as nitrogen. The HFC site had no detectable nitrate (less than 0.01 mg/L as nitrogen) present in any groundwater samples (fig. 16*D*). The low nitrate concentrations were somewhat surprising, especially at the Litchfield and Olivia sites where the broader landscape is dominated by row-crop agriculture. In Iowa, for example, nitrate concentrations of greater than 10 mg/L as nitrogen have been measured in confined aquifers (Eidem and others, 1999; Rodvang and Simpkins, 2001).

Given the low concentrations of nitrate at all sampling locations, it is difficult to evaluate if denitrification is occurring along the vertical till profiles at the study sites. If, for example, anthropogenically sourced chloride was present through a vertical profile and nitrate concentrations decreased with depth in the same profile, this would be indirect evidence that denitrification could be occurring, particularly if redox conditions in the profile are reducing. At the Cromwell site, the highest nitrate concentration (1.78 mg/L as nitrogen) is coincident with the highest chloride concentration in the shallowest piezometer (CWO2–A). Below this depth, chloride and nitrate concentrations are lower. Because the conservative analyte concentration (chloride) decreases as well as the reactive analyte concentration (nitrate), this indicates there could be hydrologic reasons (for example, dilution) for lower nitrate concentrations at depth at the Cromwell site rather than denitrification. There is slight indirect evidence for denitrification occurring in till at the Olivia site. The only detection of nitrate occurred in the shallowest piezometer, OT–13. The highest chloride concentration occurred in the next deepest piezometer, OT–20, and this concentration is marginally indicative of anthropogenically sourced chloride. DO, iron, and manganese indicate reducing conditions that would support denitrification at the depth of OT–20 (about 20 ft below land surface; fig. 17*E*).

Though not observed in this study, other studies of the Des Moines lobe tills in Iowa (Simpkins and Parkin, 1993; Parkin and Simpkins, 1995) have demonstrated nitrate removal by denitrification in till. Simpkins and Parkin (1993) detected extremely reducing, methanogenic conditions in Des Moines lobe tills and reported that denitrification would occur in the Des Moines lobe tills unless recharge rates are unusually high.

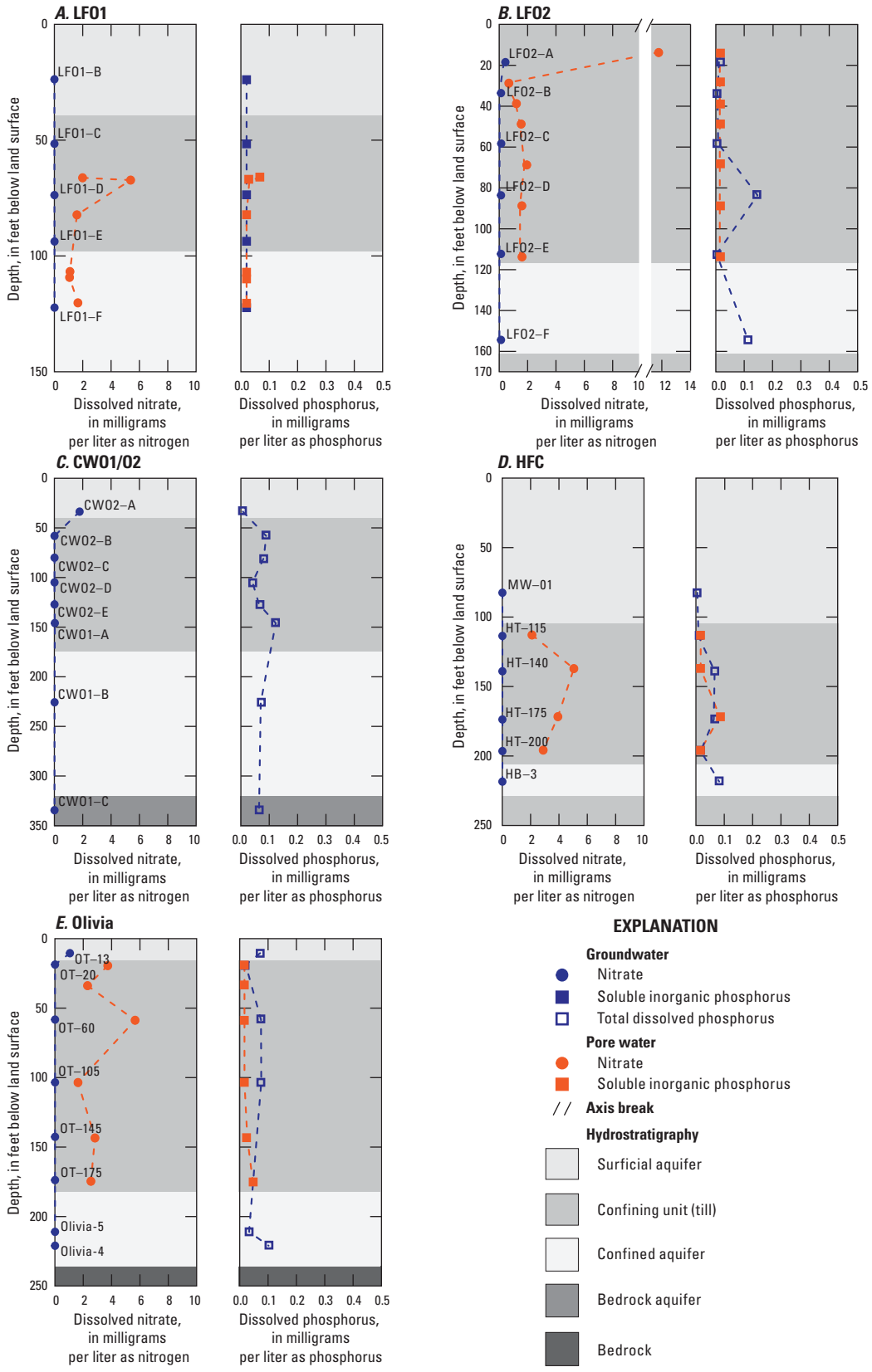

Figure 16. Vertical profiles of dissolved nitrate and phosphorus concentrations in groundwater and pore-water samples. *A*, from the Litchfield 1 (LFO1) site; *B*, from the Litchfield 2 (LFO2) site; *C*, from the Cromwell (CWO1/O2) site; *D*, from the hydrogeology field camp (HFC) site; *E*, from the Olivia site.

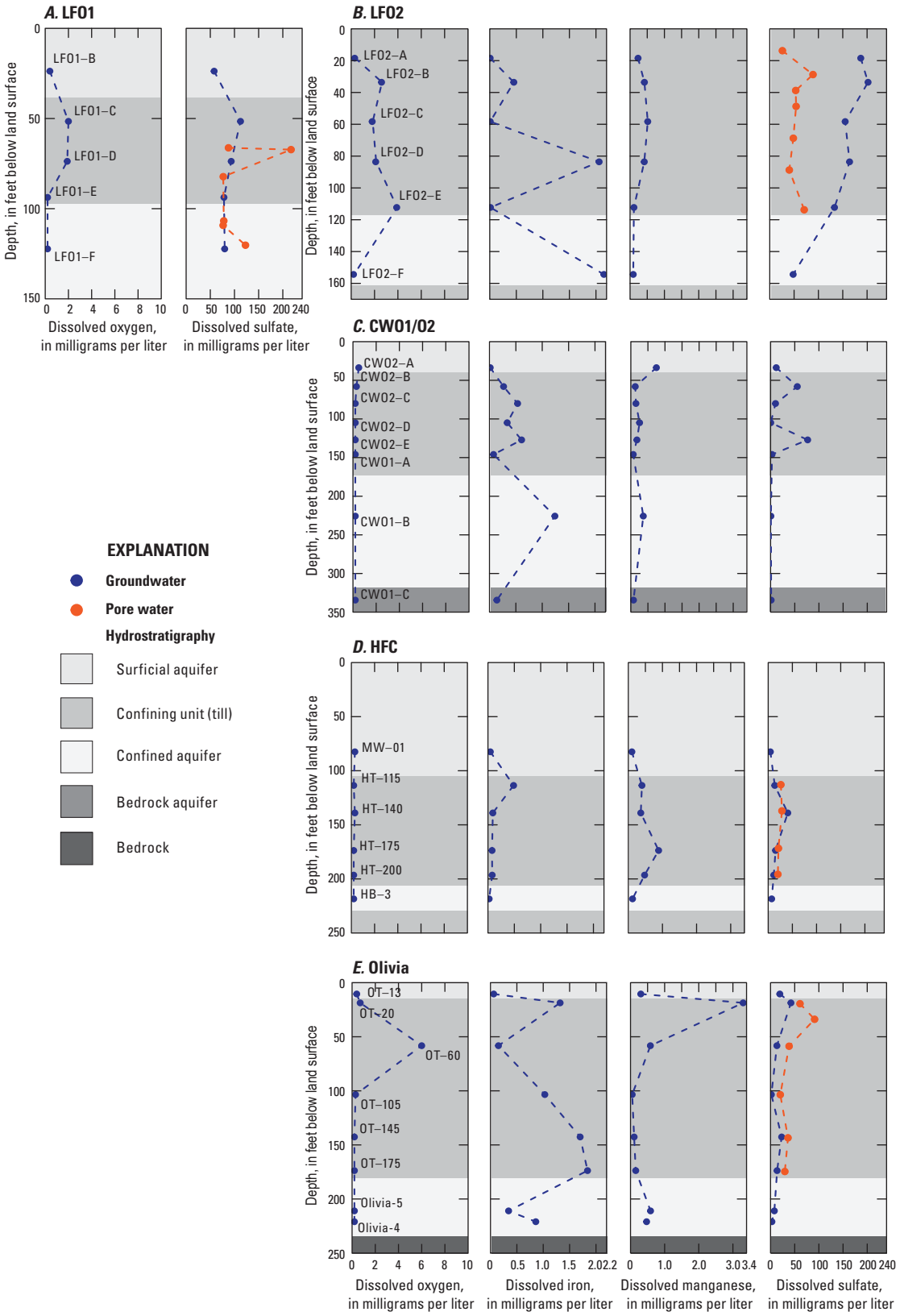

Figure 17. Vertical profiles of concentrations of oxidation-reduction (redox) indicators in groundwater and pore-water including dissolved oxygen, iron, manganese, and sulfate. *A*, at the Litchfield 1 (LFO1) site; *B*, at the Litchfield 2 (LFO2) site; *C*, at the Cromwell (CWO1/O2) site; *D*, at the hydrogeology field camp (HFC) site; *E*, at the Olivia site.

Pore-water nitrate concentrations tended to be higher than the corresponding groundwater samples (fig. 16). The higher pore-water nitrate values are likely from inadequate sample handling procedures and, therefore, are not an accurate representation of in situ pore-water nitrate. This difference is probably due to the processing of the core samples. Groundwater samples were held to strict holding times and were chilled until laboratory analyses were completed. The cores were stored for months before being squeezed. After the pore water was extracted from the core, the pore water was not chilled continuously before being analyzed for nitrate. Given that there were reducing conditions in the sediments and that cores were not processed in an anoxic environment, it is possible that ammonia was present in the pore water and was oxidized to nitrate during the sample handling.

Profiles of phosphorus concentrations along with the chloride, tritium, and travel time calculations indicate a potential geologic source of dissolved phosphorus rather than vertical penetration of anthropogenically sourced phosphorus from the surface into the subsurface (fig. 16). For example, at the LFO2 and Olivia sites, phosphorus was detected at depth in the till (fig. 16*B*,*E*) in piezometers where there was no evidence of anthropogenically sourced chloride and tritium, and Darcy calculations indicated vertical travel times of hundreds of years. At a leaky till site, LFO1, phosphorus was not detected in any piezometers despite modern water being present throughout the till profile. Phosphorus was detected throughout the tills at the HFC and Cromwell (CWO1/O2) sites (fig. 16*C*,*D*). Generally, pore-water phosphorus concentrations were lower than groundwater phosphorus concentrations, though there are a few exceptions (fig. 16). Overall, groundwater phosphorus concentrations varied from less than 0.003 to 0.147 mg/L as phosphorus. Groundwater concentrations of phosphorus in till piezometers were equal to or greater than concentrations of phosphorus in surficial aquifer piezometers. Groundwater samples from all the confined aquifers had detectable phosphorus (fig. 16), with concentrations generally lower than the statewide median (0.124 mg/L) for buried aquifers contained in Quaternary-age deposits in Minnesota (Minnesota Pollution Control Agency, 1999).

Concentrations of redox indicator species including DO, iron, manganese, and sulfate generally indicate that reducing conditions exist in the tills at each site, though there was substantial variability in concentrations of these species with depth. One consistent anomaly was the existence of higher than expected DO concentrations in several till piezometers. Concentrations of DO in six of the eight till piezometers at the LFO1 and LFO2 sites and in piezometer OT–60 at the Olivia site were higher than expected given the presence of other redox species; furthermore, a near-zero DO sample was collected in the uppermost piezometer at the LFO1, LFO2, and Olivia sites. The six Litchfield till piezometers had DO concentrations near 2 mg/L, and OT–60 had an extremely high DO concentration of 6.0 mg/L (fig. 17). For the instruments used in this study, the uncertainty of the probe DO readings is plus or minus 0.2 mg/L, which means that any reading greater than 0.2 mg/L indicates the presence of oxygen (Lewis, 2006).

Higher than expected DO in till piezometers may be explained in part by the multiday purging and low-flow methods used for sampling till piezometers in low *K* settings. At least three well volumes were purged before collecting water-quality samples. In some cases, it took multiple days to complete this purging process. This means that the water in the piezometers could have been exposed to oxygen for many hours before sampling. The pumping flow rate used for sampling the till piezometers was low (often less than 0.2 gal/min) and often resulted in dozens of feet of drawdown, allowing more time for water to be exposed to oxygen before being measured by the probe on the sonde. Therefore, the field DO measurements from till piezometers are less reliable than field DO measurements from sampling procedures used for aquifer wells. Groundwater from aquifer wells had far less opportunity for oxygen exposure because the wells could be purged and sampled with higher flow rates (typically greater than 0.7 gal/min) all on the same day.

The conditions at the Litchfield site seem to be reducing, despite the previously mentioned elevated DO concentrations in most till piezometers (fig. 17). At the LFO1 site, sulfate concentrations are low in the uppermost piezometer, corresponding to low DO. Sulfate concentrations then increase in the second piezometer and then gradually decrease down into the confined aquifer. A similar pattern in sulfate concentrations occurred at LFO2. This could mean that sulfate reduction is occurring along a vertical flow path. Aside from DO and sulfate concentrations, no other redox data are available for the LFO1 site. At the LFO2 site, dissolved iron is variable with depth; the highest values (greater than 2.0 mg/L) occur at LFO2–D (till) and LFO2–F (confined aquifer). Dissolved manganese gradually increases in concentration from the top of the till (LFO2–A) to the approximate midpoint of the till profile (LFO2–C). Below LFO2–C, the manganese concentrations then gradually decrease again.

Redox species indicate reducing conditions at the Cromwell (CWO1/O2) site. Concentrations of DO were low throughout the profile; the highest DO concentration (0.5 mg/L) was measured in the surficial aquifer. Dissolved iron and manganese were present throughout the profile. The highest manganese concentration (0.749 mg/L) occurred in the surficial aquifer, and the highest iron concentration (1.24 mg/L) occurred in the confined aquifer. The presence of manganese and iron and the absence of sulfate in the confined aquifer indicate the confined aquifer is the most reduced environment at this site. Manganese, iron, and sulfate concentrations were variable in the till piezometers at this site. Sulfate concentrations were less than 3 mg/L at the depth of CWO1–A (about 140 ft below land surface) and lower.

Redox species indicate reducing conditions at the HFC site (fig. 17*D*). Concentrations of DO were low at all piezometers, ranging from 0.2 to 0.3 mg/L (fig. 17*D*). Dissolved iron, manganese, and sulfate were comparatively low at this site relative to the other sites. These analytes all had peak

concentrations at different depths. The highest dissolved iron concentration occurred at HT–115 (0.5 mg/L), which is about 10 ft below the top of the till unit. Below this piezometer, dissolved iron concentrations were less than 0.1 mg/L. Dissolved manganese concentrations gradually increased through the till, peaking at a concentration of 0.9 mg/L at HT–175, about 70 ft below the top of the till, and then gradually decreased down into the confined aquifer. Dissolved sulfate concentrations gradually increased until HT–140, about 35 ft below the top of the till, and then gradually decreased down into the confined aquifer (fig. 17*D*).

At the Olivia site, conditions were generally reducing, though there were anomalously high DO and low iron concentrations at piezometer OT–60 (about 60 ft below land surface) (fig. 17*E*). The surficial aquifer may have been only slightly reducing as indicated by the data from OT–13. At OT–13, DO was low (0.4 mg/L), but so were dissolved iron and manganese concentrations. Nitrate was also detected at this well in the surficial aquifer (fig. 16*E*). At OT–20, DO went up slightly to 0.7 mg/L, but dissolved iron and manganese concentrations increased substantially to 1.32 mg/L and 3.3 mg/L, respectively. The next deepest piezometer, OT–60, had extremely high DO (6.0 mg/L) and low iron (0.15 mg/L) concentrations. In the remainder of the till piezometers at this site, dissolved iron concentrations increased with depth, manganese generally decreased with depth, and sulfate concentrations were low and variable (fig. 17*E*). The confined aquifer was definitely a reduced environment because of low DO and elevated iron and manganese concentrations. The steady increase in dissolved iron indicates that there may be an iron-reducing zone in the bottom half of the till confining unit.

Groundwater Type

A Piper plot (Piper, 1944) was used to characterize the groundwater type and evolution at each site (fig. 18). Major ion composition data from the two sites with the longest travel times, Olivia and LFO2, provided evidence for the evolution of groundwater geochemical composition along vertical flow paths (shallowest to deepest). At these sites, shallow, young groundwater in till had distinct major ion compositions compared to older groundwater deeper into the till profile. Groundwater in the two shallowest piezometers at the Olivia site was predominantly calcium bicarbonate and magnesium bicarbonate, whereas all till piezometers below 60 ft (OT–60 and below) contained groundwater samples that were predominantly sodium bicarbonate, or nearly so. At the LFO2 site, groundwater from the two shallowest piezometers had higher calcium and magnesium and lower sodium compared to groundwater from piezometers deeper in the till. However, at the LFO2 site, all groundwater samples were still in the water type of calcium bicarbonate and magnesium bicarbonate (or between calcium and magnesium) except for groundwater from LFO2–E, the deepest till piezometer, which approaches the sodium bicarbonate water type.

Most of the remaining piezometers at the Cromwell, LFO1, and HFC sites had calcium or magnesium as the dominant cation and bicarbonate as the dominant anion. The HFC site had one outlier groundwater sample from piezometer HT–140 that is a sodium bicarbonate water type. It is not clear if this is a unique signature caused by hydrogeological interactions or if it is caused by sodium-bentonite contamination from the piezometer installation process.

Sources of Uncertainty

Though the geology of these sites was well characterized by the MGS, there are still some uncertainties in this information. At each site, one or two continuous cores from boreholes were analyzed by the MGS and were used for understanding the stratigraphy and hydrostratigraphy for the vertical transects. Heterogeneity in the geology of the systems, such as sand or clay lenses, may have been missed because of the inability to analyze all cores from piezometer installation. Possibly, an important geologic layer with distinct hydraulic properties that affects the vertical flux of groundwater could have been missed. Fractures can be an important feature for the flux of water through till but fractures that lack staining are difficult to identify in cores. Even if unstained fractures are observed, it is unknown if they were present in situ or if they were introduced by the coring process.

Uncertainty in K estimates from slug tests can come from a variety of sources. The geometric mean K_h values for the till units are based on slug test results from the piezometer screened intervals, but K_h between the screened intervals is unknown. Drilling and installation of the piezometers may have affected the K values estimated from slug and aquifer tests. For instance, drilling, especially auger drilling, can produce a smear zone along a borehole that creates a zone of lower K_h along the wall of the borehole when the actual formation has a higher K_h (Cherry and others, 2004). A variety of drilling methods were used in this study (hollow-stem auger, mud rotary, and rotary-sonic; table 1.1), but the effects of these methods on the estimates of K_h were not evaluated. As previously discussed, there is also uncertainty in the modeling operations used to determine K_h from slug test data and K_v from aquifer test data.

This study relied on geochemistry to corroborate hydraulic data; however, each site was sampled within months of drilling, and most sites were only sampled once. It is therefore possible that water-quality samples were affected by the drilling and installation of piezometers, especially in low K zones. Sodium-bentonite contamination of groundwater and intrusion into screened intervals may have occurred during the piezometer installation process for some piezometers. Analytes that are associated with bentonite contamination include chloride, bromide, sodium, and sulfate (Remenda and van der Kamp, 1997). Other studies have indicated that these analytes will be elevated in concentration initially after

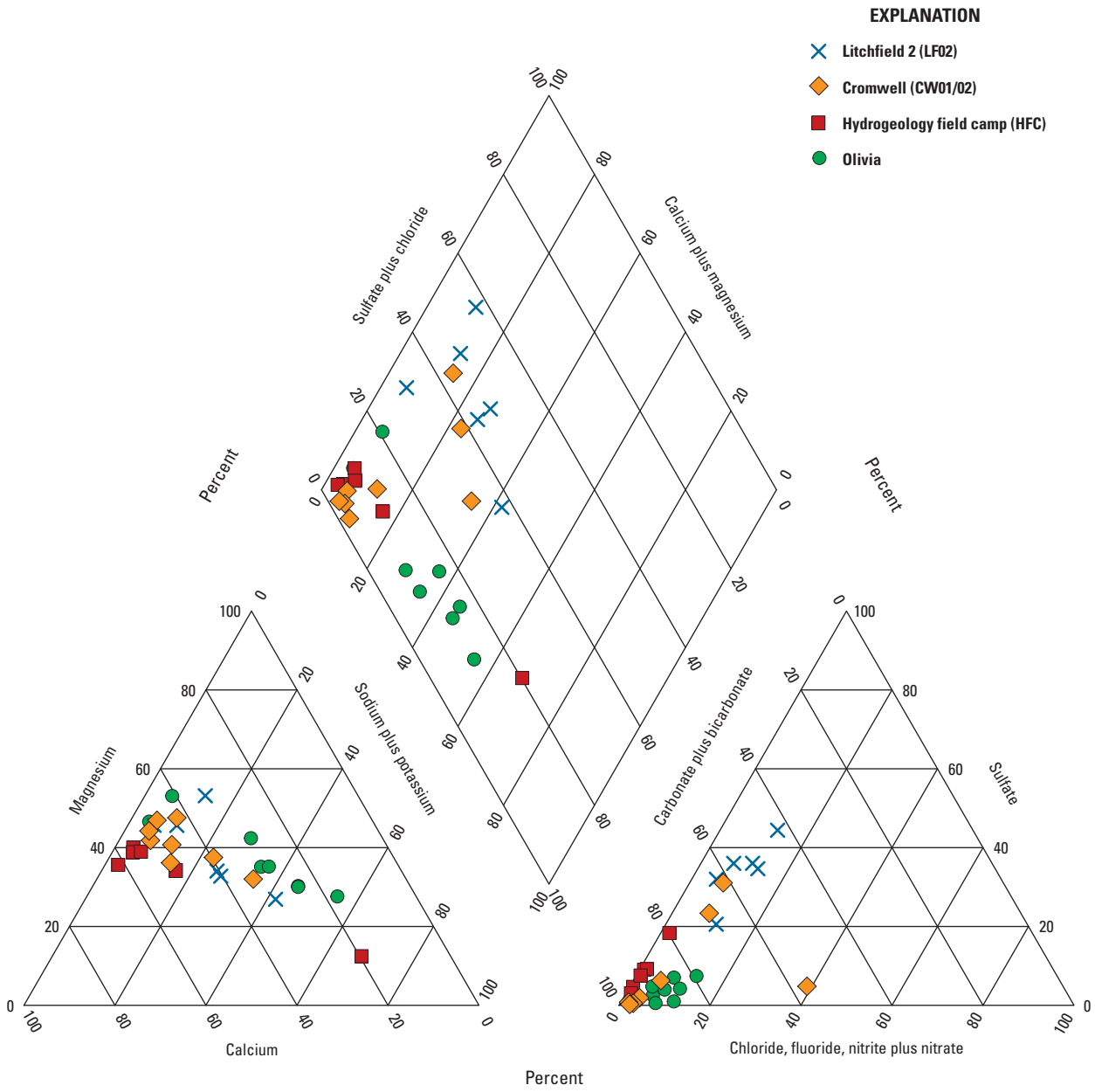

Figure 18. Piper diagram of major ion concentrations in groundwater samples from piezometer nests at the Litchfield 2 (LFO2), Cromwell (CWO1/O2), hydrogeology field camp (HFC), and Olivia sites.

installation and then decrease through time (Remenda and van der Kamp, 1997). For this study, funding was insufficient to do repeated samplings, so it is unknown of the geochemical results were affected by drilling operations. Additional samples would be beneficial for a more complete evaluation of the effect of bentonite on water-quality samples presented in this report.

Assuming that the drilling effects on water quality will be smaller in aquifer wells compared to till piezometers (because water fluxes are higher through pumped aquifers than tills), a comparison between aquifer chemistry and till chemistry may provide some insight into the potential for bentonite to affect water chemistry. Confined aquifer groundwater samples have a sodium concentration similar to till piezometer groundwater samples for the Olivia, HFC, and Cromwell sites (data available on https://doi.org/10.5066/F7P55KJN; U.S. Geological Survey, 2019). At the LFO2 site, there is less sodium in the confined aquifer compared to till piezometers, indicating a potential effect of bentonite on water-quality samples at the LFO2 till piezometers. At the HFC site, HT–140 groundwater may have sodium-bentonite contamination because the groundwater from this sample has a high sodium concentration compared to all other piezometer and well groundwater samples.

Heuristic Groundwater Modeling

A series of model scenarios demonstrated that pumping groundwater from buried aquifers affected water levels and groundwater fluxes through the till. The magnitude of the pumping effects varied substantially across the range of hydrogeological properties observed at the field sites in this study. Response variables extracted from steady-state model outputs are given in table 8. These models demonstrated that for understanding sustainability of groundwater pumping from confined aquifers, knowledge of till hydraulic properties is just as important as knowledge of aquifer hydraulic properties.

The north and south constant head boundary conditions minimally contributed to the water pumped from the buried sand unit for all but three model scenarios (table 8). In the LsLvHc, MsLvHc, HsLvHc scenarios, about 10 percent of the pumped water originated from the boundary cells (table 8). Calculations of water emanating from boundary cells were implemented as a quality assurance measure but still yielded useful information about the water source to the wells. These three scenarios all had a low K_v for till overlying the buried sand unit and a high K_h for the middle unit (LvHc). A total of 80 to 90 percent of the water entered the buried sand unit through its sides. The implication is that in this hydrogeologic setting, the contributing area for pumping is laterally extensive, extending farther than 10 mi from the well field.

The small buried sand unit size of 1.0 mi by 0.5 mi (Ls) generally could not sustain pumping at 900 gal/min, unless the buried sand unit was surrounded by conductive till (Hc). The most comparable field site to this situation is the Olivia site where two high-capacity production wells were completed in a buried sand and gravel aquifer that is mapped to be 0.08 mi^2 (Bradt, 2017), though the aquifer could be larger because its extent has been estimated with limited data. These wells pump at an approximate rate of 123 gal/min, and the geometric mean K_h of the till confining unit was 0.004 ft/d and the bulk K_v of the till confining unit was between 0.0005 and 0.001 ft/d. The pumping rate has been maintained for many years in this small confined aquifer, but substantially increasing the pumping may not be feasible under the assumption that the aquifer truly is small.

Across all the model scenarios, little water entered the buried sand unit from the till below as water was being pumped from the buried sand unit. The maximum contribution from below among all the scenarios was 9.7 percent, which occurred in an extreme case with a small, isolated buried sand unit (0.5 mi^2, Ls), under low-conductivity till (0.001 ft/d, Lv), and surrounded on all sides by low-conductivity material (0.05 ft/d, Lc). When the aquifer size was increased and surrounded by low-conductivity till, the percentage contribution from below decreased to about 4 to 5 percent. When the K_v of the overlying till and K_h of the middle unit were increased, the percentage contribution from below generally decreased to less than 1 percent of the total water entering the buried sand unit.

Leakage from the surficial unit into the till within the local area under ambient (no pumping) conditions varied in response to several hydrogeological factors and indicated that till properties as well as the fluxes of water through material underlying the till were important. Not surprisingly, as till K_v became smaller, the amount of leakage also decreased and lateral flow through the surficial unit increased; however, the size of this response was affected by the K_h of the material underlying the till. For example, in the LsHvLc (small sand unit, high till K_v, low middle unit K_h), the ambient leakage into the till was small, only about 6 percent of inputs into the surficial unit, but when the K_h of the middle unit was increased (Hc, 30 ft/d), the leakage into the top of the till increased to 37 percent (table 4). The ambient leakage into the upper till also increased as the size of the buried sand unit increased.

Till Vertical Hydraulic Conductivity, Aquifer Size, and Middle Unit Horizontal Hydraulic Conductivity Effects on Groundwater Fluxes

Three response variables across the full range of permutation parameter values are presented in figure 19: (1) maximum drawdown in the till (plots *A–C*), (2) pumping-induced increase in leakage to till from surficial unit (plots *D–F*), and (3) the amount of water entering the buried sand unit across the top face of the unit (plots *G–I*). For the following discussion, the term "sensitivity" will be used to describe, in relative terms, how much a given response variable changed across the range of model parameter values used in the series of permutation model runs. Comparing the same-colored lines across rows of graphs in figure 19 provided a visual for the sensitivity of response variables to aquifer size. The slope of the same-colored lines in each graph provided a visual for the sensitivity of each response variable to the K_v of the till unit. The vertical separation between points for a given K_v value provided a visual for the sensitivity of each response variable to the K_h of the middle unit surrounding the buried sand unit.

A couple of general patterns in response variable sensitivity to parameter changes are apparent across most of the plots in figure 19 (not *D*). First, the response variables were much more sensitive to changes in the middle unit K_h with low overlying till K_v, as demonstrated from the vertical separation of points when till K_v=0.001 ft/d. Second, the response variables tended to be more sensitive to changes in till K_v between 0.001 and 0.05 ft/d than between 0.05 and 2.0 ft/d.

The maximum drawdown in the till in model layer 3 was highly variable across the permutation runs (fig. 19, plots *A–C*). In plot *A*, the dotted lines indicated that the specified pumping rate of 900 gal/min was not sustained and therefore cannot be compared directly to the other model runs. In the remaining model runs, the maximum drawdown decreased as the K_v of the till increased. This seemed counterintuitive, especially in light of field results from this study where drawdown in response to short-term (several hours to a maximum of 5 days) pumping were not apparent in low *K* tills; however,

Table 8. Summary of sustained pumping rates, water fluxes, and drawdowns from steady-state heuristic MODFLOW model output (from Trost and others, 2020).

[gal/min, gallon per minute]

Model run name	Sustained pumping (gal/min)	Percent of water pumped by wells from boundary conditions	Percent of inputs to surficial unit (layer 1) that leaks into upper till (layer 2) within local area		Pumping-induced increase in percent of inputs leaking into upper till (layer 2)	Percent of water entering buried sand unit			Drawdown in layer 1 (surficial unit), in feet	Drawdown in layer 3 (till), in feet
			Ambient	Stressed		From below	Through the side faces	Through the top face		
LsLvLc	291	0.4	0.5	8.8	8.3	9.7	21.9	78.0	4.4	63.1
LsLvMc	501	0.3	1.8	10.4	8.6	0.9	80.7	18.4	1.7	18.4
LsLvHc	900	10.3	3.6	11.5	7.9	0.4	90.0	9.6	1.1	10.5
LsMvLc	304	0.0	2.7	8.9	6.2	2.5	3.5	94.1	5.2	8.0
LsMvMc	577	0.0	11.9	22.8	10.9	0.4	41.6	58.0	5.0	7.4
LsMvHc	900	0.1	22.2	35.5	13.3	0.2	61.7	38.2	4.4	6.4
LsHvLc	304	0.0	6.3	10.2	3.9	0.7	2.6	96.7	6.1	6.6
LsHvMc	625	0.0	18.7	29.2	10.5	0.4	35.6	63.9	6.8	7.3
LsHvHc	900	0.0	37.1	48.8	11.8	0.2	70.8	29.0	6.2	6.7
MsLvLc	900	0.0	1.3	24.0	22.7	4.9	27.0	68.2	5.2	47.6
MsLvMc	900	0.4	2.5	17.6	15.1	0.5	72.4	27.1	2.3	20.2
MsLvHc	900	10.6	3.9	11.3	7.4	0.2	89.0	10.8	1.0	9.1
MsMvLc	900	0.0	11.2	25.8	14.6	0.7	15.2	84.1	5.2	7.2
MsMvMc	900	0.0	17.5	31.1	13.6	0.2	34.7	65.1	4.4	6.4
MsMvHc	900	0.1	24.2	35.8	11.6	0.1	52.2	47.7	3.5	5.4
MsHvLc	900	0.0	21.8	32.5	10.6	0.2	21.2	78.6	5.5	6.0
MsHvMc	900	0.0	28.3	38.7	10.4	0.1	28.9	70.9	5.4	5.9
MsHvHc	900	0.0	39.1	49.1	10.0	0.1	42.3	57.6	5.1	5.5
HsLvLc	900	0.0	2.9	22.8	20.0	4.1	8.9	87.0	3.0	23.7
HsLvMc	900	0.5	3.5	15.8	12.3	0.6	56.5	42.9	1.7	13.2
HsLvHc	900	10.8	4.5	11.3	6.9	0.2	78.9	20.9	0.9	7.7
HsMvLc	900	0.0	19.9	31.7	11.8	0.6	1.5	97.9	3.5	5.4
HsMvMc	900	0.0	22.2	33.5	11.3	0.2	15.0	84.8	3.3	5.2
HsMvHc	900	0.1	25.4	35.7	10.3	0.7	30.4	69.5	3.0	4.9
HsHvLc	900	0.0	33.1	41.6	8.5	0.1	1.7	98.1	4.9	5.4
HsHvMc	900	0.0	34.7	43.3	8.6	0.1	7.4	92.5	4.9	5.3
HsHvHc	900	0.0	39.8	48.6	8.8	0.0	17.2	82.8	4.8	5.2

Table 8. Summary of sustained pumping rates, water fluxes, and drawdowns from steady-state heuristic MODFLOW model output (from Trost and others, 2020).—Continued

[gal/min, gallon per minute]

Model run name	Sustained pumping (gal/min)	Percent of water pumped by wells from boundary conditions	Percent of inputs to surficial unit (layer 1) that leaks into upper till (layer 2) within local area		Pumping-induced increase in percent of inputs leaking into upper till (layer 2)	Percent of water entering buried sand unit			Drawdown in layer 1 (surficial unit), in feet	Drawdown in layer 3 (till), in feet
			Ambient	Stressed		From below	Through the side faces	Through the top face		
BSkh_L	900	0.0	14.6	30.2	15.6	0.3	28.2	71.5	6.2	11.6
BSkh_H	900	0.0	19.9	33.1	13.2	0.2	37.5	62.3	3.7	4.4
LFtrlk	900	0.1	4.1	20.4	16.3	0.5	70.3	29.3	2.6	15.4
CRtrlk	900	0.0	23.3	35.6	12.3	0.1	19.7	80.2	6.7	8.0
Ppen_L	900	0.0	17.5	31.1	13.6	0.2	34.7	65.1	4.4	6.2
Ppen_H	900	0.0	17.5	31.1	13.6	0.2	34.7	65.1	4.4	6.3
SURF_L	900	0.0	39.0	60.4	21.3	0.3	49.0	50.7	13.3	14.0
SURF_H	900	0.0	6.3	14.1	7.8	0.1	26.3	73.5	1.4	3.8
TOTq_L	300	0.0	17.5	21.3	3.8	0.2	33.2	66.6	1.3	2.0
TOTq_H	2,250	0.0	17.5	59.7	42.2	0.3	45.4	54.4	19.2	23.0
UTtk_L	900	0.0	20.1	32.7	12.7	0.2	30.4	69.4	4.5	6.0
UTtk_H	900	0.0	14.7	29.3	14.6	0.2	39.8	59.9	4.3	7.0

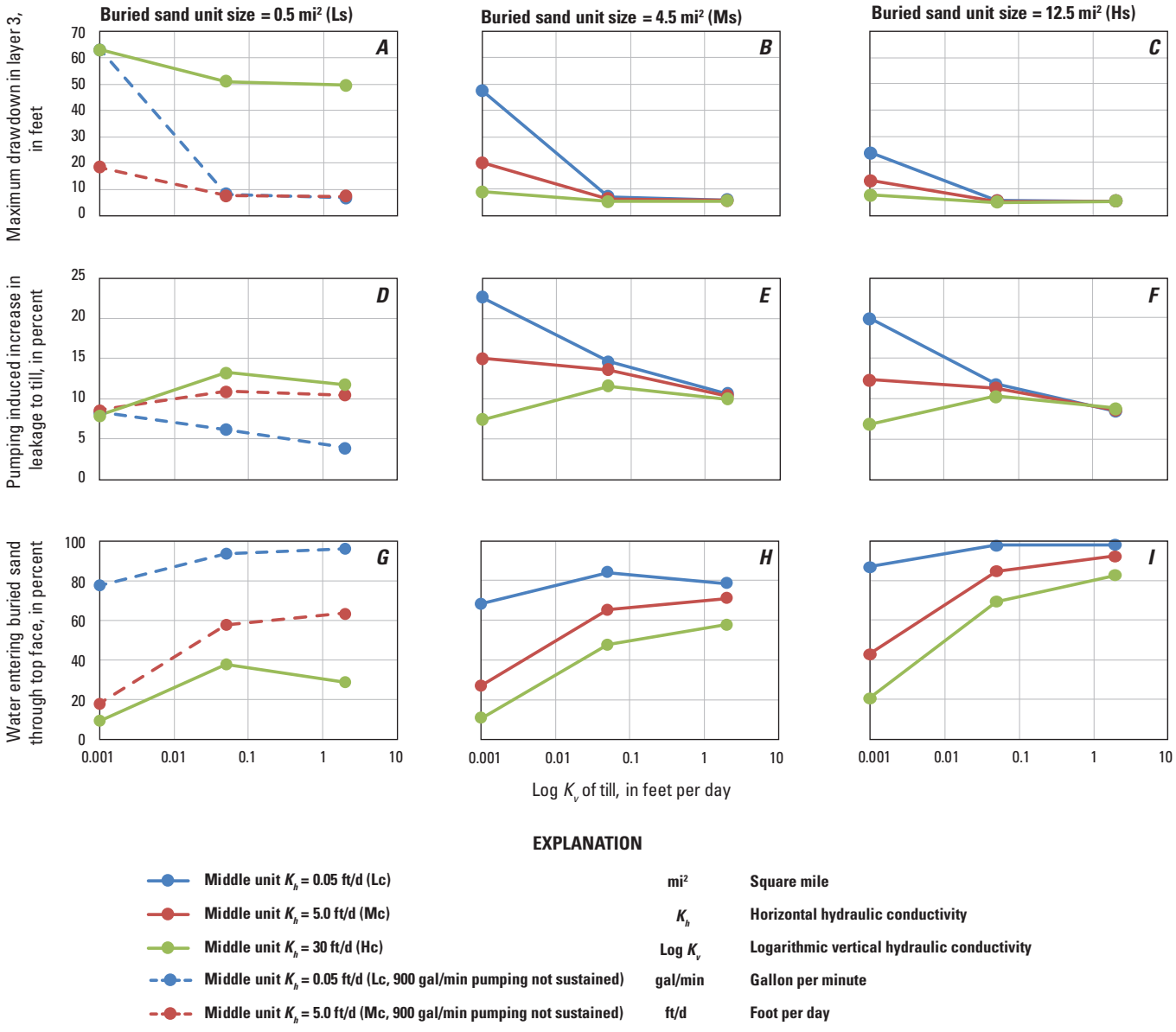

Figure 19. Heuristic MODFLOW model output including changes in maximum drawdown in till (*A*–*C*), pumping-induced increase in leakage to till from the surficial unit (*D*–*F*), and the amount of water entering the aquifer through its top face (*G*–*I*).

it is important to note that the results discussed here were from steady-state models and demonstrate conditions after 1,000 years of pumping. The maximum drawdown in the till generally decreased as the buried sand body size increased, and the maximum drawdown was especially sensitive to aquifer size less than 4.5 mi² (compare green lines in fig. 19, plots *A* and *B*). At low till K_v, there is a consistent inverse relation between the middle unit K_h and drawdown in the till.

In all cases, the introduction of pumping stress to the model system increased the amount of water leaking from the surficial unit into the top of the till unit (fig. 19, plots *D*–*F*). These pumping-induced increases in leakage represented a reduction in groundwater discharge out of the local area and groundwater discharge to local streams and lakes that is not met by increased fluxes from outside the local area (fig. 9, model layout). In some model scenarios, more than 20 percent of the inputs within the 5 mi local area were lost from the surficial unit because of pumping. Generally, the magnitude of the increase in leakage increased as the ambient leakage (no pumping) decreased (table 4). In other words, the largest pumping-induced increases in leakage occurred in low K_v tills. As with the drawdown results, this seemed counterintuitive based on our field study, but this modeling represented long-term (hundreds of years) conditions.

There is a strong interaction between the middle unit K_h and the overlying till K_v on pumping-induced leakage (fig. 19, plots *D*–*F*). Pumping-induced leakage into the till was highly sensitive to the middle unit K_h at low till K_v (0.001 ft/d) and

insensitive to middle unit K_h at high till K_v. Pumping-induced leakage was insensitive to changes in aquifer size. The practical implication of this result is that to accurately simulate these fluxes, which are important for managing water resources near the surface, reliable information on either the till K_v or the connectivity among buried aquifers is needed.

The relative amounts of water reaching a confined aquifer from above (and by implication, from the sides) changed drastically with the range of hydrogeological characteristics observed in this study (fig. 19*G*–*I*). As previously discussed, water entering the buried sand unit from below was almost always less than 1 percent of the total. Not surprisingly, the percentage of water entering the aquifer from above increased as the lateral extent of the aquifer increased. At one extreme, 98 percent of the water entered the aquifer directly from the till above. This model run had a conductive till overlying a large sand body surrounded by poorly conductive materials (HsHvLc). In the other extreme case, only about 10 percent of the water entered the aquifer directly from the till above. This model run had poorly conductive till overlying a small sand body that was adjacent to conductive till (LsLvHc). This model run had an extensive contributing area, as indicated by the increased water supplied by the model boundary 10 mi away from the well field.

Pumping and Aquifer Transmissivity Effects on Groundwater Fluxes

For the next set of model runs, one model parameter or set of parameters was varied and the remainder of the model parameters were from the base model (MsMvMc) (fig. 20; table 8).

Increases in pumping from 300 to 2,250 gal/min caused higher drawdowns in the till, substantially increased the percentage of water leaking into the till from the surficial unit, and only moderately decreased the percentage of water entering the aquifer directly from the overlying till (fig. 20). At the 300 gal/min pumping rate, pumping only increased the leakage by about 4 percent, but at the 2,250 gal/min pumping rate, the leakage increased to more than 40 percent of water inputs to the surficial unit within the local area. These pumping-induced increases in leakage represented a reduction in groundwater discharge out of the local area and a reduction in groundwater discharge to local streams and lakes that were not met by increased fluxes from outside the local area (fig. 9, model layout). These results indicated that the effect of pumping on surface-water resources depended on the pumping rate. The 900 gal/min rate was representative of the pumping rate from the confined aquifer at Litchfield. The city of Litchfield pumps at a mean rate of 630 gal/min, or 340 Mgal/yr, and there are other high-capacity permits within the same buried aquifer, as was evident from the large summer drawdowns in the buried aquifer hydrographs (fig. 10) and from the aquifer test data (Blum and Woodside, 2017). At the 900 gal/min pumping rate, pumping increased leakage into the upper till by about 14 percent, as compared to ambient conditions.

Two model runs, CRtrlk and LFtrlk, were intended to be "Cromwell transmissivity like" and "Litchfield transmissivity like." These models were not intended to replicate actual observed responses at these sites; rather, these model runs were used to compare and contrast responses to pumping. In these two scenarios, the till K_v and aquifer transmissivity were set to approximate results from aquifer tests completed at each site. The steady-state models indicate, over long periods of time, a greater drawdown in till for a Litchfield-like setting compared to a Cromwell-like setting. This was consistent with the model results presented previously, where less conductive tills demonstrated higher drawdowns in steady-state conditions. The pumping-induced increase in leakage to till was about the same between the two model runs. About 80 percent of the water in the Cromwell-like scenario entered the buried aquifer directly from the overlying till, compared to only about 30 percent in the Litchfield-like scenario. This meant that there was a more laterally extensive contributing area for a Litchfield-like setting than a Cromwell-like setting, which has implications for managing drinking water quality. Because till K_v and buried aquifer K_h were varied simultaneously in these model runs, it was difficult to tell which parameter was exerting a greater effect on the response variables. In a separate set of variation runs (BSkh), the response variables were sensitive to changes in the buried sand K_h from 30 to 100 ft/d, and the response variables were sensitive to changes in till K_v between 0.0001 and 0.05, indicating that both attributes played a role in the different responses of the Cromwell-like and Litchfield-like settings.

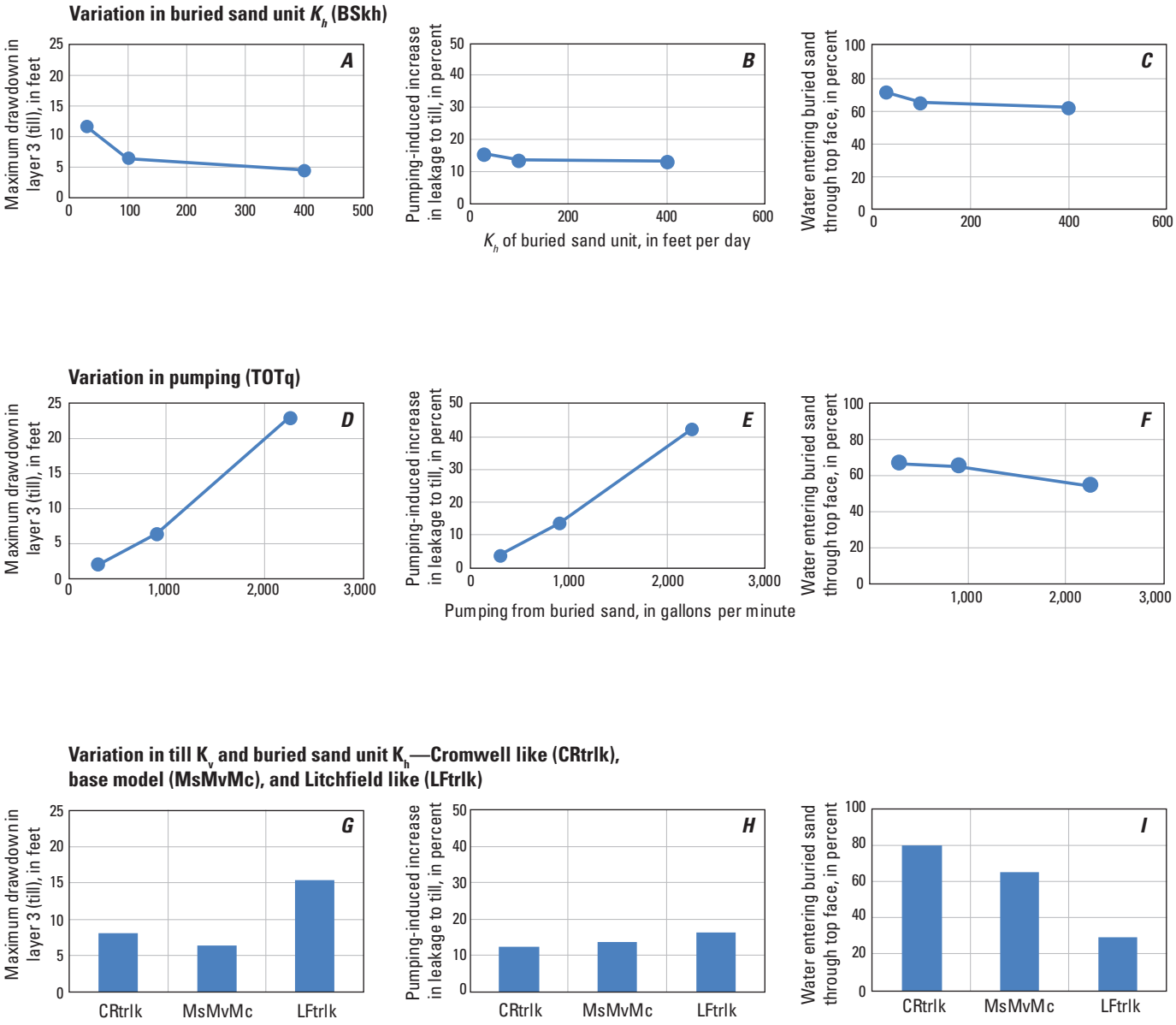

Figure 20. Heuristic MODFLOW model output for variation model runs including changes in maximum drawdown in model layer 3 (till), pumping-induced increase in leakage to model layer 2 (till) from model layer 1 (surficial unit), and the amount of water entering the buried sand unit through its top face for variations in the buried sand unit horizontal hydraulic conductivity (K_h, *A–C*), variations in total pumping (*D–F*), and variations in till vertical hydraulic conductivity (K_v) and buried sand K_h (*G–I*).

Summary

Confined (or buried) aquifers of glacial origin overlain by till confining units provide drinking water to hundreds of thousands of Minnesota residents. The sustainability of these groundwater resources is not well understood because hydraulic properties of till that control vertical groundwater fluxes (leakage) to underlying aquifers are largely unknown. The U.S. Geological Survey, Iowa State University, Minnesota Geological Survey, and Minnesota Department of Health investigated hydraulic properties and groundwater flow through till confining units using field studies and heuristic MODFLOW simulations. Till confining units in the following late-Wisconsinan stratigraphic units (with locations in parentheses) were characterized: Des Moines lobe till of the New Ulm Formation (Litchfield, Minnesota); Superior lobe tills of the Cromwell and Aitkin Formations (Cromwell, Minn.); and Wadena lobe till of the Hewitt Formation (hydrogeology field camp [HFC] near Akeley, Minn.). Pre-Illinoian till of the Good Thunder formation (Olivia, Minn.) was also characterized.

Hydraulic and geochemical field data were collected from sediment cores and a series of five piezometer nests. Each nest consisted of five to eight piezometers screened at short vertical

intervals in hydrostratigraphic units including (if present) surficial aquifers, till confining units, confined/buried aquifers, and underlying bedrock. Till hydraulic conductivity (K) was estimated from slug tests (horizontal [K_h]) and constant-rate aquifer tests in the confined aquifer (vertical [K_v]). Pressure transducers were emplaced to measure hydraulic-head fluctuations. Groundwater samples from the piezometers and pore-water samples from till cores were analyzed for major ions, nutrients, enriched tritium, and stable isotopes (oxygen [$\delta^{18}O$] and hydrogen [$\delta^{2}H$]) of water. Travel times through the till were evaluated with Darcy's law and stable isotope concentrations. A series of heuristic MODFLOW simulations were used to evaluate groundwater fluxes through till across the range of till hydraulic properties and pumping rates observed at the field sites.

The first Litchfield piezometer nest (LFO1) was in a leaky 60-foot (ft)-thick till profile with a mean composition of 47-percent sand, 34-percent silt, and 19-percent clay. The site had a mean downward hydraulic gradient of 0.55 in the till, and the largest hydraulic gradient was near the base of the till. Drawdown responses were observed in all till piezometers during the aquifer test at the site. The geometric mean K_h of two till piezometers was 0.07 foot per day (ft/d), whereas the bulk K_v determined from an aquifer test at Litchfield was 0.001 ft/d. These two K values along with other site information were used to calculate specific discharge and travel time through till according to Darcy's law. Specific discharge ranged from 2.4 (K_v) to 176 inches per year (in/yr) (K_h) and travel times varied from 1 (K_h) to 74 years (K_v). Tritium was detected in all till piezometers, indicating the presence of modern water throughout the till profile. "Modern" indicates groundwater that was last exposed to the atmosphere sometime after 1953. Chloride to bromide ratios were near 250 throughout the till, indicating a possible presence of anthropogenically sourced chloride throughout the till.

The second Litchfield piezometer nest (LFO2) was only one-half mile away from LFO1 and in the same New Ulm Formation but contained an effective confining unit in the lower part of the till. The 115-ft-thick till profile at this site had a mean composition of 52-percent sand, 31-percent silt, and 17-percent clay. The site had a mean downward hydraulic gradient of 0.48 in the till, and the largest hydraulic gradient was near the base of the till. Drawdown responses were not observed in any till piezometers during the aquifer test at the site. The geometric mean K_h of five till piezometers was 0.0002 ft/d, whereas the bulk K_v determined from an aquifer test at Litchfield was 0.001 ft/d. These two K values along with other site information were used to calculate specific discharge and travel time through till according to Darcy's law. Specific discharge ranged from 0.4 (K_h) to 2.1 in/yr (K_v) and travel times varied from 165 (K_v) to 913 years (K_h). Tritium was only detected in the two uppermost till piezometers, to about 35 ft into the till, indicating nonmodern water (older than 1953) was present through most of the till profile. Chloride to bromide ratios were near 250 to a depth of about 60 ft into the till, indicating a possible presence of anthropogenically sourced chloride to this depth.

The Cromwell nest was in a leaky 120-ft-thick till profile with a mean composition of 57-percent sand, 31-percent silt, and 13-percent clay (greater than 100 percent because of rounding). The site had a mean upward hydraulic gradient of 0.02 in the till, but hydraulic gradient directions were variable throughout the till. Drawdown responses were observed in all till piezometers during the aquifer test at the site. The geometric mean K_h of five till piezometers was 0.06 ft/d, whereas the bulk K_v determined from an aquifer test was 1.1 ft/d. These two K values along with other site information were used to calculate specific discharge and travel time through till according to Darcy's law. Because of the upward hydraulic gradient at this site, fluxes are from the base of the till to the overlying surficial aquifer. Specific discharge ranges from 4.5 (K_h) to 86 in/yr (K_v), and travel times vary from 4 (K_v) to 80 years (K_h); however, these calculations ignore the broader flow environment at this site. Tritium was not detected in till but was detected in the surficial aquifer and the confined aquifer. The hydraulic gradient data and the tritium data indicate that recharge to the confined aquifer enters the system somewhere upgradient in the same buried aquifer system or perhaps through a stratigraphic window in the overlying till confining unit where the hydraulic gradient in the till is downward. This indicates that the till sequence observed near the production well may have little direct effect on the quality and quantity of water at the Cromwell site. Rather, the anthropogenic activities and geologic materials at a distal recharge area (yet to be defined) may affect the water observed in the confined aquifer at the Cromwell site. Chloride to bromide ratios were variable in the till and were greater than 250 at multiple locations.

The HFC nest was in a leaky 100-ft-thick till profile with a mean composition of 67-percent sand, 22-percent silt, and 11-percent clay. The site had a mean downward hydraulic gradient of 0.04 in the till. Drawdown responses were observed in all but the uppermost till piezometer during the aquifer test at the site. The geometric mean K_h of till piezometers was 0.03 ft/d, and the bulk K_v determined from an aquifer test was 0.031 ft/d. These two K values along with other site information were used to calculate specific discharge and travel time through till according to Darcy's law. Specific discharge ranged from 5.3 (K_h) to 6.0 in/yr (K_v), and travel times varied from 50 (K_v) to 57 years (K_h). Tritium was detected in all till piezometers, indicating the presence of modern water throughout the till profile. Chloride to bromide ratios were much less than 250 throughout the till, indicating that anthropogenically sourced chloride is not a major factor at this site, likely because this site is in a remote forested region.

The Olivia nest contained an effective confining unit in the lower part of the till above the confined aquifer. The 166-ft-thick till profile at the Olivia site had a mean composition of 37-percent sand, 40-percent silt, and 23-percent clay. The site had a mean downward hydraulic gradient of 0.13 in the till, with the largest hydraulic gradients at the base of the till and an extremely large hydraulic gradient of 2.26 across the till/confined aquifer boundary. Drawdown responses during an aquifer test were not observed in any

till piezometers because of a prolonged reverse water-level fluctuation response in most till piezometers. The geometric mean K_h of five till piezometers was 0.004 ft/d, and the bulk K_v determined from an aquifer test was 0.0012 ft/d according to a leaky confined aquifer analytical approach or 0.0005 ft/d according to a time-delay analytical approach. These K estimates along with other site information were used to calculate specific discharge and travel time through till according to Darcy's law. Specific discharge ranged from 0.7 (K_v) to 2.3 in/yr (K_h), and travel times varied from 217 (K_h) to 1,770 years (K_v). Tritium was only detected in the uppermost till piezometer, at a depth of about 8 ft into the till, indicating nonmodern water (older than 1953) was present through most of the till profile. In this same piezometer, chloride to bromide ratios were greater than 250, indicating anthropogenically sourced chloride may be present. Chloride to bromide ratios were far greater than 250 in the lower one-half of the till, but primarily because of extremely low bromide concentrations and not from elevated chloride concentrations compared to the uppermost till piezometer.

Diverse tills were evaluated at the four study sites, and comparisons across sites yield some useful insights for generalizing these results. The field data demonstrated variability in hydraulic properties between and within till stratigraphic units horizontally and vertically. The variability in hydraulic properties resulted in substantial differences in groundwater flux through till across the sites. A conceptual understanding that emerges from the vertical till profiles is that they are not homogeneous hydrostratigraphic units with uniform properties; rather, each vertical sequence is a heterogeneous mixture of glacial sediment with differing abilities to transmit water.

Till thicknesses varied from 60 to 166 ft, and till textures ranged from a sandy loam (Hewitt Formation, HFC site) to a silt loam/clay loam (Good Thunder formation, Olivia site). Till K_h varied by one to three orders of magnitude within each piezometer nest. Four piezometer nests had downward hydraulic gradients ranging from 0.04 to 0.56, and one nest had a slight upward hydraulic gradient of 0.02. The Cromwell, HFC, and LFO1 sites were examples of "leaky" tills with high K_v (0.001 to 1.1 ft/d) and geometric mean K_h (0.03 to 0.07 ft/d), and extensive vertical hydraulic connectivity between the confined aquifer and the overlying till. Estimated groundwater travel times through these sites ranged from 1 to 81 years, and two of these sites had tritium throughout their till profiles. The tills at the other two sites, Olivia and LFO2, were effective confining units that had low K_v (0.001 to 0.0005 ft/d) and geometric mean K_h (0.0002 to 0.004 ft/d). The till piezometers at these sites had no drawdown response to short-term (up to 10 hours for Olivia and up to 5 days for Litchfield) high-capacity pumping from the confined aquifer. Estimated groundwater travel times through the tills at these sites ranged from 165 to nearly 1,800 years, and tritium was only detected in the upper one-third of these till profiles. Across all sites, the till vertical anisotropy (ratio of K_h to K_v) ranged by four orders of magnitude from 0.05 at the Cromwell nest to 70 at the LFO1 nest. Stable isotopes of oxygen and hydrogen indicate that groundwater throughout all five till profiles is younger than the last glacial advance into Minnesota about 11,000 years ago.

A drawdown response to pumping from the confined aquifer was typically observed in till piezometers screened in sediments with at least 55-percent sand and less than 15-percent clay. The mean percentages of sand and clay for a given till profile were correlated with the logarithm of the bulk K_v determined from aquifer tests; however, the percentages of sand or clay from core sections at the same depth as piezometer screens were not correlated with the K_h determined from slug tests. This indicates that factors in addition to textural composition are affecting the hydraulic properties of till (or measurement thereof) at the localized scale of slug tests, but at the larger aquifer-test scale, textural composition is indicative of bulk till hydraulic characteristics.

The heuristic modeling demonstrated that, for understanding sustainability of groundwater pumping from confined aquifers, knowledge of till hydraulic properties is just as important as knowledge of aquifer hydraulic properties. In particular, it is important to have information about the K_v of overlying till, the areal extent of the buried aquifer, and the lateral connectivity of the buried aquifer to other aquifers. Three response variables were examined in detail from the steady-state models: maximum drawdown in till, pumping-induced leakage from the surficial unit into the till confining unit, and the source of water to the buried sand unit (expressed as the percentage of water entering the aquifer directly from the overlying till). Over long periods of time (hundreds of years), pumping-induced hydraulic gradients can be established in buried aquifer systems, and even in low K tills, these hydraulic gradients increased leakage into and through till. The percentage of water entering a buried aquifer directly from the overlying till ranged from 10 to 98 percent among the model scenarios; when only 10 percent of the water entered the aquifer from above, water fluxes increased at the model boundary, 10 miles away from the well field. The percentage of water entering the aquifer from above was demonstrated to be sensitive to buried aquifer size, K_v of till, and K_h of material adjacent to the buried aquifer. In almost all cases, less than 1 percent of the water entered the buried sand from the underlying till.

In conclusion, groundwater flowing vertically downward through till confining units (leakage) replenishes water pumped from confined aquifers. Till hydraulic properties, such as those presented in this report, provide important information that can be used to quantify leakage rates through till. Till hydraulic properties are variable over short distances and profoundly affect leakage rates, demonstrating the importance of site-specific till hydraulic data for evaluating the sustainability of groundwater withdrawals from confined aquifers.

References Cited

Alcalá, F.J., and Custodio, E., 2008, Using the Cl/Br ratio as a tracer to identify the origin of salinity in aquifers in Spain and Portugal: Journal of Hydrology (Amsterdam), v. 359, no. 1–2, p. 189–207. [Also available at https://doi.org/10.1016/j.jhydrol.2008.06.028.]

American Public Health Association, American Water Works Association, and Water Environment Federation, 1998, Standard methods for the examination of water and wastewater (20th ed.): Washington, D.C., p. 3–37 to 3–43.

Beckie, R., and Harvey, C.F., 2002, What does a slug test measure—An investigation of instrument response and the effects of heterogeneity: Water Resources Research, v. 38, no. 12, p. 1–14. [Also available at https://doi.org/10.1029/2001WR001072.]

Berg, J.A., 2018, Geologic atlas of Clay County, Minnesota: St. Paul, Minn., Minnesota Department of Natural Resources, County Atlas Series C–29, Part B, Report and Plates 6–8. [Also available at https://www.dnr.state.mn.us/waters/programs/gw_section/mapping/platesum/claycga.html.]

Berg, J.A., 2019, Groundwater atlas of Washington County, Minnesota: St. Paul, Minn., Minnesota Department of Natural Resources, County Atlas Series C–39, Part B, Report and Plates 7–9. [Also available at https://www.dnr.state.mn.us/waters/programs/gw_section/mapping/platesum/washcga.html.]

Berg, S.J., Hsieh, P.A., and Illman, W.A., 2011, Estimating hydraulic parameters when poroelastic effects are significant: Ground Water, v. 49, no. 6, p. 815–829. [Also available at https://doi.org/10.1111/j.1745-6584.2010.00781.x.]

Blanchette, D., Lefebvre, R., Nastev, M., and Cloutier, V., 2010, Groundwater quality, geochemical processes and groundwater evolution in the Chateauguay River watershed, Quebec, Canada: Canadian Water Resources Journal, v. 35, no. 4, p. 503–526. [Also available at https://doi.org/10.4296/cwrj3504503.]

Blum, J.L., 2019a, Analysis of the University of Minnesota HB-1 (809697) pumping test, July 20, 2018, confined glacial-fluvial aquifer—Aquifer test 2327: Minnesota Department of Health Technical Memorandum 1–43, 42 p.

Blum, J.L., 2019b, Analysis of the Olivia 4 (228797) pumping test, July 11, 2108, confined Quaternary glacial-fluvial aquifer—Aquifer test 2329: Minnesota Department of Health, 56 p.

Blum, J.L., 2020, Preliminary analysis of poroelastic response of aquitards during pumping tests at Cromwell and Olivia: Minnesota, Minnesota Department of Health, 29 p.

Blum, J.L., and Woodside, J., 2017, Analysis of the Litchfield, Minnesota well 2 (607420) aquifer test conducted on June 29, 2017, confined Quaternary glacial-fluvial sand aquifer: Minnesota Department of Health, aquifer test 2617, 81 p. [Also available at https://www.health.state.mn.us/communities/environment/water/docs/swp/testlitchfield.pdf.]

Boerboom, T.J., 2009, C–19 geologic atlas of Carlton County, Minnesota [part A]: Minnesota Geological Survey, 6 plates. [Also available at https://conservancy.umn.edu/handle/11299/58760.]

Bradbury, K.R., and Muldoon, M.A., 1990, Hydraulic conductivity determinations in unlithified glacial and fluvial materials, *in* Nielsen, D.M., and Johnson, A.I., eds., Ground water and vadose zone monitoring: Philadelphia, Pa., American Society for Testing and Materials, p. 138–151., ASTM STP 1053.

Bradbury, K.R., Gotkowitz, M.B., Hart, D.J., Eaton, T.T., Cherry, J.A., Parker, B.L., and Borchardt, M.A., 2006, Contaminant transport through aquitards—Technical guidance for aquitard assessment: Awwa Research Foundation, 144 p.

Bradt, R.J., 2017, Geologic atlas of Renville County, Minnesota: Minnesota Department of Natural Resources, County Atlas Series C–28, Part B, 31 p. report, 27 map figures, and plates 6–8. [Also available at https://www.dnr.state.mn.us/waters/programs/gw_section/mapping/platesum/renvcga.html.]

Burkart, M.R., Simpkins, W.W., Morrow, A.J., and Gannon, J.M., 2004, Occurrence of total dissolved phosphorus in unconsolidated aquifers and aquitards in Iowa: Journal of the American Water Resources Association, v. 40, no. 3, p. 827–834. [Also available at https://doi.org/10.1111/j.1752-1688.2004.tb04461.x.]

Butler, J.J., Jr., 1998, The design, performance, and analysis of slug tests: Boca Raton, Fla., CRC Press, 280 p.

Butler, J.J., Jr., McElwee, C.D., and Liu, W., 1996, Improving the quality of parameter estimates obtained from slug tests: Ground Water, v. 34, no. 3, p. 480–490. [Also available at https://doi.org/10.1111/j.1745-6584.1996.tb02029.x.]

Cherry, J.A., Parker, B.L., Bradbury, K.R., Eaton, T.T., Gotkowitz, M.G., Hart, D.J., and Borchardt, M.A., 2004, Role of aquitards in the protection of aquifers from contamination—A "state of the science" report: Denver, Colo., Awwa Research Foundation, 124 p. [Also available at https://clu-in.org/download/contaminantfocus/dnapl/Chemistry_and_Behavior/Aquitard_State_of_Science_Reportfor_AWWARF_draft_of1-3-05.pdf.]

Clayton, L., and Moran, S.R., 1982, Chronology of late Wisconsinan glaciation in middle North America: Quaternary Science Reviews, v. 1, no. 1, p. 55–82. [Also available at https://doi.org/10.1016/0277-3791(82)90019-1.]

Craig, H., 1961, Isotopic variations in meteoric waters: Science, v. 133, no. 3465, p. 1702–1703. [Also available at https://doi.org/10.1126/science.133.3465.1702.]

Cunningham, W.L., and Schalk, C.W., comps., 2011, Groundwater technical procedures of the U.S. Geological Survey: U.S. Geological Survey Techniques and Methods 1–A1, 151 p.

Delin, G.N., 1986, Hydrogeology of confined-drift aquifers near the Pomme de Terre and Chippewa Rivers, western Minnesota: U.S. Geological Survey Water-Resources Investigations Report 86–4098, 90 p., 6 plates. [Also available at https://doi.org/10.3133/wri864098.]

Driscoll, F.G., 1986, Groundwater and wells (2d ed.): St. Paul, Minn., Johnson Screens, 1,089 p.

Duffield, G.M., 2007, AQTESOLV for Windows—Version 4.5 user's guide: Reston, Va., HydroSOLVE, Inc., 529 p.

Eidem, J.M., Simpkins, W.W., and Burkart, M.R., 1999, Geology, groundwater flow, and water quality in the Walnut Creek watershed: Journal of Environmental Quality, v. 28, no. 1, p. 60–69. [Also available at https://doi.org/10.2134/jeq1999.00472425002800010006x.]

Fishman, M.J., ed., 1993, Methods of analysis by the U.S. Geological Survey National Water Quality Laboratory—Determination of inorganic and organic constituents in water and fluvial sediments: U.S. Geological Survey Open-File Report 93–125, 217 p. [Also available at https://doi.org/10.3133/ofr93125.]

Fishman, M.J., and Friedman, L.C., 1989, Methods for determination of inorganic substances in water and fluvial sediments: U.S. Geological Survey Techniques of Water-Resources Investigations, book 5, chap. A1, 545 p. [Also available at https://doi.org/10.3133/twri05A1.]

Fortin, G., van der Kamp, G., and Cherry, J.A., 1991, Hydrogeology and hydrochemistry of an aquifer-aquitard system within glacial deposits, Saskatchewan, Canada: Journal of Hydrology (Amsterdam), v. 126, no. 3–4, p. 265–292. [Also available at https://doi.org/10.1016/0022-1694(91)90160-J.]

Gerber, R.E., and Howard, K.W.F., 1996, Evidence for recent groundwater flow through late Wisconsinan till near Toronto, Ontario: Canadian Geotechnical Journal, v. 33, no. 4, p. 538–555. [Also available at https://doi.org/10.1139/t96-080-302.]

Gerber, R.E., and Howard, K., 2000, Recharge through a regional till aquitard—Three-dimensional flow model water balance approach: Ground Water, v. 38, no. 3, p. 410–422. [Also available at https://doi.org/10.1111/j.1745-6584.2000.tb00227.x.]

Goldberg, S., and Kabengi, N.J., 2010, Bromide adsorption by reference minerals and soils: Vadose Zone Journal, v. 9, no. 3, p. 780–786. [Also available at https://doi.org/10.2136/vzj2010.0028.]

Grisak, G.E., and Cherry, J.A., 1975, Hydrologic characteristics and response of fractured till and clay confining a shallow aquifer: Canadian Geotechnical Journal, v. 12, no. 1, p. 23–43. [Also available at https://doi.org/10.1139/t75-003.]

Grisak, G.E., Cherry, J.A., Vonhof, J.A., and Blumele, J.P., 1976, Hydrogeologic and hydrochemical properties of fractured till in the interior plains region, *in* Legget, R.F., ed., Glacial till: Ottawa, Royal Society of Canada, Special Publication 12, p. 304–335.

Haglund, G.L., and Robertson, S.W., 2000, Wellhead protection plan part 1, wellhead protection area and drinking water supply management area delineations for the City of Litchfield, First District Association, and Towmaster Trailers: Minnesota Department of Health, 15 p.

Hantush, M.S., and Jacob, C.E., 1955, Non-steady radial flow in an infinite leaky aquifer: American Geophysical Union Transactions, v. 36, no. 1, p. 95–100.

Harbaugh, A.W., 2005, MODFLOW-2005—The U.S. Geological Survey modular ground-water model—The ground-water flow process: U.S. Geological Survey Techniques and Methods, book 6, chap. A16, variously paged. [Also available at https://doi.org/10.3133/tm6A16.]

Harbaugh, A.W., Banta, E.R., Hill, M.C., and McDonald, M.G., 2000, MODFLOW-2000—The U.S. Geological Survey modular ground-water model—User guide to modularization concepts and the ground-water flow process: U.S. Geological Survey Open-File Report 2000–92, 121 p. [Also available at https://doi.org/10.3133/ofr200092.]

Hart, D.J., Bradbury, K.R., and Gotkowitz, M.B., 2008, Is one an upper limit for natural hydraulic gradients?: Ground Water, v. 46, no. 4, p. 518–520. [Also available at https://doi.org/10.1111/j.1745-6584.2008.00433.x.]

Helmke, M.F., Simpkins, W.W., and Horton, R., 2005a, Fracture-controlled nitrate and atrazine transport in four Iowa till units: Journal of Environmental Quality, v. 34, no. 1, p. 227–236. [Also available at https://doi.org/10.2134/jeq2005.0227.]

Helmke, M.F., Simpkins, W.W., and Horton, R., 2005b, Simulating conservative tracers in fractured till under realistic timescales: Ground Water, v. 43, no. 6, p. 877–889. [Also available at https://doi.org/10.1111/j.1745-6584.2005.00129.x.]

Hendry, M.J., and Schwartz, F.W., 1990, The chemical evolution of ground water in the Milk River aquifer, Canada: Ground Water, v. 28, no. 2, p. 253–261. [Also available at https://doi.org/10.1111/j.1745-6584.1990.tb02253.x.]

Hendry, M.J., and Wassenaar, L.I., 1999, Implications of the distribution of δD in pore waters for groundwater flow and the timing of geologic events in a thick aquitard system: Water Resources Research, v. 35, no. 6, p. 1751–1760. [Also available at https://doi.org/10.1029/1999WR900046.]

Hobbs, H.C., and Goebel, J.E., 1982, S–01 Geologic map of Minnesota—Quaternary geology: Minnesota Geological Survey, scale 1:500,000, accessed November 22, 2017, at http://hdl.handle.net/11299/60085.

Howard, K.W.F., and Beck, P.J., 1993, Hydrogeochemical implications of groundwater contamination by road de-icing chemicals: Journal of Contaminant Hydrology, v. 12, no. 3, p. 245–268. [Also available at https://doi.org/10.1016/0169-7722(93)90010-P.]

Hsieh, P.A., 1996, Deformation-induced changes in hydraulic head during ground-water withdrawal: Ground Water, v. 34, no. 6, p. 1082–1089. [Also available at https://doi.org/10.1111/j.1745-6584.1996.tb02174.x.]

Husain, M.M., Cherry, J.A., Fidler, S., and Frape, S.K., 1998, On the long-term hydraulic gradient in the thick clayey aquitard in the Sarnia region, Ontario: Canadian Geotechnical Journal, v. 35, no. 6, p. 986–1003. [Also available at https://doi.org/10.1139/t98-057.]

Hyder, Z., Butler, J.J., Jr., McElwee, C.D., and Liu, W., 1994, Slug tests in partially penetrating wells: Water Resources Research, v. 30, no. 11, p. 2945–2957. [Also available at https://doi.org/10.1029/94WR01670.]

Jennings, C.E., and Johnson, M.D., 2011, The Quaternary of Minnesota: Developments in Quaternary Science, v. 15, p. 499–511. [Also available at https://doi.org/10.1016/B978-0-444-53447-7.00038-6.]

Johnson, M.D., Adams, R.S., Gowan, A.S., Harris, K.L., Hobbs, H.C., Jennings, C.E., Knaeble, A.R., Lusardi, B.A., and Meyer, G.N., 2016, Quaternary lithostratigraphic units of Minnesota: Minnesota Geological Survey Report of Investigations 68, 262 p.

Katz, B.G., Eberts, S.M., and Kauffman, L.J., 2011, Using Cl/Br ratios and other indicators to assess potential impacts on groundwater quality from septic systems—A review and examples from principal aquifers in the United States: Journal of Hydrology (Amsterdam), v. 397, no. 3–4, p. 151–166. [Also available at https://doi.org/10.1016/j.jhydrol.2010.11.017.]

Keller, C.K., van der Kamp, G., and Cherry, J.A., 1989, Multiscale study of the permeability of a thick clayey till: Water Resources Research, v. 25, no. 11, p. 2299–2317. [Also available at https://doi.org/10.1029/WR025i011p02299.]

Kelly, W.R., Panno, S.V., and Hackley, K., 2012, The sources, distribution, and trends of chloride in the waters of Illinois: Champaign, Ill., Illinois State Water Survey, Prairie Research Institute, Bulletin B–74, 59 p.

Kim, J.M., and Parizek, R.R., 2005, Numerical simulation of the Rhade effect in layered aquifer systems due to groundwater pumping shutoff: Advances in Water Resources, v. 28, no. 6, p. 627–642. [Also available at https://doi.org/10.1016/j.advwatres.2004.12.005.]

Knaeble, A.R., coordinator, 2006, Landforms, stratigraphy, and lithologic characteristics of glacial deposits in central Minnesota: Minnesota Geological Survey Guidebook 22, 44 p.

Knaeble, A.R., 2013, Plate 4—Quaternary stratigraphy, *in* Setterholm, D.R., ed., C–28 geologic atlas of Renville County, Minnesota [part A]: Minnesota Geological Survey, 6 plates. [Also available at https://conservancy.umn.edu/handle/11299/159398.]

Knaeble, A.R., and Hobbs, H.C., 2009, Plate 3—Surficial geology, *in* Boerboom, T.J., ed., C–19 geologic atlas of Carlton County, Minnesota [part A]: Minnesota Geological Survey, 6 plates. [Also available at https://conservancy.umn.edu/handle/11299/58760.]

Knaeble, A.R., and Hougardy, D.D., 2018, Plate 3—Surficial geology, *in* Lusardi, B.A., ed., C–41, geologic atlas of Hubbard County, Minnesota: Minnesota Geological Survey, 6 plates. [Also available at https://conservancy.umn.edu/handle/11299/198898.]

Kroening, S., and Ferrey, M., 2013, The condition of Minnesota's groundwater, 2007–2011: St. Paul, Minn., Minnesota Pollution Control Agency, 59 p.

Lewis, M.E., 2006, Dissolved oxygen, *in* Wilde, F.D., ed., Field measurements: U.S. Geological Survey Techniques of Water-Resources Investigations, book 9, chap. A6, variously paged. [Also available at https://doi.org/10.3133/twri09A6.]

Lindgren, R.J., 1996, Availability and quality of water from drift aquifers in Marshall, Pennington, Polk, and Red Lake Counties, northwestern Minnesota: U.S. Geological Survey Water-Resources Investigations Report 95–4201, 144 p.

Lindgren, R.J., 2002, Ground-water resources of the uppermost confined aquifers, southern Wadena County and parts of Ottertail, Todd, and Cass Counties, central Minnesota, 1997–2000: U.S. Geological Survey Water-Resources Investigations Report 02–4023, 50 p.

Lund, T., and Blum, J.L., 2017, Analysis of the Cromwell, Minnesota, well 4 (593593) aquifer test conducted on May 24, 2017: St. Paul, Minn., Minnesota Department of Health, Aquifer Test 2612, 75 p., accessed March 15, 2018, at https://www.health.state.mn.us/communities/environment/water/docs/swp/testcromwell.pdf.

Maher, A.-T., 2020, Hydrogeology and groundwater geochemistry of two glacigenic aquitard/aquifer systems in north-central and south-central Minnesota: Iowa State University, master's thesis, 212 p. [Also available at https://lib.dr.iastate.edu/cgi/viewcontent.cgi?article=9013&context=etd.]

Maher, A.-T., Trost, J.J., Witt, A.N., Berg, A.M., Simpkins, W.W., and Stark, J.R., 2020, Geochemical data, water-level data, and slug test analysis results from till confining units and confined aquifers in glacial deposits near Akeley, Cromwell, Litchfield, and Olivia, Minnesota, 2015–2018: U.S. Geological Survey data release, https://doi.org/10.5066/P9IXC7D3.

McKay, L.D., Cherry, J.A., and Gillham, R.W., 1993, Field experiments in a fractured clay till hydraulic conductivity and fracture aperture: Water Resources Research, v. 29, no. 4, p. 1149–1162. [Also available at https://doi.org/10.1029/92WR02592.]

McKay, L.D., and Fredericia, J., 1995, Distribution, origin, and hydraulic influence of fractures in a clay-rich glacial deposit: Canadian Geotechnical Journal, v. 32, no. 6, p. 957–975. [Also available at https://doi.org/10.1139/t95-095.]

McMahon, P.B., Chapelle, F.H., and Bradley, P.M., 2011, Evolution of redox processes in groundwater: ACS Symposium Series 1071, p. 581–597. [Also available at https://doi.org/10.1021/bk-2011-1071.ch026.]

McMahon, P.B., Cowdery, T.K., Chapelle, F.H., and Jurgens, B.C., 2009, Redox conditions in selected principal aquifers of the United States: U.S. Geological Survey Fact Sheet 2009–3041, 6 p. [Also available at https://doi.org/10.3133/fs20093041.]

Meyer, G.N., 2015, C–35, geologic atlas of Meeker County, Minnesota [part A]: Minnesota Geological Survey, 5 plates. [Also available at https://conservancy.umn.edu/handle/11299/166576.]

Minnesota Department of Health, 2017, Minnesota well index online: accessed November 20, 2017, at https://apps.health.state.mn.us/cwi/.

Minnesota Department of Natural Resources, 2006, Geologic map of Minnesota—Quaternary geology (MGS map S–1), 1982: Minnesota Geological Survey web page, accessed June 2020 at https://gisdata.mn.gov/dataset/geos-quaternary-geology-mn.

Minnesota Department of Natural Resources, 2014, Minnesota county boundaries: Minnesota Geographic Metadata Guidelines, accessed June 2020 at https://gisdata.mn.gov/dataset/bdry-counties-in-minnesota.

Minnesota Department of Natural Resources, 2017, Minnesota Water Use Data, ArcGIS Layer: accessed November 20, 2017, at http://files.dnr.state.mn.us/waters/watermgmt_section/appropriations/mpars_wa_permits_installations_uses.zip.

Minnesota Department of Natural Resources, 2018, MNDNR hydrography: Minnesota Geographic Metadata Guidelines, accessed June 2020 at https://gisdata.mn.gov/dataset/water-dnr-hydrography.

Minnesota Department of Natural Resources, 2020, 1981–2010 normal precipitation maps—Annual (January–December): Minnesota Department of Natural Resources web page, accessed August 2020 at https://www.dnr.state.mn.us/climate/summaries_and_publications/precip_norm_1981-2010_annual.html.

Minnesota Pollution Control Agency, 1999, Phosphorous in Minnesota's ground water: St. Paul, Minn., Minnesota Pollution Control Agency, 2 p. [Also available at https://www.pca.state.mn.us/sites/default/files/phospho.pdf.]

Moench, A.F., 1985, Transient flow to a large-diameter well in an aquifer with storative semiconfining layers: Water Resources Research, v. 21, no. 8, p. 1121–1131. [Also available at https://doi.org/10.1029/WR021i008p01121.]

Mullaney, J.R., Lorenz, D.L., and Arntson, A.D., 2009, Chloride in groundwater and surface water in areas underlain by the glacial aquifer system, northern United States: U.S. Geological Survey Scientific Investigations Report 2009–5086, 41 p. [Also available at https://doi.org/10.3133/sir20095086.]

Neuman, S.P., and Witherspoon, P.A., 1969, Applicability of current theories of flow in leaky aquifers: Water Resources Research, v. 5, no. 4, p. 817–829. [Also available at https://doi.org/10.1029/WR005i004p00817.]

Neuman, S.P., and Witherspoon, P.A., 1972, Field determination of the hydraulic properties of leaky multiple aquifer systems: Water Resources Research, v. 8, no. 5, p. 1284–1298. [Also available at https://doi.org/10.1029/WR008i005p01284.]

Odell, J.W., ed., 1993, Method 365.1, revision 2.0—Determination of phosphorus by semi-automated colorimetry: Cincinnati, Ohio, U.S. Environmental Protection Agency, 18 p., accessed June 12, 2020, at https://www.epa.gov/sites/production/files/2015-08/documents/method_365-1_1993.pdf.

Palmer, P.C., Gannett, M.W., and Hinkle, S.R., 2007, Isotopic characterization of three groundwater recharge sources and inferences for selected aquifers in the upper Klamath Basin of Oregon and California, USA: Journal of Hydrology (Amsterdam), v. 336, no. 1–2, p. 17–29. [Also available at https://doi.org/10.1016/j.jhydrol.2006.12.008.]

Parkin, T.B., and Simpkins, W.W., 1995, Contemporary groundwater methane production from Pleistocene carbon: Journal of Environmental Quality, v. 24, no. 2, p. 367–372. [Also available at https://doi.org/10.2134/jeq1995.00472425002400020021x.]

Patton, C.J., and Kryskalla, J.R., 2011, Colorimetric determination of nitrate plus nitrite in water by enzymatic reduction, automated discrete analyzer methods: U.S. Geological Survey Techniques and Methods, book 5, chap. B8, 34 p. [Also available at https://doi.org/10.3133/tm5B8.]

Piper, A.M., 1944, A graphic procedure in the geochemical interpretation of water-analyses: Eos (Washington, D.C.), v. 25, no. 6, p. 914–928. [Also available at https://doi.org/10.1029/TR025i006p00914.]

Remenda, V.H., Cherry, J.A., and Edwards, T.W.D., 1994, Isotopic composition of old ground water from Lake Agassiz—Implications for late Pleistocene climate: Science, v. 266, no. 5193, p. 1975–1978. [Also available at https://doi.org/10.1126/science.266.5193.1975.]

Remenda, V.H., and van der Kamp, G., 1997, Contamination from sand-bentonite seal in monitoring wells installed in aquitards: Ground Water, v. 35, no. 1, p. 39–46. [Also available at https://doi.org/10.1111/j.1745-6584.1997.tb00058.x.]

Robertson, S., 2011, Well head protection plan part i—Well head protection area delineation drinking water supply management area delineation well and drinking water supply management area vulnerability assessments for the city of Olivia: Minnesota Department of Health, p. 1–21.

Rodvang, S., and Simpkins, W., 2001, Agricultural contaminants in Quaternary aquitards—A review of occurrence and fate in North America: Hydrogeology Journal, v. 9, no. 1, p. 44–59. [Also available at https://doi.org/10.1007/s100400000114.]

Ruhl, J.F., and Adolphson, D.G., 1986, Hydrogeologic and water-quality characteristics of the Red River-Winnipeg aquifer northwestern Minnesota: Water-Resources Investigations Report 84–4111, 2 plates. [Also available at https://doi.org/10.3133/wri844111.]

Sebilo, M., Mayer, B., Nicolardot, B., Pinay, G., and Mariotti, A., 2013, Long-term fate of nitrate fertilizer in agricultural soils: Proceedings of the National Academy of Sciences of the United States of America, v. 110, no. 45, p. 18185–18189. [Also available at https://doi.org/10.1073/pnas.1305372110.]

Seo, H.H., 1996, Hydraulic properties of quaternary stratigraphic units in the Walnut Creek watershed: Iowa State University, master's thesis, 145 p.

Shaw, R.J., and Hendry, M.J., 1998, Hydrogeology of a thick clay till and Cretaceous clay sequence, Saskatchewan, Canada: Canadian Geotechnical Journal, v. 35, no. 6, p. 1041–1052. [Also available at https://doi.org/10.1139/t98-060.]

Simpkins, W.W., and Bradbury, K.R., 1992, Groundwater flow, velocity, and age in a thick, fine-grained till unit in southeastern Wisconsin: Journal of Hydrology (Amsterdam), v. 132, no. 1–4, p. 283–319. [Also available at https://doi.org/10.1016/0022-1694(92)90183-V.]

Simpkins, W.W., and Parkin, T.B., 1993, Hydrogeology and redox geochemistry of CH_4 in a late Wisconsinan till and loess sequence in central Iowa: Water Resources Research, v. 29, no. 11, p. 3643–3657. [Also available at https://doi.org/10.1029/93WR01687.]

Smith, E.A., and Westenbroek, S.M., 2015, Potential groundwater recharge for the state of Minnesota using the Soil-Water-Balance model, 1996–2010: U.S. Geological Survey Scientific Investigations Report 2015–5038, 85 p. [Also available at https://doi.org/10.3133/sir20155038.]

Spalding, R.F., and Exner, M.E., 1993, Occurrence of nitrate in groundwater—A review: Journal of Environmental Quality, v. 22, no. 3, p. 392–402. [Also available at https://doi.org/10.2134/jeq1993.00472425002200030002x.]

Springer, R.K., and Gelhar, L.W., 1991, Characterization of large-scale aquifer heterogeneity in glacial outwash by analysis of slug tests with oscillatory responses, Cape Cod, Massachusetts, *in* Mallard, G.E., and Aronson, D.A., eds., U.S. Geological Survey Toxic Substances Hydrology Program—Proceedings of the technical meeting, Monterey, California, March 11–15, 1991: U.S. Geological Survey Water-Resources Investigations Report 91–4034, p. 36–40. [Also available at https://doi.org/10.3133/wri914034.]

Staley, A., and Nguyen, M., 2018, Core descriptions and unit interpretations in support of hydrologic properties of till investigation, Olivia and University of Minnesota hydrogeology-field site: St. Paul, Minn., Minnesota Geological Survey, 20 p.

Staley, A.E., Wagner, K., Nguyen, M., and Tipping, R., 2018, Core descriptions, borehole geophysics, and unit interpretations in support of phase I and II USGS hydrologic properties of till investigation: St. Paul, Minn., Minnesota Geological Survey Open File Report 18–03, 29 p.

Trost, J.J., Feinstein, D.T., and Jones, P.M., 2020, Heuristic MODFLOW models used to evaluate the effects of pumping groundwater from confined aquifers overlain by till confining units: U.S. Geological Survey data release, https://doi.org/10.5066/P9KOI6T3.

U.S. Census Bureau, 2012, 2010 Census of Population and Housing, Population and Housing Unit Counts, CPH-2-25, Minnesota: Washington, D.C., U.S. Government Printing Office.

U.S. Geological Survey, variously dated, National field manual for the collection of water-quality data: U.S. Geological Survey Techniques of Water-Resources Investigations, book 9, chaps. A1–A9, accessed April 1, 2016, at https://water.usgs.gov/owq/FieldManual/.

U.S. Geological Survey, 2019, USGS water data for the Nation: U.S. Geological Survey National Water Information System database, accessed May 20, 2020, at https://doi.org/10.5066/F7P55KJN.

Wagner, K., and Tipping, R., 2016, Core descriptions and borehole geophysics in support of USGS hydrologic properties of till investigation, Litchfield and Cromwell, Minnesota: University of Minnesota and Minnesota Geological Survey, 15 p., accessed November 20, 2017, at https://www.lccmr.leg.mn/projects/2014/finals/2014_03h_MGS_report.pdf.

Walsh, J.F., 2012, Amendment to the wellhead protection plan for the city of Cromwell, Public water supply identification number 1090007: Minnesota Department of Health, 13 p.

Wang, H.F., 2001, Theory of linear poroelasticity with applications to geomechanics and hydrogeology: Princeton, N.J., Princeton University Press, 287 p.

Witt, A.N., 2017, Hydrogeological and geochemical investigation of recharge (leakage) through till aquitards to buried-valley aquifers in central and northeastern Minnesota: Iowa State University, master's thesis, 168 p. [Also available at https://lib.dr.iastate.edu/etd/15462/ https://doi.org/10.31274/etd-180810-5080.]

Young, N.L., Simpkins, W.W., Reber, J.E., and Helmke, M.F., 2020, Estimation of the representative elementary volume of a fractured till—A field and groundwater modeling approach: Hydrogeology Journal, v. 28, p. 781–793.

Appendix 1 Well and Piezometer Construction Details

This appendix contains table 1.1, which has detailed well and piezometer construction information.

References Cited

Staley, A., and Nguyen, M., 2018, Core descriptions and unit interpretations in support of hydrologic properties of till investigation, Olivia and University of Minnesota hydrogeology-field site: St. Paul, Minn., Minnesota Geological Survey, 20 p.

Staley, A.E., Wagner, K., Nguyen, M., and Tipping, R., 2018, Core descriptions, borehole geophysics, and unit interpretations in support of phase I and II USGS hydrologic properties of till investigation: St. Paul, Minn., Minnesota Geological Survey Open File Report 18–03, 29 p.

Wagner, K., and Tipping, R., 2016, Core descriptions and borehole geophysics in support of USGS hydrologic properties of till investigation, Litchfield and Cromwell, Minnesota: University of Minnesota and Minnesota Geological Survey, 15 p., accessed November 20, 2017, at https://www.lccmr.leg.mn/projects/2014/finals/2014_03h_MGS_report.pdf.

Table 1.1. Construction information, types of data collected, and adjacent sediment texture properties for wells and piezometers sampled at the Litchfield, Cromwell, Olivia, and hydrogeology field camp field sites in Minnesota.

[ft, foot; BLS, below land surface; N, no; Y, yes; WQ, water quality; WL, water level; --, unknown or data not collected]

Well or piezometer name	Drilling method	Completion date	Tipping bucket precipitation	Continuous water levels	Types of discrete data collected	Screen slot size	Mesh size of silica sand for filter pack	Top of filter pack (ft BLS)	Filter pack length (ft)	Textural description of material at well screen	Number of well volumes purged to develop well	Sediment texture properties within 10 ft of well screen[a]		
												Sand percent	Silt percent	Clay percent
Litchfield field sites														
LFO1–B	Hollow-stem auger	6/12/2015	N	Y	WQ, WL	10	20/40	19.0	6.3	Fine-grained sand	51	--	--	--
LFO1–C	Hollow-stem auger	6/12/2015	N	N	WQ, WL	10	20/40	47.1	6.1	Sandy loam till	9	58	29	13
LFO1–D	Hollow-stem auger	6/11/2015	N	Y	WQ, WL	10	20/40	70.0	5.3	Loamy till	14	47	32	21
LFO1–E	Hollow-stem auger	6/10/2015	N	N	WQ, WL	10	20/40	89.8	5.5	Sandy loam till	53	--	--	--
LFO1–F	Hollow-stem auger	6/15/2015	N	Y	WQ, WL	20	12/20	94.8	32.7	Sand and gravel	14	--	--	--
LFO2–A	Hollow-stem auger	6/24/2015	Y	Y	WQ, WL	10	20/40	15.0	5.0	Loamy till	9	52	35	13
LFO2–B	Hollow-stem auger	6/24/2015	N	N	WQ, WL	10	20/40	30.1	5.0	Sandy loam till	5	49	32	19
LFO2–C	Hollow-stem auger	6/22/2015	N	Y	WQ, WL	10	20/40	52.0	8.7	Loamy till	4	46	34	20
LFO2–D	Hollow-stem auger	6/23/2015	N	Y	WQ, WL	10	20/40	79.3	5.9	Sandy loam till	4	47	32	21
LFO2–E	Hollow-stem auger	6/20/2015	N	N	WQ, WL	10	20/40	108.8	5.0	Sandy loam till	6	58	29	13
LFO2–F	Hollow-stem auger	6/16/2015	N	Y	WQ, WL	20	12/20	137.5	24.9	Sand and gravel	21	--	--	--
LF–OB1	Auger (nonspecified)	12/18/1997	N	N	WL	10	--	--	--	Sand and gravel	--	--	--	--
LF–CM1	Nonspecified rotary	10/30/2008	N	N	WL	60	--	--	--	Sand and gravel	--	--	--	--
LF–CM2	Nonspecified rotary	2/19/1998	N	N	WL	115	--	--	--	Sand and gravel	--	--	--	--
LF–CM3	Nonspecified rotary	12/9/1999	N	N	WL	70	--	--	--	Sand	--	--	--	--
LF–CM4	Nonspecified rotary	12/9/1999	N	N	WL	70	--	--	--	Sand and gravel	--	--	--	--

Table 1.1. Construction information, types of data collected, and adjacent sediment texture properties for wells and piezometers sampled at the Litchfield, Cromwell, Olivia, and hydrogeology field camp field sites in Minnesota.—Continued

[ft, foot; BLS, below land surface; N, no; Y, yes; WQ, water quality; WL, water level; --, unknown or data not collected]

Well or piezometer name	Drilling method	Completion date	Tipping bucket precipitation	Continuous water levels	Types of discrete data collected	Screen slot size	Mesh size of silica sand for filter pack	Top of filter pack (ft BLS)	Filter pack length (ft)	Textural description of material at well screen	Number of well volumes purged to develop well	Sediment texture properties within 10 ft of well screen[a]		
												Sand percent	Silt percent	Clay percent
Cromwell field sites														
CWO1–A	Mud rotary	7/21/2015	N	Y	WQ, WL	10	12/20	142.0	6.0	Sandy loam till	14	--	--	--
CWO1–B	Mud rotary	7/20/2015	N	Y	WQ, WL	20	12/20	220.9	14.8	Sand and gravel	15	--	--	--
CWO1–C	Mud rotary	7/18/2015	N	Y	WQ, WL	20	12/20	329.6	16.0	Slate	7	--	--	--
CWO2–A	Hollow-stem auger	7/9/2015	Y	Y	WQ, WL	10	20/40	30.2	7.5	Sand and gravel	71	99	0	1
CWO2–B	Hollow-stem auger	7/13/2015	N	N	WQ, WL	10	20/40	54.4	5.5	Sandy loam till	10	63	27	10
CWO2–C	Hollow-stem auger	7/10/2015	N	N	WQ, WL	10	20/40	74.4	7.5	Sandy loam till	65	56	30	14
CWO2–D	Hollow-stem auger	6/29/2015	N	Y	WQ, WL	10	20/40	93.2	13.5	Sandy loam till	4	54	32	14
CWO2–E	Hollow-stem auger	7/12/2015	N	N	WQ, WL	10	20/40	123.6	5.3	Sandy loam till	14	56	33	11
CW–CM3	Nonspecified rotary	10/21/1992	N	N	--	25	--	--	--	Sand and gravel	--	--	--	--
CW–CM4	Cable tool	4/16/1999	N	N	WL	50	--	--	--	Sand and gravel	--	--	--	--
Hydrogeology field camp field sites														
HT–115	Rotary sonic	5/30/2017	N	Y	WQ, WL	10	20/40	109.0	6.0	Sand	21	70	19	11
HT–140	Rotary sonic	5/31/2017	N	Y	WQ, WL	10	20/40	134.0	6.4	Sandy loam till	4	66	22	12
HT–175	Rotary sonic	5/26/2017	N	Y	WQ, WL	10	20/40	170.0	5.1	Sandy loam till	6	73	19	8
HT–200	Rotary sonic	5/25/2017	N	Y	WQ, WL	10	20/40	191.0	6.9	Sandy loam till	10	68	22	10
HB–1	Rotary sonic	12/19/2014	N	N	WL	10	--	--	--	Sand and clay	--	--	--	--

Table 1.1. Construction information, types of data collected, and adjacent sediment texture properties for wells and piezometers sampled at the Litchfield, Cromwell, Olivia, and hydrogeology field camp field sites in Minnesota.—Continued

[ft, foot; BLS, below land surface; N, no; Y, yes; WQ, water quality; WL, water level; --, unknown or data not collected]

Well or piezometer name	Drilling method	Completion date	Tipping bucket precipitation	Continuous water levels	Types of discrete data collected	Screen slot size	Mesh size of silica sand for filter pack	Top of filter pack (ft BLS)	Filter pack length (ft)	Textural description of material at well screen	Number of well volumes purged to develop well	Sediment texture properties within 10 ft of well screen[a]		
												Sand percent	Silt percent	Clay percent
HB–2	Nonspecified rotary	6/22/2016	N	Y	WL	10	--	--	--	Sand	--	--	--	--
HB–3	Mud rotary	7/18/2017	N	Y	WL	7	12/20	200.0	23.7	Sand and gravel	--	100	0	0
MW–01	Unknown	7/20/1995	Y	Y	WQ, WL	--	--	--	--	Sand and gravel	--	98.5	1	0.5
WL07	Unknown	10/19/1977	N	N	WL	--	--	--	--	Sand and gravel	--	--	--	--
WL12	Unknown	6/13/1978	N	N	WL	--	--	--	--	Sand	--	--	--	--
WL299	Unknown	6/25/1978	N	N	WL	--	--	--	--	Sand and gravel	--	--	--	--
Olivia field sites														
OT–13	Rotary sonic	8/9/2017	Y	Y	WQ, WL	10	20/40	8.0	5.2	Sand and gravel	178	60	25	15
OT–20	Rotary sonic	8/9/2017	N	Y	WQ, WL	10	20/40	15.0	5.2	Silty to clayey loam till	17	45	38	17
OT–35	Rotary sonic	8/9/2017	N	N	WQ, WL	10	20/40	30.0	4.8	Silty to clayey loam till	--	--	--	--
OT–60	Rotary sonic	8/9/2017	N	Y	WQ, WL	10	20/40	55.0	4.9	Silty to clayey loam till	3	36	38	26
OT–105	Rotary sonic	8/8/2017	N	Y	WQ, WL	10	20/40	100.0	5.1	Silty to clayey loam till	6	32	45	23
OT–145	Rotary sonic	8/3/2017	N	Y	WQ, WL	10	20/40	140.0	4.3	Silty to clayey loam till	4	34	36	30

Table 1.1. Construction information, types of data collected, and adjacent sediment texture properties for wells and piezometers sampled at the Litchfield, Cromwell, Olivia, and hydrogeology field camp field sites in Minnesota.—Continued

[ft, foot; BLS, below land surface; N, no; Y, yes; WQ, water quality; WL, water level; --, unknown or data not collected]

Well or piezometer name	Drilling method	Completion date	Tipping bucket precipitation	Continuous water levels	Types of discrete data collected	Screen slot size	Mesh size of silica sand for filter pack	Top of filter pack (ft BLS)	Filter pack length (ft)	Textural description of material at well screen	Number of well volumes purged to develop well	Sediment texture properties within 10 ft of well screen[a]		
												Sand percent	Silt percent	Clay percent
OT–175	Rotary sonic	8/2/2017	N	Y	WQ, WL	10	20/40	169.5	5.9	Silty to clayey loam till	5	14	60	26
OB–7	Rotary sonic	8/1/2017	N	Y	WL	10	12/20	201.0	8.8	Sand and gravel	11	--	--	--
Olivia-4	Unknown	9/3/1964	N	N	WQ, WL	40, 30	--	--	--	Sand and gravel	--	--	--	--
Olivia-5	Unknown	5/18/1972	N	N	WQ, WL	15, 30, 40	--	--	--	Sand and gravel	--	--	--	--
Olivia-6	Unknown	1977	N	N	WL	--	--	--	--	Sand and gravel	--	--	--	--

[a]Data provided by the Minnesota Geological Survey. Data are summarized in Wagner and Tipping (2016), Staley and Nguyen (2018), and Staley and others (2018).

Appendix 2 Slug Test Information

All water-level data used for slug test analyses, AQTESOLV files, and plots are available in the accompanying data release for this report (Maher and others, 2020). Three tables (tables 2.1, 2.2, and 2.3) are included in this appendix. Detailed in table 2.1 is the field information gathered on the slug tests completed at all sites, including the number of tests done, the type of slug test (rising or falling), the volume of the slug used in the tests, and water-level information (static water levels, observed initial displacements, and the calculated theoretical water-level displacement of the slug used). Detailed in table 2.2 are the water-level (static water column height and the saturated thickness) and piezometer construction parameters entered into AQTESOLV for the model runs. Detailed in table 2.3 are several statistical analyses outputted by AQTESOLV for each model run completed, including the mean residual, standard deviation of the residuals, and the 95-percent confidence interval for K_h results.

The program AQTESOLV (Duffield, 2007) has curve matching solutions for slug tests done in confined and unconfined aquifers. During the slug test analyses, the Kansas Geological Survey (KGS) model (Hyder and others, 1994) was used to analyze the water-level response to slug tests. The KGS model has a solution for confined and unconfined aquifers. This method applies a curved solution to declining or rising water-level data collected during a single-well slug test in an unconfined or a confined aquifer with a completely or partially penetrating well. The KGS method assumes the following:

1. the unconfined or confined aquifer is infinite in extent, homogeneous, and of uniform thickness;
2. the potentiometric surface of the aquifer is initially horizontal;
3. the slug is introduced or removed instantaneously to/from the well;
4. head losses during the test are negligible;
5. the water-level response from the slug test is classified as unsteady or overdamped (nonoscillating); and
6. water is released instantaneously from storage with decline of hydraulic head.

The KGS model provides corrections for low permeability materials around the well screen, such as mud residue from well installation, and can consider hydraulic conductivity anisotropy (Arnold, 2015).

A confined KGS model without wellbore skin is identical to the Dougherty-Babu (Dougherty and Babu, 1984) solution (Duffield, 2007). This equation takes into account the following physical parameters of where the piezometer is emplaced: confined aquifer thickness/saturated thickness, the distance from the water table to the top of the screen, the distance from the water table to the bottom of the piezometer screen, the screen thickness, the elevation of the piezometer from the base of the aquifer, and the elevation of the top of the piezometer screen from the base of the aquifer (Duffield, 2007). For the unconfined KGS model without a wellbore skin, the following physical parameters of where the piezometer is emplaced are considered: the depth to the top of the well screen, the depth below top of aquifer, the screen length, and the saturated thickness of the unconfined aquifer (Duffield, 2007).

Because the piezometers in the till are not below the confining unit (the piezometers are in the confining unit), they are not confined and do not have a potentiometric surface as a piezometer screened in a confined aquifer does. Therefore, because the till piezometers are physically not confined, the unconfined solution was used to estimate hydraulic conductivity.

Different solutions were used for the piezometers screened in the confined aquifers and the unconfined aquifers at the sites. The KGS model for confined aquifers without a wellbore skin was used for analyzing the results from slug tests from piezometers in the confined aquifers that did not have an oscillatory response. The KGS model for confined aquifers has the same assumptions as for unconfined aquifers, except that the aquifer is confined instead of unconfined (Duffield, 2007). The Butler (1998) inertial solution was used for results in confined aquifers that indicated inertial effects because of an oscillatory water-level response. The Butler (1998) inertial solution accounts for oscillatory responses in confined aquifers because of a high hydraulic conductivity (Duffield, 2007). Assumptions of the Butler (1998) solution were the same as the KGS solution, except that the flow is in a quasi-steady state and the wells must be partially penetrating (Duffield, 2007).

For unconfined aquifer results that indicated inertial effects present during the slug tests, the Springer-Gelhar (Springer and Gelhar, 1991) inertial solution was used to account for the oscillatory effects. The assumptions of the Springer-Gelhar (Springer and Gelhar,1991) inertial solution are the same as the Butler (1998) solution, except that the aquifer is unconfined and the wells can be either fully or partially penetrating.

References Cited

Arnold, L.R., 2015, Monitoring-well installation, slug testing, and groundwater quality for selected sites in South Park, Park County, Colorado, 2013: U.S. Geological Survey Open-File Report 2014–1231, 32 p., accessed June 2020 at https://doi.org/10.3133/ofr20141231.

Butler, J.J., Jr., 1998, The design, performance, and analysis of slug tests: Boca Raton, Fla., CRC Press, 280 p.

Dougherty, D.E., and Babu, D.K., 1984, Flow to a partially penetrating well in a double-porosity reservoir: Water Resources Research, v. 20, no. 8, p. 1116–1122. [Also available at https://doi.org/10.1029/WR020i008p01116.]

Duffield, G.M., 2007, AQTESOLV for Windows—Version 4.5 user's guide: Reston, Va., HydroSOLVE, Inc., 529 p.

Hyder, Z., Butler, J.J., Jr., McElwee, C.D., and Liu, W., 1994, Slug tests in partially penetrating wells: Water Resources Research, v. 30, no. 11, p. 2945–2957. [Also available at https://doi.org/10.1029/94WR01670.]

Maher, A.-T., Trost, J.J., Witt, A.N., Berg, A.M., Simpkins, W.W., and Stark, J.R., 2020, Geochemical data, water-level data, and slug test analysis results from till confining units and confined aquifers in glacial deposits near Akeley, Cromwell, Litchfield, and Olivia, Minnesota, 2015–2018: U.S. Geological Survey data release, https://doi.org/10.5066/P9IXC7D3.

Springer, R.K., and Gelhar, L.W., 1991, Characterization of large-scale aquifer heterogeneity in glacial outwash by analysis of slug tests with oscillatory responses, Cape Cod, Massachusetts, *in* Mallard, G.E., and Aronson, D.A., eds., U.S. Geological Survey Toxic Substances Hydrology Program—Proceedings of the technical meeting, Monterey, California, March 11–15, 1991: U.S. Geological Survey Water-Resources Investigations Report 91–4034, p. 36–40. [Also available at https://doi.org/10.3133/wri914034.]

Table 2.1. Water-level and displacement data from slug tests done in piezometers at the Litchfield, Cromwell, Olivia, and hydrogeology field camp field sites in Minnesota.

[ft, foot; BLS, below land surface; gal, gallon; H(0), observed initial displacement; ±, plus or minus; − (negative value), water level change below the initial water level; --, unknown]

Piezometer name	Slug test number	Approximate static water level before falling-head slug test (ft BLS)	Approximate static water level before rising-head slug test (ft BLS)	Volume of slug (gal)	Falling head observed initial displacement, H(0) (ft)	Rising head observed initial displacement, H(0) (ft)	Theoretical water-level displacement (±ft)
Litchfield field sites							
LFO1–B	1	11	11	0.080	0.29	−0.44	1.25
LFO1–B	2	11	11	0.080	0.37	−0.50	1.25
LFO1–B	3	11	11	0.080	0.55	−0.62	1.25
LFO1–C	1	13	13	0.161	2.23	−1.97	2.54
LFO1–D	1	26	26	0.160	2.35	−2.47	2.51
LFO1–E	1	35	35	0.081	0.68	−0.57	1.28
LFO1–E	2	35	35	0.081	1.21	−1.33	1.28
LFO1–E	3	35	35	0.081	1.18	−1.50	1.28
LFO1–F	1	35	35	0.199	1.05	−1.27	1.17
LFO1–F	2	35	35	0.199	1.26	−1.64	1.17
LFO2–A	1	11	11	0.080	0.97	−0.93	1.25
LFO2–B	1	13	13	0.080	1.13	−1.04	1.26
LFO2–C	1	16	16	0.160	2.71	−2.84	2.51
LFO2–D	1	36	--	0.160	2.75	--	2.50
LFO2–E	1	62	62	0.160	2.76	−2.94	2.50
LFO2–F	1	63	63	0.378	2.63	−3.15	2.22
LFO2–F	2	63	63	0.378	2.65	−2.42	2.22
LFO2–F	3	63	63	0.378	2.84	−4.02	2.22
Cromwell field sites							
CWO1–A	1	20	20	0.389	2.37	−2.31	2.29
CWO1–B	1	16	16	0.378	2.87	−3.86	2.22
CWO1–B	2	16	16	0.378	2.64	−3.15	2.22
CWO1–B	3	16	16	0.378	0.56	−3.72	2.22
CWO1–C	1	16	16	0.378	5.85	−3.13	2.22
CWO1–C	2	16	16	0.378	3.86	−2.60	2.22
CWO1–C	3	16	16	0.378	3.78	−2.65	2.22
CWO2–A	1	26	26	0.081	1.52	−1.19	1.28
CWO2–A	2	26	26	0.081	1.12	−2.46	1.28
CWO2–A	3	26	26	0.081	3.18	−4.56	1.28

Table 2.1. Water-level and displacement data from slug tests done in piezometers at the Litchfield, Cromwell, Olivia, and hydrogeology field camp field sites in Minnesota.—Continued

[ft, foot; BLS, below land surface; gal, gallon; H(0), observed initial displacement; ±, plus or minus; − (negative value), water level change below the initial water level; --, unknown]

Piezometer name	Slug test number	Approximate static water level before falling-head slug test (ft BLS)	Approximate static water level before rising-head slug test (ft BLS)	Volume of slug (gal)	Falling head observed initial displacement, H(0) (ft)	Rising head observed initial displacement, H(0) (ft)	Theoretical water-level displacement (±ft)
CWO2–B	1	28	28	0.162	2.64	−2.81	2.54
CWO2–C	1	26	26	0.175	2.48	−2.51	2.75
CWO2–D	1	23	23	0.162	2.77	−2.83	2.54
CWO2–E	1	24	24	0.161	2.70	−2.65	2.52
Hydrogeology field camp field sites							
HT–115	1	60	60	0.161	2.64	−2.44	2.24
HT–115	2	60	60	0.161	2.47	−2.49	2.24
HT–115	3	60	60	0.161	2.51	−2.28	2.24
HT–140	1	61	61	0.080	1.24	−1.31	1.12
HT–140	2	61	61	0.080	1.22	−1.22	1.12
HT–140	3	61	61	0.080	1.28	−1.04	1.12
HT–175	1	63	63	0.080	1.18	−1.28	1.12
HT–175	2	63	63	0.080	1.23	−1.42	1.12
HT–175	3	63	63	0.080	1.34	−1.47	1.12
HT–200	1	64	64	0.161	2.5	−2.39	2.24
HT–200	2	64	64	0.161	2.57	−2.43	2.24
HT–200	3	64	64	0.161	2.58	−2.39	2.24
HB–3	1	66	66	0.411	2.21	−2.01	2.35
HB–3	2	66	66	0.411	1.95	−1.94	2.35
HB–3	3	66	66	0.411	2.81	−2.34	2.35
MW–01	1	62	62	0.411	2.99	−2.25	2.52
MW–01	2	62	62	0.411	3.29	−1.87	2.52
MW–01	3	62	62	0.411	3.99	−2.11	2.52
Olivia field sites							
OT–13	1	1	1	0.161	1.71	−2.24	2.25
OT–13	2	1	1	0.080	0.91	−0.97	1.12
OT–13	3	1	1	0.080	0.84	−1.07	1.12
OT–20	1	5	5	0.080	1.07	−0.86	1.12
OT–20	2	5	5	0.080	0.97	−0.97	1.12

Table 2.1. Water-level and displacement data from slug tests done in piezometers at the Litchfield, Cromwell, Olivia, and hydrogeology field camp field sites in Minnesota.—Continued

[ft, foot; BLS, below land surface; gal, gallon; H(0), observed initial displacement; ±, plus or minus; − (negative value), water level change below the initial water level; --, unknown]

Piezometer name	Slug test number	Approximate static water level before falling-head slug test (ft BLS)	Approximate static water level before rising-head slug test (ft BLS)	Volume of slug (gal)	Falling head observed initial displacement, H(0) (ft)	Rising head observed initial displacement, H(0) (ft)	Theoretical water-level displacement (±ft)
OT–20	3	5	5	0.080	1.07	−1.05	1.12
OT–60	1	6	6	0.080	1.18	−1.24	1.12
OT–60	2	6	6	0.080	1.17	−0.91	1.12
OT–60	3	6	6	0.080	1.19	--	1.12
OT–105	1	15	15	0.080	1.27	−1.37	1.12
OT–105	2	15	15	0.080	1.27	−1.32	1.12
OT–105	3	15	15	0.080	1.27	−1.36	1.12
OT–145	1	22	21	0.080	1.21	−1.33	1.12
OT–145	2	18	18	0.080	1.24	−1.19	1.12
OT–145	3	17	17	0.080	1.43	−1.03	1.12
OT–175	1	28	28	0.080	1.22	−1.27	1.12
OT–175	1	28	28	0.080	0.88	−1.09	1.12
OT–175	3	28	28	0.080	1.09	−1.19	1.12
OB–7	1	100	100	0.161	0.90	−0.98	0.91
OB–7	2	100	100	0.161	1.71	−1.45	0.91
OB–7	3	100	100	0.161	1.36	−1.46	0.91

Table 2.2. Aquifer and piezometer parameters specified in AQTESOLV for the analysis of slug test data for piezometers at the Litchfield, Cromwell, Olivia, and hydrogeology field camp field sites in Minnesota.

Piezometer name	Static water column height	Aquifer saturated thickness	Depth to top of filter pack (or screen for aquifers) below reference point[a]	Length of filter pack (or screen for aquifers)	Radius casing	Radius of borehole (or well for aquifers)
	Feet					
Litchfield field sites						
LFO1–B	14	27.94	11.34	2.7	0.0521	0.0521
LFO1–C	40.45	86.71	35.76	6.1	0.0521	0.3438
LFO1–D	49.54	86.71	58.84	5.3	0.0521	0.3438
LFO1–E	59.46	86.71	78.79	5.5	0.0521	0.3438
LFO1–F	91.56	44.00	19.50	9.6	0.0833	0.085
LFO2–A	8.61	105.83	3.82	5.0	0.0521	0.3438
LFO2–B	21.84	105.83	19.12	5.0	0.0521	0.3438
LFO2–C	43.29	105.83	62.91	8.7	0.0521	0.3438
LFO2–D	51.04	105.83	82.35	5.9	0.0521	0.3438
LFO2–E	51.38	105.83	96.83	5.0	0.0521	0.3438
LFO2–F	99.96	44.00	32.54	9.6	0.0833	0.085
Cromwell field sites						
CWO1–A	128.38	150.69	119.82	6.0	0.0833	0.2813
CWO1–B	211.28	147.00	47.91	9.6	0.0833	0.085
CWO1–C	323.91	187.03	156.66	16.0	0.0833	0.2813
CWO2–A	6.81	15.85	4.15	2.7	0.0521	0.0521
CWO2–B	31.88	136.54	25.94	5.5	0.0521	0.3438
CWO2–C	55.39	136.54	46.95	7.5	0.0521	0.3438
CWO2–D	83.39	136.54	65.23	13.5	0.0521	0.3438
CWO2–E	104.95	136.54	95.29	5.3	0.0521	0.3438
Hydrogeology field camp field sites						
HT–115	52.07	144.00	49.54	6.4	0.055	0.28125
HT–140	76.97	144.00	74.14	6.5	0.055	0.28125
HT–175	109.59	144.00	110.50	6.0	0.055	0.28125
HT–200	133.23	144.00	131.50	9.0	0.055	0.28125
HB–3	157	22.00	8.33	10.2	0.0863	0.08500
MW–01	24	44.00	19.00	5.0	0.0833	0.08500
Olivia field sites						
OT–13	9.61	9.61	4.46	5.1	0.055	0.0575
OT–20	16.26	177.00	11.22	5.2	0.055	0.28125
OT–35	28.13	177.00	26.37	5.0	0.055	0.28125
OT–60	50.62	177.00	51.30	5.0	0.055	0.28125
OT–105	87.24	177.00	95.46	5.2	0.055	0.28125
OT–145	121.94	177.00	135.53	5.5	0.055	0.28125
OT–175	145.14	177.00	165.01	6.0	0.055	0.28125
OB–7	109.71	54.00	24.92	4.8	0.0863	0.08333

[a]Reference point is the water table surface for piezometers screened in unconfined aquifers and till; reference point is the till-aquifer boundary for wells screened in confined aquifers.

Table 2.3. Residual statistics and confidence interval of each horizontal hydraulic conductivity estimate made from slug tests done in piezometers at the Litchfield, Cromwell, Olivia, and hydrogeology field camp field sites in Minnesota.

[mean residual, the mean difference between the recorded water-level recovery by modeled water-level recovery; %, percent; K_h, horizontal hydraulic conductivity; E, scientific notation denoting exponentiation; for example −2.30E−03 = -2.30×10^{-3}; --, unknown]

Piezometer name	Slug test number	Falling head			Rising head		
		Mean residual	Standard deviation of the residuals	95% confidence interval of K_h (plus or minus)	Mean residual	Standard deviation of the residuals	95% confidence interval of K_h (plus or minus)
		Feet		Feet per day	Feet		Feet per day
Litchfield field sites							
LFO1–B	1	−2.30E−03	3.76E−02	1.22E+02	1.38E−03	3.60E−02	7.36E+01
LFO1–B	2	2.81E−03	1.09E−02	4.08E+01	4.18E−11	9.28E−11	9.15E−07
LFO1–B	3	−1.99E−01	5.84E−01	7.22E+02	9.05E−03	2.67E−02	6.70E+01
LFO1–C	1	6.01E−03	2.04E−02	9.75E−04	6.57E−02	2.23E−02	1.60E−03
LFO1–D	1	2.27E−02	5.86E−02	6.17E−02	6.89E−03	2.04E−02	1.37E−02
LFO1–E	1	3.27E−03	2.91E−02	2.33E−01	−8.06E−03	2.95E−02	2.45E−01
LFO1–E	2	2.05E−02	7.86E−02	1.43E−01	−5.41E−03	4.75E−02	9.80E−02
LFO1–E	3	−9.36E−02	1.51E−01	2.41E−01	1.71E−02	6.00E−02	7.96E−02
LFO1–F	1	−3.47E−02	9.63E−02	6.37E+01	1.60E−02	9.80E−02	4.94E+01
LFO1–F	2	−2.49E−02	1.36E−01	6.81E+01	3.40E−03	1.21E−01	3.76E+01
LFO2–A	1	−8.31E−03	6.95E−02	8.21E−05	−2.62E−02	6.14E−02	4.09E−05
LFO2–B	1	−3.40E−02	1.12E−01	2.57E−04	−2.74E−03	3.25E−02	5.82E−05
LFO2–C	1	1.84E−01	3.28E−01	7.64E−04	1.79E−01	3.39E−01	5.81E−04
LFO2–D	1	7.01E−04	2.49E−02	1.99E−06	--	--	--
LFO2–E	1	3.70E−03	5.26E−02	4.63E−05	2.60E−02	1.88E−01	7.45E−05
LFO2–F	1	−9.34E−02	4.37E−01	9.45E+01	−8.80E−02	2.41E−01	3.45E+01
LFO2–F	2	−1.93E−01	3.16E−01	7.16E+01	−2.26E−01	2.55E−01	5.77E+01
LFO2–F	3	−5.10E−02	4.34E−01	9.72E+01	2.79E−02	3.36E−01	3.50E+01
Cromwell field sites							
CWO1–A	1	9.01E−03	7.95E−02	3.36E−02	5.06E−02	9.23E−02	3.32E−02
CWO1–B	1	2.08E−02	3.19E−01	8.15E+02	−3.39E−02	1.90E−01	8.84E+00
CWO1–B	2	−8.73E−03	7.29E−02	1.97E+00	−1.20E−02	5.21E−02	8.73E+01
CWO1–B	3	9.56E−03	2.21E−01	6.01E+02	8.54E−02	3.84E−01	5.05E+00
CWO1–C	1	−2.36E−01	6.09E−01	2.66E−01	−2.63E−02	9.88E−02	3.36E−02
CWO1–C	2	−1.23E−01	2.43E−01	8.34E−02	2.51E−02	8.94E−02	2.74E−02
CWO1–C	3	−1.80E−01	2.64E−01	8.76E−02	−1.82E−01	4.35E−01	1.31E−01
CWO2–A	1	−3.79E−02	1.62E−01	2.15E+00	−3.37E−03	1.53E−02	1.84E−01
CWO2–A	2	−1.94E−03	1.38E−02	1.52E−01	2.78E−01	4.44E−01	4.08E+00
CWO2–A	3	−5.42E−01	8.06E−01	4.08E+00	−7.36E−01	1.16E+00	6.15E+00
CWO2–B	1	1.46E−02	3.79E−02	3.18E−03	2.27E−02	5.75E−02	3.72E−03
CWO2–C	1	7.33E−03	3.32E−02	5.75E−03	1.74E−02	1.86E−01	4.74E−02
CWO2–D	1	−1.20E−02	5.59E−02	7.00E−04	3.52E−02	9.32E−02	1.40E−03
CWO2–E	1	−8.24E−03	3.44E−02	2.42E−03	7.95E−04	2.87E−02	1.87E−03
Hydrogeology field camp field sites							
HT–115	1	−5.01E−02	3.50E−01	5.44E−02	−2.73E−02	2.63E−01	3.62E−02
HT–115	2	−2.13E−02	1.96E−01	2.80E−02	−2.74E−02	2.96E−01	4.04E−02
HT–115	3	−1.90E−02	2.03E−01	3.05E−02	−7.96E−03	1.90E−01	2.71E−02

Table 2.3. Residual statistics and confidence interval of each horizontal hydraulic conductivity estimate made from slug tests done in piezometers at the Litchfield, Cromwell, Olivia, and hydrogeology field camp field sites in Minnesota.—Continued

[mean residual, the mean difference between the recorded water-level recovery by modeled water-level recovery; %, percent; K_h, horizontal hydraulic conductivity; E, scientific notation denoting exponentiation; for example −2.30E−03 = -2.30×10^{-3}; --, unknown]

Piezometer name	Slug test number	Falling head			Rising head		
		Mean residual	Standard deviation of the residuals	95% confidence interval of K_h (plus or minus)	Mean residual	Standard deviation of the residuals	95% confidence interval of K_h (plus or minus)
		Feet		Feet per day	Feet		Feet per day
HT–140	1	3.28E−03	4.82E−02	1.89E−05	−5.89E−03	5.33E−02	1.71E−05
HT–140	2	−2.96E−03	9.24E−02	2.71E−05	−1.37E−02	1.41E−01	5.06E−05
HT–140	3	−1.32E−02	1.43E−01	5.67E−05	−2.76E−03	3.96E−02	7.02E−06
HT–175	1	−1.21E−02	9.99E−02	7.35E−04	−2.88E−03	8.53E−02	8.68E−04
HT–175	2	−2.70E−03	5.88E−02	3.47E−04	−8.54E−03	1.01E−01	7.05E−04
HT–175	3	−9.66E−04	3.85E−02	2.18E−04	−7.29E−03	9.02E−02	6.56E−04
HT–200	1	−4.37E−02	2.95E−01	1.66E−02	−1.70E−02	1.56E−01	8.54E−03
HT–200	2	−2.16E−02	2.03E−01	1.09E−02	−1.02E−02	1.39E−01	8.32E−03
HT–200	3	−1.94E−02	1.98E−01	1.32E−02	−1.44E−02	1.44E−01	9.61E−03
HB–3	1	−1.62E−02	1.30E−01	7.34E+00	6.45E−03	1.14E−01	8.27E+00
HB–3	2	−1.01E−02	1.57E−01	1.10E+01	2.24E−02	1.18E−01	7.88E+00
HB–3	3	−1.80E−03	3.08E−01	1.58E+01	4.74E−03	1.13E−01	5.43E+00
MW–01	1	−4.45E−02	5.59E−01	8.56E+00	−6.70E−03	1.27E−01	1.55E+00
MW–01	2	−3.37E−02	4.38E−01	6.47E+00	−1.09E−02	1.50E−01	1.80E+00
MW–01	3	2.68E−03	3.86E−01	5.50E+00	−9.94E−03	1.94E−01	1.95E+00
				Olivia field sites			
OT–13	1	−4.45E−02	2.65E−01	2.73E−01	−1.40E−02	1.54E−01	1.18E−01
OT–13	2	−1.78E−02	1.11E−01	1.23E−01	7.96E−04	7.59E−02	1.02E−01
OT–13	3	−1.02E−02	8.95E−02	1.08E−01	3.28E−05	4.90E−02	9.74E−02
OT–20	1	−1.27E−03	7.96E−03	1.90E−05	−2.94E−03	1.59E−02	3.48E−05
OT–20	2	−1.85E−03	9.95E−03	2.11E−05	−1.10E−02	3.52E−02	2.87E−04
OT–20	3	−2.65E−03	1.43E−02	1.89E−05	−1.42E−03	4.73E−02	2.35E−04
OT–60	1	1.32E−03	6.02E−02	4.95E−05	−2.37E−03	5.66E−02	1.28E−05
OT–60	2	−2.81E−03	3.10E−02	1.20E−05	−5.68E−03	2.57E−02	6.45E−06
OT–60	3	−9.82E−03	5.18E−02	2.09E−05	--	--	--
OT–105	1	−3.33E−03	3.85E−02	5.58E−07	−2.36E−03	2.61E−02	9.91E−07
OT–105	2	−6.50E−05	1.09E−02	3.08E−07	−1.32E−04	6.57E−02	2.13E−06
OT–105	3	−2.36E−03	2.36E−02	4.99E−07	−2.07E−04	2.75E−02	8.88E−07
OT–145	1	−4.45E−03	3.38E−02	1.44E−04	−7.67E−03	3.82E−02	1.10E−04
OT–145	2	1.45E−03	1.50E−02	2.73E−05	−4.81E−02	1.00E−01	2.64E−04
OT–145	3	1.36E−03	1.94E−02	3.98E−05	−5.36E−02	9.34E−02	2.62E−04
OT–175	1	−5.40E−03	2.92E−02	8.46E−05	−2.48E−03	3.15E−02	1.06E−04
OT–175	2	3.58E−03	1.88E−02	1.09E−04	2.07E−03	1.68E−02	8.43E−05
OT–175	3	1.51E-03	9.99E−03	5.17E−05	−2.45E−04	1.32E−02	5.69E−05
OB–7	1	−1.24E−03	4.39E−02	4.03E−01	2.13E−03	2.07E−02	8.87E−02
OB–7	2	−3.12E−02	1.13E−02	1.17E+01	5.49E−03	3.07E−02	6.41E−02
OB–7	3	−2.05E−02	5.58E−02	5.79E+00	5.18E−03	2.99E−02	6.26E−02
OT–35	1	--	--	--	3.01E−02	1.32E+00	8.77E−12

Appendix 3 Quality Assurance for Water-Quality Samples

Two tables (tables 3.1 and 3.2) are included in appendix 3. Listed in table 3.1 is information on replicates of groundwater samples for three piezometers, HT–200 from the hydrogeology field camp (HFC) site, OT–145 from the Olivia site, and LFO2–F from the Litchfield site. Also included in table 3.1 is information on equipment blanks analyzed for three piezometers, CWO2–C from the Cromwell site, HT–175 from the HFC site, and OT–60 from the Olivia site. Detailed in table 3.2 are laboratory comparisons done for groundwater samples from the OT–13, OT–20, and OT–35 piezometers, which were collected at the same time for the U.S. Geological Survey National Water Quality Laboratory (USGS NWQL) and for Rick Knurr (who worked at the University of Minnesota Laboratory during the Litchfield and Cromwell site analyses and then worked at the Ion Chrom Analytical Laboratory during the Olivia and HFC site analyses).

Most analyte concentrations in replicate samples have a relative percent difference from the field sample of less than 10 percent. The following analytes from the HT–200 replicate sample had a relative percent difference from the field sample of greater than 10 percent: filtered, inflection-point titration carbonate concentration with a relative percent difference of 80 percent, filtered iron concentration with a relative percent difference of 11.1 percent, filtered phosphorus concentration with a relative percent difference of 11.1 percent, and filtered nitrate with a relative percent difference of 10.5 percent. Analyte concentrations in replicate groundwater samples collected at OT–145 had no relative percent differences greater than 10 percent. The following analyte from the LFO2–F replicate sample had a relative percent difference from the field sample of greater than 10 percent: filtered, inflection-point titration carbonate with a percentage difference of 18.2 percent.

Almost all equipment blanks analyzed were less than detection limits for the analytes sampled. The only exception was the filtered, inflection-point titration alkalinity for all three piezometers, ranging from 1 to 3 milligrams per liter (mg/L) as calcium carbonate; filtered, inflection-point titration bicarbonate where the piezometers ranged from 1.6 to 5.2 mg/L; and manganese where two of the piezometers (CWO2–C and OT–60) had detectable manganese ranging from 0.22 to 0.24 microgram per liter. These concentrations are still low, especially when compared to the concentrations observed in the samples.

Three split replicate groundwater samples collected at the Olivia site were sent to the USGS NWQL and the Ion Chrom Analytical Laboratory and analyzed for major anions (table 3.2). Relative percent differences may be large, especially with lower concentrations of analytes. The holding time between when the whole samples were first delivered to the USGS NWQL and the split samples were sent to the Ion Chrom Analytical Laboratory was most likely exceeded for the nitrate and nitrite samples. Because of the sensitivity on nutrient anions, this may have led to the presence of nitrate or nitrite occurring in the sample analyzed by the Ion Chrom Analytical Laboratory, when the sample originally had no occurrence of the analytes, as seen in the USGS NWQL analysis.

Chloride and bromide concentrations between the two laboratories indicate that relative percent differences were low for chloride concentrations (less than 2 percent) and tended to be higher for bromide concentrations (9 to 20 percent), perhaps because of the lower concentrations of bromide compared to chloride. Fluoride concentrations tended to be slightly higher for the USGS NWQL compared to Ion Chrom Analytical Laboratory. Sulfate concentrations were similar between both laboratories and all had a relative percent difference of less than 5 percent. Only one piezometer groundwater sample can be compared for nitrate as nitrogen (OT–13), because the rest of the samples had one or both concentrations less than the detection limit. The resulting comparison of nitrate as nitrogen had a low relative percent difference, at 3.5 percent. The relative percent differences may represent variation between the laboratory analyses and uncertainty with laboratory procedures.

Reference Cited

U.S. Geological Survey, 2019, USGS water data for the Nation: U.S. Geological Survey National Water Information System database, accessed May 20, 2020, at https://doi.org/10.5066/F7P55KJN.

Table 3.1. Quality assurance data, including field replicates and field blanks, for groundwater samples collected from piezometers at the Litchfield, Cromwell, Olivia, and hydrogeology field camp field sites in Minnesota.

[HT–200 and HT–175, hydrogeology field camp piezometers; OT–145 and OT–60, Olivia piezometers; LFO2–F, Litchfield piezometer; CWO2–C, Cromwell piezometer; mg/L, milligram per liter; $CaCO_3$, calcium carbonate; <, less than; --, unknown; µg/L, microgram per liter; N, nitrogen; P, phosphorus; SiO_2, silica]

Constituent	HT–200	OT–145	LFO2–F	CWO2–C	HT–175	OT–60
	[a]Groundwater replicate value ([b]relative percent difference)			Equipment blank value		
Alkalinity, water, filtered, inflection-point titration (mg/L as $CaCO_3$)	190 (2.1)	359 (1.7)	219 (3.7)	3	3	1
Ammonia (NH_3 + NH_4^+), water, filtered (mg/L)	0.14 (0)	1.28 (0.8)	0.66 (1.5)	<0.01	<0.01	0.02
Bicarbonate, water, filtered, inflection-point titration (mg/L)	230 (1.8)	434 (1.8)	266 (3.4)	5.2	4.5	1.6
Bromide, water, filtered (mg/L)	<0.01 (0)	0.023 (9.1)	0.045 (6.5)	<0.01	<0.01	<0.01
Calcium, water, filtered (mg/L)	52.4 (0.9)	46.2 (3.1)	76.6 (0)	<0.022	<0.022	0.031
Carbon dioxide, water, unfiltered (mg/L)	11 (0)	24 (4.1)	18 (0)	--	--	--
Carbonate, water, filtered, inflection-point titration (mg/L)	0.7 (80)	1.7 (6.1)	0.6 (18.2)	<0.1	<0.1	<0.1
Chloride, water, filtered (mg/L)	0.56 (3.5)	13.4 (2.2)	13.6 (0.7)	<0.02	<0.02	<0.02
Dissolved oxygen, water, unfiltered, percent of saturation (%)	2 (0)	2 (0)	2 (0)	--	--	--
Dissolved solids dried at 180 degrees Celsius, water (mg/L)	213 (2.4)	465 (1.5)	316 (7.9)	<20	<20	<20
Dissolved solids, water, filtered, sum of constituents (mg/L)	219 (0.5)	452 (1.8)	342 (1.5)	<3	<3	<1
Dissolved oxygen, water, unfiltered (mg/L)	0.2 (0)	0.2 (0)	0.2 (0)	--	--	--
Fluoride, water, filtered (mg/L)	0.1 (0)	0.69 (2.9)	0.21 (4.7)	<0.01	<0.01	<0.01
Hardness, water mg/L as $CaCO_3$	186 (1.6)	198 (2.6)	299 (0)	<0.1	<0.1	<0.12
Iron, water, filtered (µg/L)	71.8 (11.1)	1630 (4.2)	2120 (1.4)	<4	<10	<10
Magnesium, water, filtered (mg/L)	13.4 (2.2)	20 (1.0)	26.1 (0.4)	<0.011	<0.011	<0.011
Manganese, water, filtered (µg/L)	485 (1.7)	100 (5.8)	92.1 (0.4)	0.22	<0.2	0.24
Nitrate, water, filtered (mg/L as N)	<0.009 (10.5)	<0.01 (0)	<0.01 (0)	<0.01	<0.01	<0.01
Nitrite, water, filtered (mg/L as N)	<0.001 (0)	<0.001 (0)	<0.001 (0)	<0.001	<0.001	<0.001
Nitrate plus nitrite, water (mg/L as N)	<0.01 (0)	<0.01 (0)	<0.01 (0)	<0.01	<0.01	<0.01
pH, water, unfiltered, field, standard units	7.5 (0)	7.5 (0)	7.4 (0)	--	--	--
Phosphorus, water, filtered (mg/L as P)	0.019 (11.1)	0.134 (--)	0.119 (5.2)	<0.003	<0.003	<0.003
Potassium, water, filtered (mg/L)	1.53 (1.3)	1.84 (4.3)	3.52 (0.6)	<0.03	<0.1	<0.1
Silica, water, filtered (mg/L as SiO_2)	17.6 (1.1)	26.1 (0)	29.1 (1.0)	<0.018	<0.018	<0.018
Sodium, water, filtered (mg/L)	7.08 (0.6)	104 (2.8)	9.91 (0)	<0.06	<0.1	<0.1
Sulfate, water, filtered (mg/L)	11.5 (0.9)	21.3 (7.7)	48.1 (0)	<0.02	<0.02	<0.02

[a]Only the replicate value is shown in this table, the regular sample concentrations can be retrieved from the U.S. Geological Survey National Water Information System (U.S. Geological Survey, 2019).

[b](Concentration1 – concentration2)/[(concentration1 + concentration2)/2].

Table 3.2. Comparison of anion concentrations measured in split replicate groundwater samples by Rick Knurr (University of Minnesota and Ion Chrom Analytical Laboratory) and the U.S. Geological Survey National Water Quality Laboratory (USGS NWQL).

[lab, laboratory; mg/L, milligram per liter; N, nitrogen; <, less than; --, not calculated]

Constituent	Samples collected October 24, 2017								
	Sample OT–13			Sample OT–20			Sample OT–60		
	R. Knurr lab	USGS NWQL	[a]Relative percent difference	R. Knurr lab	USGS NWQL	Relative percent difference	R. Knurr lab	USGS NWQL	[a]Relative percent difference
	Concentration			Concentration			Concentration		
Bromide, water, filtered (mg/L)	0.041	0.034	18.7	0.112	0.125	11.0	0.274	0.302	9.7
Chloride, water, filtered (mg/L)	7.242	7.12	1.7	39.714	40	0.7	13.196	13.1	0.7
Fluoride, water, filtered (mg/L)	0.368	0.48	26.4	0.242	0.34	33.7	0.625	0.65	3.9
Nitrate, water, filtered (mg/L as N)	1.098	1.06	3.5	0.022	<0.009	--	0.013	<0.01	--
Nitrite, water, filtered (mg/L as N)	<0.003	0.012	--	<0.237	<0.001	--	0.677	<0.001	--
Sulfate, water, filtered (mg/L)	19.331	19.2	0.7	41.826	42.2	0.9	13.755	13.2	4.1

[a](Concentration1 – concentration2)/[(concentration1 + concentration2)/2].

For more information about this publication, contact
Director, USGS Upper Midwest Water Science Center
2280 Woodale Drive
Mounds View, MN 55112
(763) 783–3100
For additional information visit https://www.usgs.gov/centers/umid-water
Publishing support provided by the
Rolla Publishing Service Center

ISSN2328-0328 (online)
https://doi.org/10.3133/sir20205127